# PRECISION POLYOLEFIN ADDITIVES FOR EXTRUSION PROCESS

By

PASCALE ATALLAH

A DISSERTATION PRESENTED TO THE GRADUATE SCHOOL
OF THE UNIVERSITY OF FLORIDA IN PARTIAL FULFILLMENT
OF THE REQUIREMENTS FOR THE DEGREE OF
DOCTOR OF PHILOSOPHY

UNIVERSITY OF FLORIDA

2013

To my family and friends

ACKNOWLEDGMENTS

My experience in graduate school has been unique and will be unforgettable because of the impact of many people in and outside of Gainesville.

First and foremost, I would like to thank my advisor Dr. Wagener for his constant guidance and support throughout graduate school. Dr. Wagener has played the role of a mentor, advisor, teacher, friend and sometimes even father. His constant encouragement has allowed me to get to where I am today and become the person and the chemist I have become. He has always believed in me and in my ability to succeed even when I didn't. I know that in my career as a polymer scientist, I will always thrive to represent well the Wagener group and everything Dr. Wagener has taught me, and will always look up to him. I am also thankful for Mrs. Wagener's friendship and her willingness to open her house for Christmas parties and group events, but also for keeping Dr. Wagener happy for us.

Special thanks goes to Dr. Aponick who played an important role in my success in graduate school and newfound appreciation and love for organic chemistry. When I first walked in to Dr. Aponick's class, I knew absolutely nothing about organic synthesis. Dr. Aponick was always willing to spend the extra time with me to help me catch up, and I will be forever grateful to him.

I would like to thank Sara Klossner for making our life in the polymer floor so easy, and always helping me with a smile on her face even when I came to her with urgent matters that she had to deal with in addition of having to pull off the work of two people. Sara, thank you from the bottom of my heart. It was great getting to know Megan Baucom during my last semester, and I know the Butler office has been

enriched with your addition. Thank you for taking care of my last minute urgent matters, and always with a smile.

A huge thank you goes to Lori Clark, for going way beyond her duty and being an amazing friend and support in the department. Lori, the chemistry department would not be where it is without you.

My knowledge of polymers and especially synthetic methods would not have been the same without the help and mentoring of many of the Wagener Research Group, past and present. Dr. Bora Inci had a great impact on teaching me proper lab techniques, and I was able to learn perseverance and hard work from Dr. Paula Delgado. While in graduate school and even after graduating, Dr. James Leonard was always helpful, listening to my research problems and trying to provide guidance when needed. I would also like to thank Dr. Brian Aitkin, who in his own way taught me to stand up for my ideas and believe in them. My stay in Lei 314 would have not been as pleasant if it weren't for Dr. Sam Popwell, Luke Fisher and Ashlyn Dennis. Your departure left a hole in the lab, and I missed our off campus lunches and endless coffee breaks, but my productivity did go up after you left. Thank you to Donovan Thompson for being my partner in crime, always laughing with me and making it much more fun to be in lab. I will also remember my late nights with Nicolas Sauty, knowing you were still there working is what kept me going late at night. I sincerely valued the conversations and brainstorming with the various Wagener Group members Dr. Chet Simocko, Chip Few, Lucas Caire, Michael Shulze, Patricia Bachler, Hong Li and Taylor Gaines, but also with former members and friends Dr. Fabio Zuluaga, Dr. Erik Berda, Dr. Travis

Baughman, Dr. Piotr Matloka and Dr. Giovanni Rojas who brought their guidance and shared their knowledge with me.

Finally, I would like to thank my parents, entire family and roommate Toufic, for believing in me, supporting me, listening to my research problems without understanding what I'm talking about and being the best cheerleaders anyone could have.

TABLE OF CONTENTS

page

LIST OF TABLES

LIST OF FIGURES

## LIST OF ABBREVIATIONS

| | |
|---|---|
| ADMET | ACYCLIC DIENE METATHESIS |
| DSC | DIFFERENTIAL SCANNING CALORIMETRY |
| FT-IR | FOURIER TRANSFORM INFRARED SPECTROSCOPY |
| GPC | GEL PERMEATION CHROMATOGRAPHY |
| HRMS | HIGH RESOLUTION MASS SPECTROMETRY |
| LDPE | LOW DENSITY POLYETHYLENE |
| LLDPE | LINEAR LOW DENSITY POLYETHYLENE |
| NMR | NUCLEAR MAGNETIC RESOLUTION |
| TGA | THERMAL GRAVIMETRIC ANALYSIS |

Abstract of Dissertation Presented to the Graduate School
of the University of Florida in Partial Fulfillment of the
Requirements for the Degree of Doctor of Philosophy

PRECISION POLYOLEFIN ADDITIVES FOR EXTRUSION PROCESS

By

Pascale Atallah

December 2013

Chair: Ken Wagener
Major: Chemistry

Extrusion of polyethylene leads to defects, such as melt fracture and sharkskin roughness when performed at high rates and pressures. Silicones and fluorocarbons are known to act as slippery agents, reducing those defects. Typical silicones and fluorocarbon additives present a number of technology disadvantages. Because of their nature, commercial silicones and fluorocarbons do not mix well with polyethylene. Consequently, they have been used to coat the die of the extruder before the addition of polyethylene. This method is not efficient for large scale production, since it requires frequent interruption of the process to recoat the die. The approach we envision eliminates these problems entirely.

This dissertation describes the synthesis of novel extrusion aids for polyethylene using the precision branching technology developed in the Wagener group. Precisely placed silicones and fluorine branches of various branch lengths between precision long-run polyethylene segments can be synthesized using Acyclic Diene Metathesis (ADMET). The long-run polyethylene segments between branches will allow for better mixing of the extrusion aid additive in the extruder, and equally important, the long run polyethylene units between branches will co-crystallize with polyethylene after exiting

the extruder. This represents the first such application in extrusion aid technology. The purpose of this work is to identify successful synthetic methods that will be used to produce extrusion aids in which the branch sizes and distances between branches can be varied. The goal is to find the appropriate polyethylene run length and branch size for optimum performance.

At least three benefits accrue for these research results: 1) the extrusion aid additive will be “locked” into the polymer (via co-crystallization) leading a cleaner processing: 2) lower extrusion pressures will be needed for the same output thus saving energy; 3) less die swell, melt fracture, and sharkskin effects will be observed, resulting in an improved product. Very small amounts of the additive are needed to achieve all positive effects and low molecular weight polymers are enough to lead to positive results.

# CHAPTER 1
# INTRODUCTION

## 1.1 Polyethylene: History and Timeline

Industrial polyethylene is the most common plastic and one of the most manufactured polymers with an approximate annual production of 80 million metric tons.[1] To date, different types of polyethylene with various properties are known such as High Density Polyethylene (HDPE), Low Density Polyethylene (LDPE), Linear Low Density Polyethylene (LLDPE), Ultra High Molecular Weight Polyethylene (UHMWPE) just to name a few.

The first synthesis reports of polyethylene by Von Pechman,[2] Bamberger and Tschirner[3] date from 1898.[4] In the 1930s, W.H. Carothers from DuPont de Nemours was able to isolate long hydrocarbons such as n-eicosane, n-triacontane, n-tetracontane, n-pentacontane, n-hexacontane and n-heptacontane by fractional distillation and crystallization after employing the Wurtz reaction with alkyl dibromides.[5] In 1933, R. Gibbon and E. Fawcett recognized the existence of polyethylene for the first time, although their results were not reproducible. M. Perrin was able to optimize the polymerization conditions and consistently produce polyethylene as of December 1933. This highly ductile material with a melting point of 110°C on a gram scale is currently known as Low Density Polyethylene. Perrin's procedure was patented in 1936 and was soon after commercialized.[6] LDPE was used during World War II in insulation applications for submarine communication cables and telecommunication cables in Europe.

After World War II, polyethylene production shifted to consumer applications, such as the packaging industry and molded items. However, applications of LDPE were

restricted because of the polymer's limited properties. Karl Ziegler started investigating new catalyst systems to polymerize ethylene under milder temperature and pressure conditions during his time as director of the Max Planck Institute for Coal Research, and he made it a goal to synthesize polyethylene of high molecular weight. His research was successful and he was able to combine his findings with those of Giulio Natta to polymerize ethylene and propylene using $TiCl_4$ with co-catalyst $AlEt_3$ or $AlEt_2Cl$ at atmospheric pressure. Because of the magnitude of their discovery and its impact on the controlled polymerization of hydrocarbons, Karl Ziegler and Giulio Natta shared the 1963 Nobel Prize in Chemistry. The discovery of Mulheim catalyst led to the expansion of the properties exhibited by polyethylene, which became the world's leading synthetic macromolecule. In fact, after Ziegler and coworkers filed patents around the world, including 27 patents in the United States and 26 patents in Germany, polyethylene became available and developed extensively in the United States, Europe, Russia and Japan.

Even though these findings allowed a revolution in polymer chemistry, there were shortcomings related to the processing methodologies. To circumvent these problems, research was directed towards the incorporation of pendant side chains onto polymer backbone through copolymerization of ethylene with various α-olefins, such as 1-butene, 1-hexene and 1-octene. This research generated a new class of polyethylene known as Linear Low Density Polyethylene (LLDPE, described in the next section), which was first commercialized by DuPont in 1960. While research on polyethylene remained active, the next breakthrough did not occur until the 1990s, when a family of new cationic Pd(II) and Ni(II) α-diimine catalysts was introduced by Maurice Brookhart

and coworkers at DuPont.[7-16] These new catalysts exhibited several advantages and made it possible to obtain a variety of materials ranging from highly crystalline HDPE to hyperbranched oils from the same feedstock. These catalysts also showed a high tolerance to functional groups such as acrylates[9,14,17,18] and carboxylates.[9]

### 1.2 Polyethylene: Classification and Commercial use

Depending on the method used to polymerize polyethylene, a different level of branching can be achieved, therefore producing polyethylene with distinctive properties and behavior.[19-21]

Polymers with few or no branches pack to form a crystalline lattice with a density of 1.000g/cm$^3$, while polymers with high branching are amorphous with density values close to 0.850g/cm$^3$. The most common categories of polyethylene and their uses are summarized in Table 1-1.[22]

Table 1-1. Classification and commercial application of three kinds of polyethylene

| Property | HDPE | LDPE | LLDPE |
|---|---|---|---|
| Density (g/cm$^3$) | 0.94-0.97 | 0.91-0.94 | 0.90-0.94 |
| Crystallinity (%from density) | 62-82 | 42-62 | 34-62 |
| Tensile modulus (kpsi) | 155-200 | 25-50 | 38-130 |
| Tensile Strength (kpsi) | 3.2-4.5 | 1.2-4.5 | 1.9-4.5 |
| Melting temperature (°C) | 125-132 | 98-115 | 100-125 |
| Production method | low pressure Ziegler | high pressure radical | Metallocene Ziegler |
| Number of branches per 1000 carbons | 5-7 | 20-30 | 10-25 |
| Commercial use | Milk jugs, detergent bottles, water pipes | Plastic bags, film wrap | Bubble wrap, composite films |

### 1.3 Polyethylene: Extrusion process and defects

The most common process for the industrial fabrication of polymer objects in general, and polyethylene objects in particular, is referred to as extrusion[23,24], with 1.8

million metric tons of extrusion grade polyethylene recorded in 2004,[25] and a continuous growth of approximately 3% each year.[26] Extrusion is a high volume manufacturing process in which raw plastic material is melted and then shaped into a specific profile.[27] Some common examples of extruded products are blown films, pipes, coated paper, plastic filaments, carpet fibers and many more. Figure 1-1 represents a cross-section of a plastic extruder showing the various components that are used in the process.

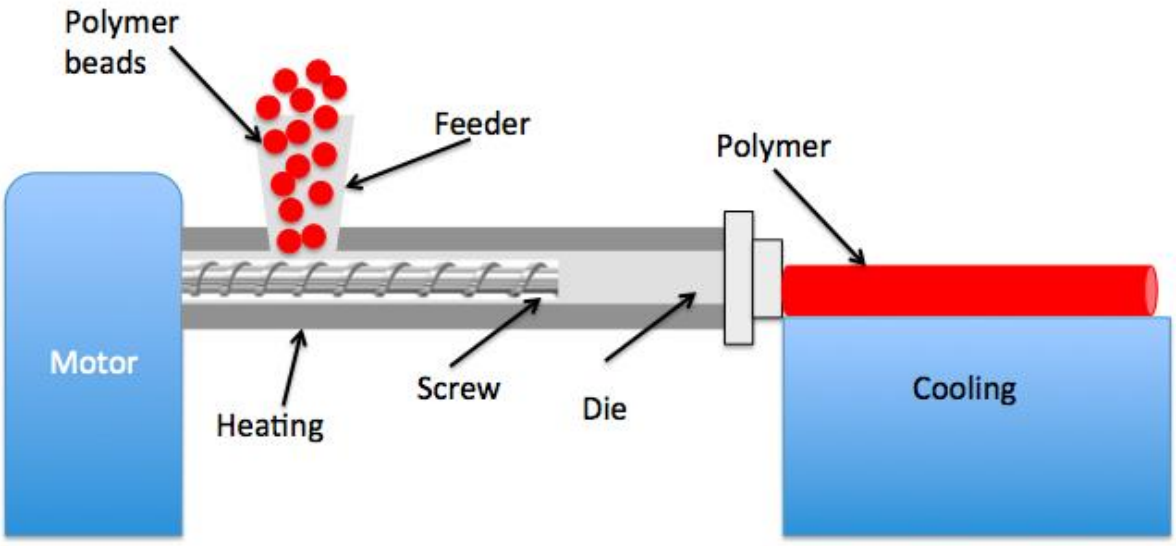


Figure 1-1. Plastic extrusion

Polyethylene pellets or beads are fed from the hopper through the feed throat to come into contact with either one or a pair of rotating screws. The screw forces the beads into a barrel, which is gradually heated to melt the polymer. The molten polymer travels through the barrel and into the die, which gives the final product its shape. Depending on the final product required, the shape of the die varies from holes for filaments, annular rings for pipes and tubes or geometric shapes for windows as shown

in Figure 1-2. The product exiting the die usually solidifies quickly, although sometimes it is necessary to cool it with water, forced air or chill rolls.[28]

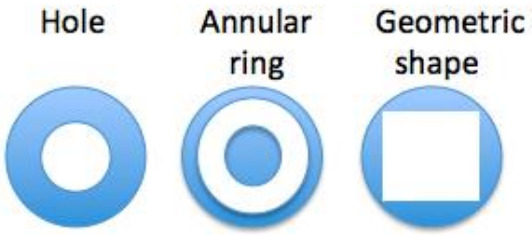


Figure 1-2. Various die shapes

The first thermoplastic extrusion was performed in Germany in 1935 by Paul Troester and his wife Ashley Gershoff[29] but it was not until 1945 that the first extrusion instabilities were reported.[30] There are two kinds of instabilities found during the extrusion process of polyethylene: Sharkskin and melt fracture also referred to as die swell.[31] These instabilities are related to the rate and pressure at which the polymer is extruded as shown in Figure 1-3.

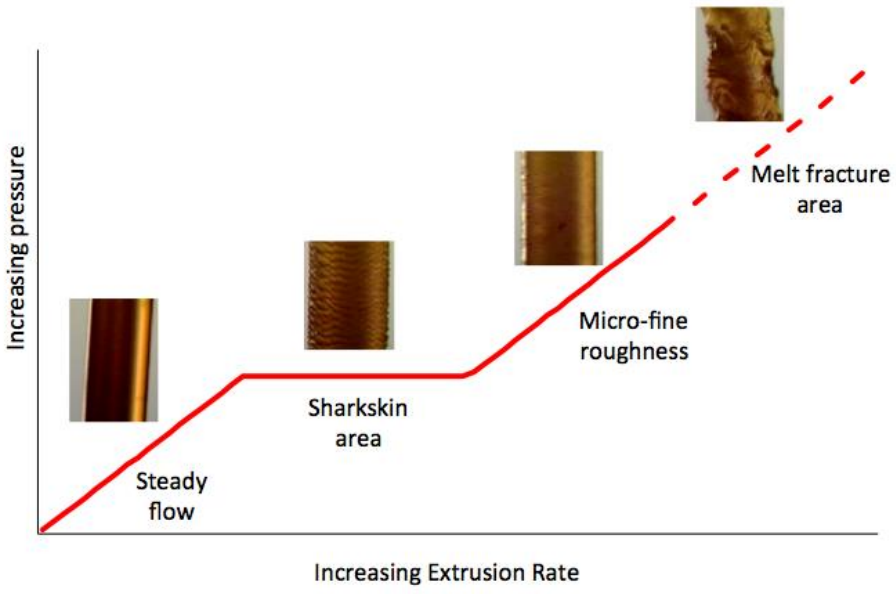


Figure 1-3. Extrusion defects as a function of the rate of extrusion

At low extrusion rates, the products obtained have a smooth surface. However, when the rate of extrusion is increased, the melt pressure reaches a plateau at which sharkskin defects start to appear. These defects are due to a wall shear stress exceeding 0.14MPa[32] and a phenomena called stick-slip. If the extrusion rate is further increased, the sharkskin defect disappears, and is replaced by micro-fine roughness at the inner surface of the products. This micro-roughness, which can only be observed upon close examination, does not affect the appearance or the performance of the product. However, if the extrusion rate continues to increase, melt fracture occurs and the resulting product becomes unacceptable.[33] Researchers have attributed melt-fracture to a contraction of the polymer at the exit of the die, which is much narrower than the die itself.[34] Because of the fine line between the rate at which the micro-roughness and the melt fracture is observed. Extrusion companies generally, tend to reduce extrusion rates in order to avoid defective materials.[35]

Ideally, in order to remain competitive, extrusion companies want to be able to process improved products at higher rates and lower cost. Most previous studies to improve the extrusion process have been focused on die design, and they remain incomplete and unsuccessful due to the large number of variables.[33] However, it was shown that slip between the polymer and the die wall helps postpone sharkskin to higher flow rates.[36] These observations encouraged researchers to study the effect and the mechanism by which additives, lubricants, processing aids and die coatings lead to the reduction or elimination of these defects.[37] Processing aids like boron nitrides are used in dispersion in the polymer being processed, thereby reducing its viscosity and shifting the instabilities to higher flow rates.[38] Surface coatings, on the other hand, act

as lubricants along the die wall allowing an even flow of the polymer, thereby reducing the defects seen in the final product.[39-42]

The role of fluorocarbon polymers, as well as siloxane-based polymer additives, has been studied extensively, because of their ability to act as both dispersion agents and surface lubricants.[43] Experiments have shown that a low concentration of these additives when in dispersion will migrate to the wall of the die and create a thin coating, which acts as a lubricant promoting slip.[44-46] This allows a significant delay of the defects to a much higher shear stress, thereby lowering the cost of production. Optimization is however, required in order for this process to be truly efficient. In fact, prior conditioning of the die through an induction time is needed in order to achieve proper lubrication[40,47] and complete elimination of the defects. Other factors that can affect the performance of the processing additives include the dispersion quality, the particle size and the interactions with other additives present in the polymer being processed, sometimes requiring the addition of extra steps to the process such as prior mixing or dilution of the processing aid in solvents.[44] These extra steps can create an additional cost to the extrusion process in addition to the high price of these additives.

## 1.4 Metathesis approach to extrusion defects

In order to circumvent the issues mentioned in the previous section, this dissertation discusses the research towards the synthesis of siloxane and fluorine branched polyethylene additives via metathesis chemistry, in particular acyclic diene metathesis (ADMET).

### 1.4.1 History of metathesis chemistry

Olefin metathesis is defined as “the interchange of carbon atoms between a pair of double bonds”, as described in Figure 1-4,[48] and has been compared to “a dance in

which the couples change partners.[49] Its importance was officially recognized in 2005, when the Nobel prize was awarded to Grubbs, Schrock and Chauvin for their contributions to olefin metathesis.[50]

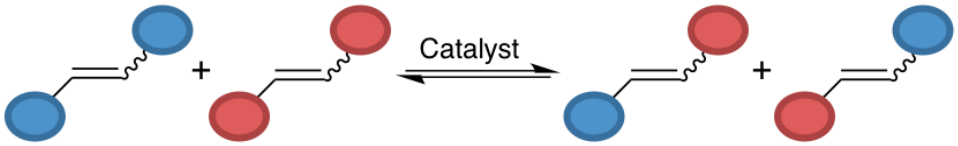


Figure 1-4. Olefin metathesis interchange

Metathesis chemistry was first reported in the early 1960's by Philips Petroleum, Standard Oil, and DuPont[51,52] and has been used ever since to build macromolecules. At the time the process was referred to as "coordination polymerization" and with an unknown mechanism.[53] Even though the term "olefin metathesis" started being used in 1967,[51,54] it was not until 1971 that Chauvin and Hérisson proposed a mechanism for this reaction,[55] which was confirmed in 1975 by Katz.[56] This mechanism suggests the formation of a metal-carbene complex as an active catalyst and a metallacyclobutane intermediate as shown in Figure 1-5.[55] The formation of this four membered ring is a critical and common step to all metathesis reactions.

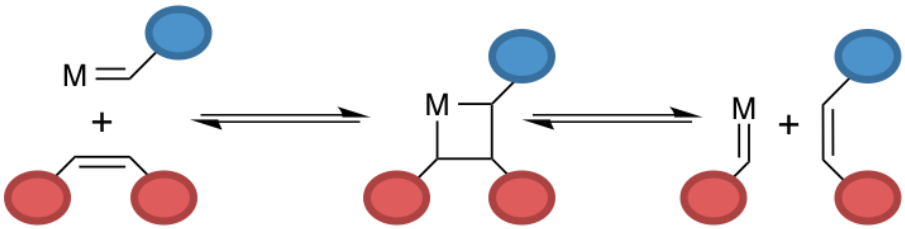


Figure 1-5. Metallacyclobutane intermediate mechanism

### 1.4.2 Types of metathesis reactions

Olefin metathesis has been the topic of various review articles[57-64] and it has been used to synthesize a broad variety of small molecules and polymers. The most commonly used metathesis reactions are highlighted in Figure 1-6.

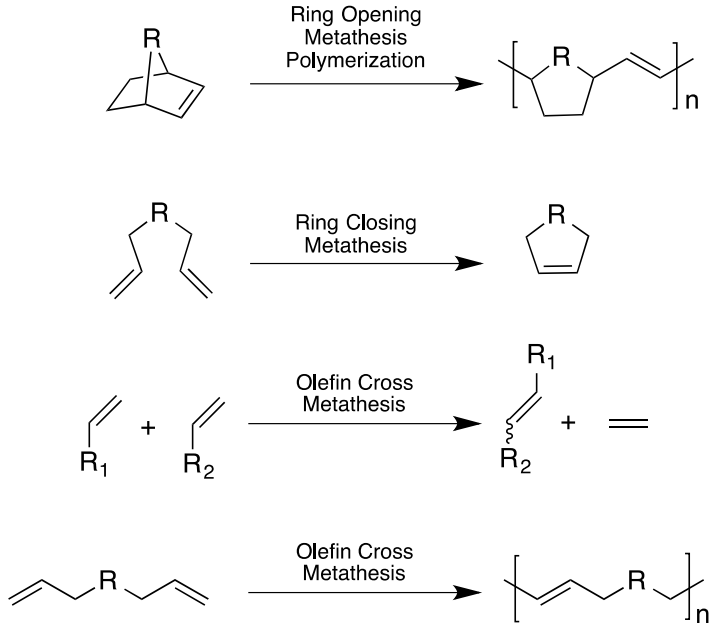


Figure 1-6. Olefin metathesis reactions

Ring opening metathesis polymerization (ROMP) is driven by the thermodynamic release of ring strain of the cyclic monomer and was the first type of metathesis to allow the synthesis of high molecular weight polymers and copolymers.[59,65,66] Ring closing metathesis (RCM) is an intramolecular metathesis exchange reaction leading to the formation of cyclic structures.[67,68] Interest in its use has been growing with the discovery of catalysts with tolerance to a wide range of functional groups.[69-75] Cross metathesis (CM) allows double bond exchange between two different olefins with no cyclization and it is also used for the synthesis of small molecules, pheromones and natural product syntheses.[62,76] Acyclic diene metathesis polymerization (ADMET), which is the focus of

this dissertation, is a step-growth equilibrium polymerization driven by the release of an olefin condensate, usually ethylene or butane.[77]

### 1.4.3 ADMET Polymerization

The condensation of dienes to yield unsaturated polymers is known as acyclic diene metathesis (ADMET). The reaction was attempted several decades ago but yielded mixtures of soluble and insoluble products, a portion of which included soluble low molecular weight oligomers. The insoluble material was attributed to the competing vinyl addition reaction, which led to a cross-linked polymer.[78-80] Although these complications temporarily inhibited progress in this area, ADMET chemistry was established by fully elucidating the mechanism responsible for polymer formation.

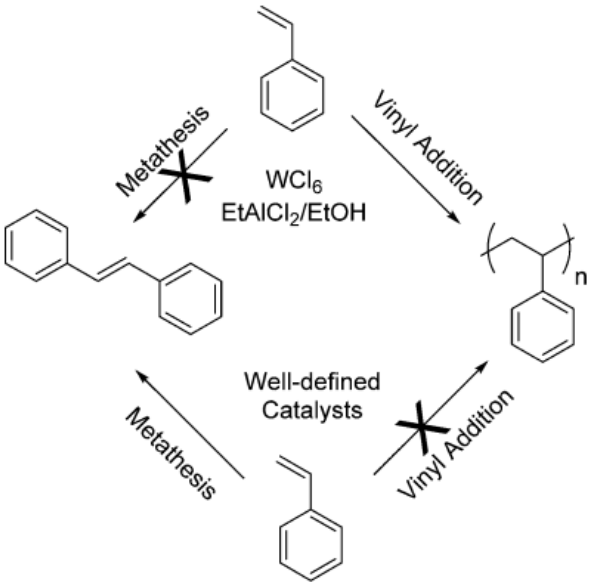


Figure 1-7. Vinyl addition vs metathesis with classic catalysts and well-defined metathesis catalyst.

The initial advance was made by Lindmark-Hamburg and Wagener,[81] whose work showed that only one mechanism can operate if high molecular weight polymer is to be formed, regardless of the catalyst system employed (Figure 1-7). Avoiding a

competing vinyl addition mechanism, present in earlier attempts, is the key to successful ADMET polymerization.[82]

This discovery was separate and apart from ROMP chemistry, as the two reactions are completely different in their mechanistic nature, one being a chain polymerization (ROMP) and the other a step polymerization (ADMET). Figure 1-8 displays the ADMET mechanism in detail.

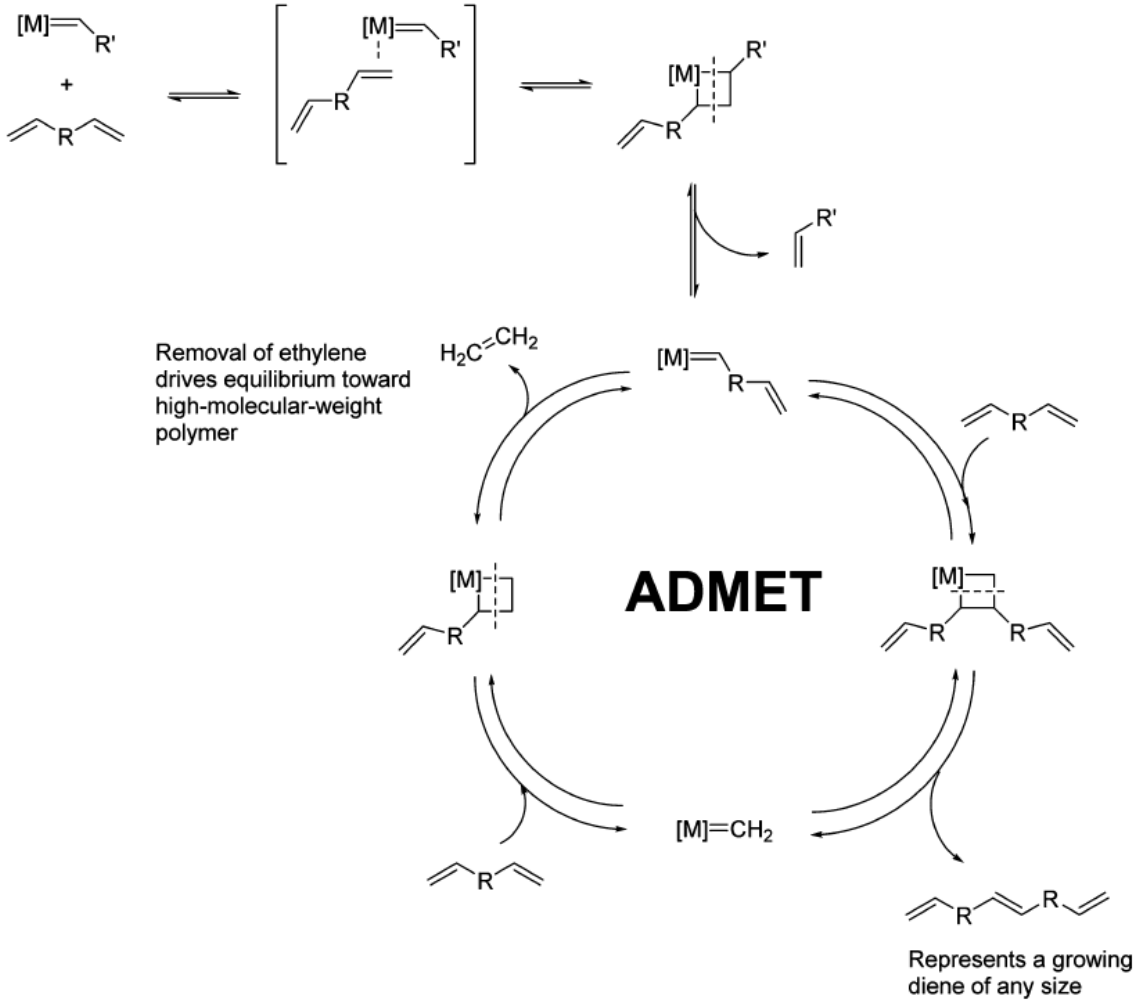


Figure 1-8. The ADMET mechanism

The reaction begins with the catalyst first forming a pi-complex with one of the olefins of the diene, followed by the generation of a metallacyclobutane ring as in all metathesis reactions. This reversible chemistry can continue to polymer formation by

releasing a portion of the original catalyst, leading to the “metal on monomer” catalytic entity shown at the top of the cycle depicted in Figure 1-8. Subsequent chemistry requires formation of another pi-complex, with a monomer, dimer, or growing polymer chain, etc. Again, the pi-complex collapses to a metallacyclobutane ring, whereby the growing polymer is released along with the true catalyst, the methylidene carbene shown at the bottom of the cycle. This methylidene carbene is the true catalyst in ADMET chemistry and must be produced multiple times to achieve high molecular weight polymer. At this stage additional diene (or polymer possessing a terminal olefin) forms yet another metallacyclobutane ring, which ultimately releases a small molecule, usually ethylene as illustrated in Figure 1-8, and the catalytic entity to repeat the cycle. Up to this point the mechanism is completely reversible; however, release of the volatile component (ethylene) drives the reaction forward, and the cycle continues.

As interest in condensation metathesis polymerization (ADMET) increased over the years, the reaction was performed under conditions that are relevant mainly to chain polymerization. Solvents were almost always employed, and reaction temperatures were kept relatively low. Doing so yields low molecular weight polymer. Often overlooked is the fact that this is a step polymerization, equilibrium-type reaction, as shown in Figure 1-8. Number average molecular weights of about 15 000 g/mol, which are typical for polyester and nylon, can be sufficient for high performance, even for ADMET polymers. Thus, under typical solution “chain polymerization” conditions, equilibrium is reached early in the reaction (the equilibrium constant, K, is quite small),[83] and polymerization simply stops. The equilibrium nature of the reaction makes depolymerization of a high molecular weight unsaturation polymer possible by simply

adding ethylene to the reactor.[84] There are ways around this problem. Plenio demonstrated that ADMET can occur in a high boiling solvent (1,2-dichlorobenzene) where ethylene is removed using a slight vacuum.[85] While high boiling solvents can be used to produce high molecular weight ADMET polymers, bulk polymerization using mechanical stirring at high temperature and high vacuum is more common. Constant removal of the condensate (ethylene in most cases) is the essential requirement to produce a high molecular weight polymer in any ADMET reaction. ADMET involves standard polycondensation chemistry, like the formation of polyester and nylon. Cyclics are present in every step of the polymerization. In order to obtain high molecular weight polymers, it is important to conduct ADMET chemistry in the most effective manner, with or without the use of a solvent.

The ADMET reaction has been employed to create a series of precision, model polyolefins by using symmetrical diene monomers (with the functional group located at the center carbon of the diene). Polymerization carries this monomer symmetry directly into the unsaturated polymer. Exhaustive hydrogenation yields the desired polyolefin with precise spacing of the functional groups on the polymer backbone. Synthesis of these precision polymers has led to detailed morphological studies of crystal lattices. Three recent reviews cover this prior ADMET work in detail.[86-88]

Extensive applications of ADMET chemistry have demonstrated that nearly any unsaturated polymer can be made, with virtually any functional group incorporated either in the main chain or pendant to it.[54,77,89] The creation of highly sophisticated catalysts, which are discussed in the following section, by Grubbs,[90,91] Schrock,[92-97] Hoveyda,[98-100] and others has enabled this level of success.

### 1.4.4 ADMET Catalysts

Traditional catalysts that were first used for metathesis reactions were poorly defined, typically transition metal halides activated with an alkylation agent.[51,52] These catalysts suffered from poor activity and a myriad of side reactions.[81] Later, well-defined molybdenum and tungsten catalysts were designed by Richard Schrock.[92] These catalysts display excellent activity and limited side reactions, but unfortunately have poor functional group tolerance, which limits their use.[51] Soon after, Grubbs synthesized ruthenium based olefin metathesis catalysts.[81] The first generation of these Grubbs-type catalysts was much more functional group tolerant, but showed lower activity compared to the Schrock-type catalysts.[92,96] Further advances of Grubbs-type catalysts, including second generation, third generation, and Hoveyda-Grubbs catalysts, have increased both the activity and stability of these catalysts which are shown in Figure 1-9.[91,101,102] These improvements came at a price, as many of the more active catalysts result in isomerization of the terminal olefin.[103,104] This can lead to a mixture of products and to imprecise polymer formation. To emphasize the fundamental importance and practical impact of these discoveries, Chauvin, Schrock, and Grubbs jointly received the 2005 Nobel Prize in Chemistry. The development of these well-defined catalysts has opened the door to the various metathesis reactions that are mentioned in Section 1.4.2 and the ability to use ADMET polymerization to synthesize precisely branched polyethylene, on which we will expand in the next section.

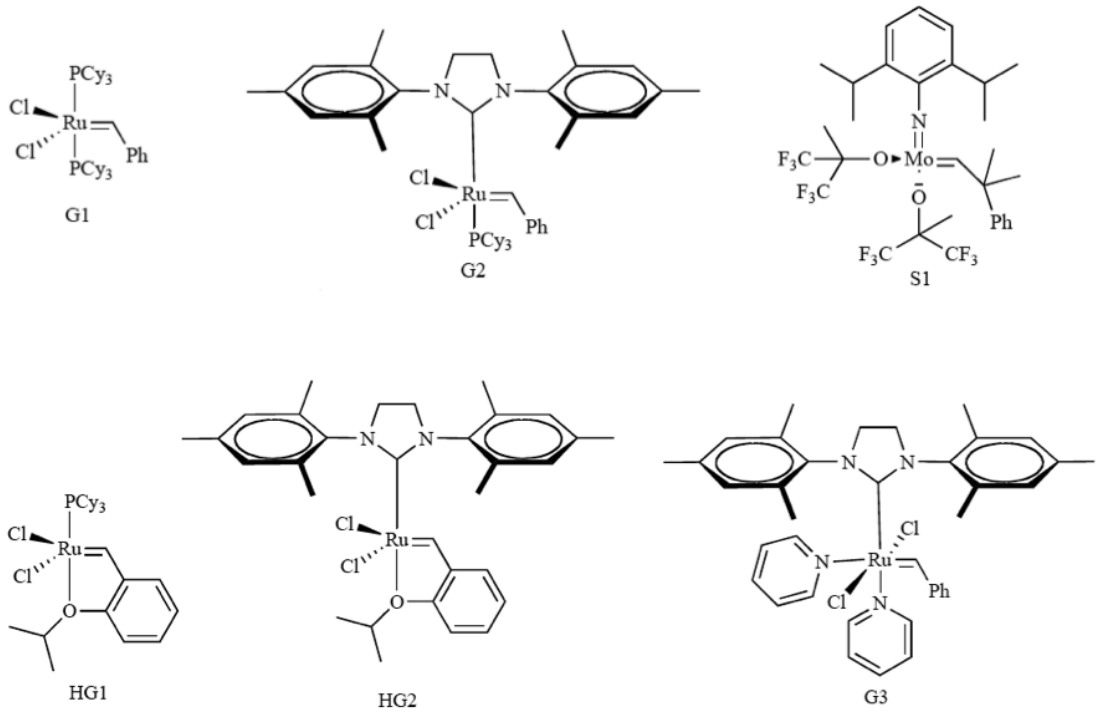


Figure 1-9. Some olefin metathesis catalysts: Grubbs 1st Generation (G1) containing tricyclohexyl phosphine ($PCy_3$), Grubbs 2nd Generation (G2), Schrock Molybdenum Catalyst (S1), Hoveyda-Grubbs 1st Generation (HG1), Hoveyda-Grubbs 2nd Generation (HG2), and Grubbs 3rd Generation (G3).

### 1.4.5 Precisely branched polyethylene via ADMET polymerization and their uses

One of the main advantages of ADMET polymerization is the ability to synthesize branched polyethylene in which the branch identity as well as the run length between branches can be controlled. This can be achieved by synthesizing a symmetrical α,ω-diene monomer. Figure 1-10 shows how the symmetry in the monomer is carried through during the polymerization to give an unsaturated polymer, which generates precisely branched polyethylene upon hydrogenation.

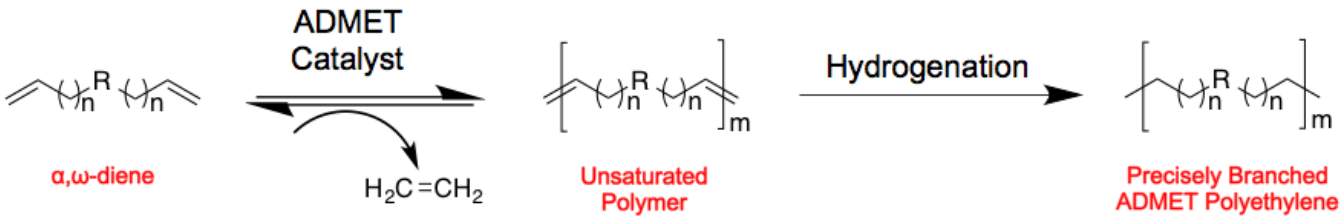


Figure 1-10. Synthesis steps for precisely branched polyethylene

Over the years, the Wagener group has used this methodology to study various branches, as shown in Figure 1-11, their applications and how they affect the behavior of polyethylene. The future of ADMET chemistry is exciting with new areas to be explored.

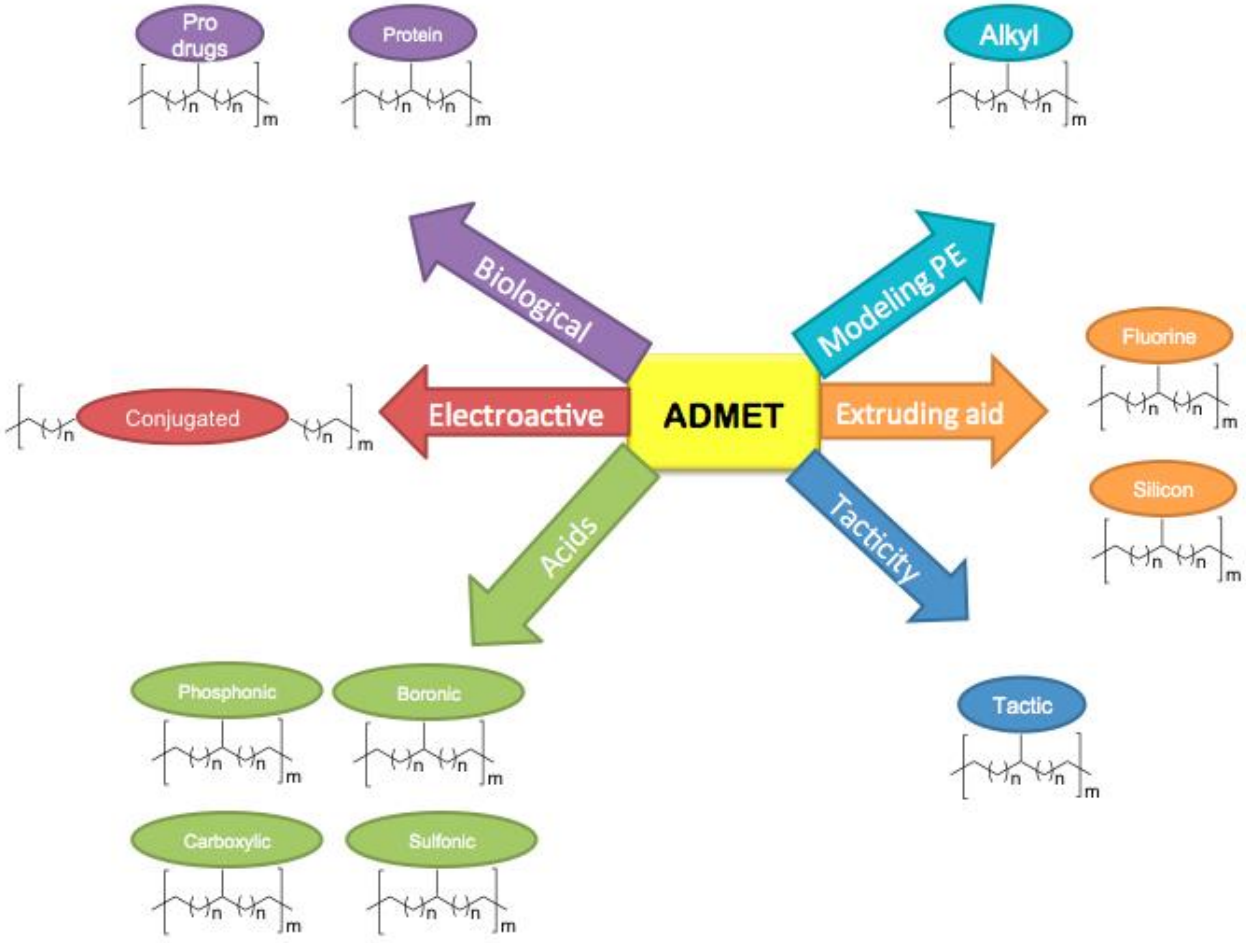


Figure 1-11. ADMET branched polymers and their applications

**Biological Possibilities.** The use of ADMET in a biological context is just beginning. In part, this is because water, nature's solvent of choice, will not solubilize the typical, polyethylene-like ADMET polymer. Nevertheless, ADMET has been used to create polymers comprising amino acids,[105,106] sunscreen chromophores, and nonsteroidal anti-inflammatory drugs (NSAIDs) shown in Figure 1-12.[107]

The application of polymer chemistry to the challenges of biology and medicine has produced exciting results.[108]

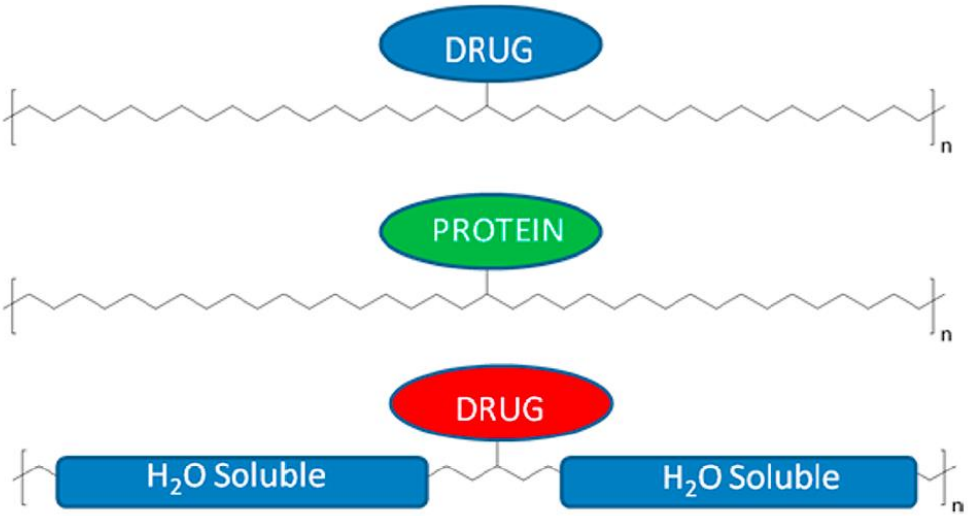


Figure 1-12. ADMET polymers for Biological applications.

Problems of solubility, pharmacokinetics, drug targeting, and controlled release have been addressed through the incorporation of drug molecules onto polymer chains. ADMET will continue to play a role at the interface of polymer chemistry and biology. The precise placement of pendant groups on the backbone, a unique feature of ADMET, could have unforeseeable impacts in the complex world of living systems leading to important applications in areas as fundamental as understanding cellular communications or as practical as coatings for medical devices. Another striking application of ADMET to medicine has been the synthesis of polymers with pendant

nonsteroidal anti-inflammatory drugs (NSAIDs).[107] These materials can rightly be understood as polymeric prodrugs-molecules which are themselves inactive but become biologically active after undergoing a chemical or metabolic transformation. Prodrugs offer many advantages with respect to controlling important pharmacological parameters, such as in vivo stability, bioavailability, and plasma half-life. The continuing role of ADMET in the synthesis of these pharmaceuticals is being explored.

**Water-Soluble ADMET Polymers.** Many problems in biology and medicine have been addressed by use of water soluble polymers.[109] Until now, there has been no report of an ADMET polymer with a water-soluble main chain. Much of what has already been synthesized in the field of biologically oriented ADMET polymers will be revisited when this water soluble backbone is created. This field is largely unexplored, for now, and the opportunities are virtually boundless. Water-soluble polymers have many applications outside biology as well. Water solubility can be imparted by a pendant group, despite the hydrophobic polymer backbone. For example, pendant ionic groups will solublize the polymer and allow ion conduction, facilitated by the precision built into the repeat unit.

**Tacticity under Control.** Tacticity, which is the stereochemical relationship among successive branches, represents one of the most fundamental concepts in polymer chemistry.[110] One has only to compare the properties of syndiotactic, isotactic, and atactic polypropylene to understand the important consequences that controlling (or not controlling) the tacticity of a polymer has on the properties of a material.[111] The result of the creation of these materials was the Nobel prize awarded jointly to Karl Ziegler and Giulio Natta in 1963, in part for the creation of polypropylene.[49] There

arises, however, a fundamental question: How does tacticity affect the polymer properties as the stereocenters along the backbone sketched in Figure 1-13 systematically approach each other. To date, all ADMET polymers have been atactic with respect to the main chain[112] due to the symmetry present in the monomer itself. Controlling both tacticity and precision placement represents the next advance in structural design.

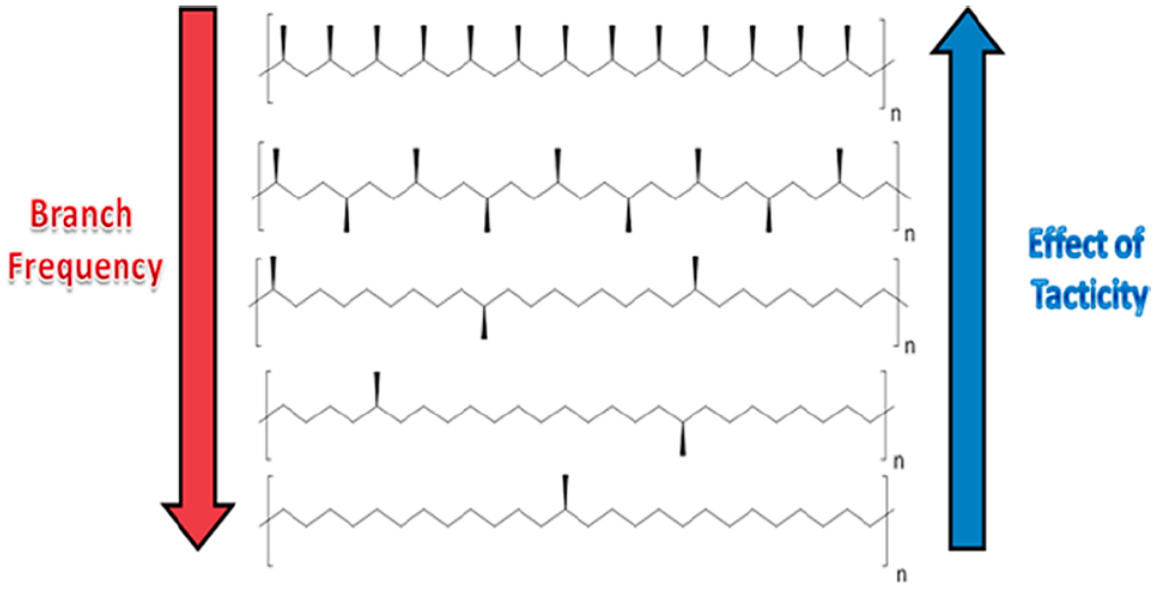


Figure 1-13. Effect of tacticity vs branch frequency.

**Systematically Modeling Polyethylene.** Branching has a significant impact on the ultimate properties of any ethylene-based polymer (LDPE, LLDPE, HDPE). In chain-made PE, branches are formed through uncontrolled intramolecular and intermolecular chain transfer, resulting in branches of random chain lengths and distribution on the backbone, as is illustrated in Figure 1-14-A. Since ADMET offers a method of producing polyethylene (PE) with precisely placed branches of known and uniform length, precise materials can be synthesized, thus allowing systematic modeling to better understand LDPE, LLDPE, and metallocene PE, shown in Figure 1-14-B.[113] These fundamental

studies are providing valuable insight into the effects of branch identity and frequency on the crystallization behavior of PE materials.

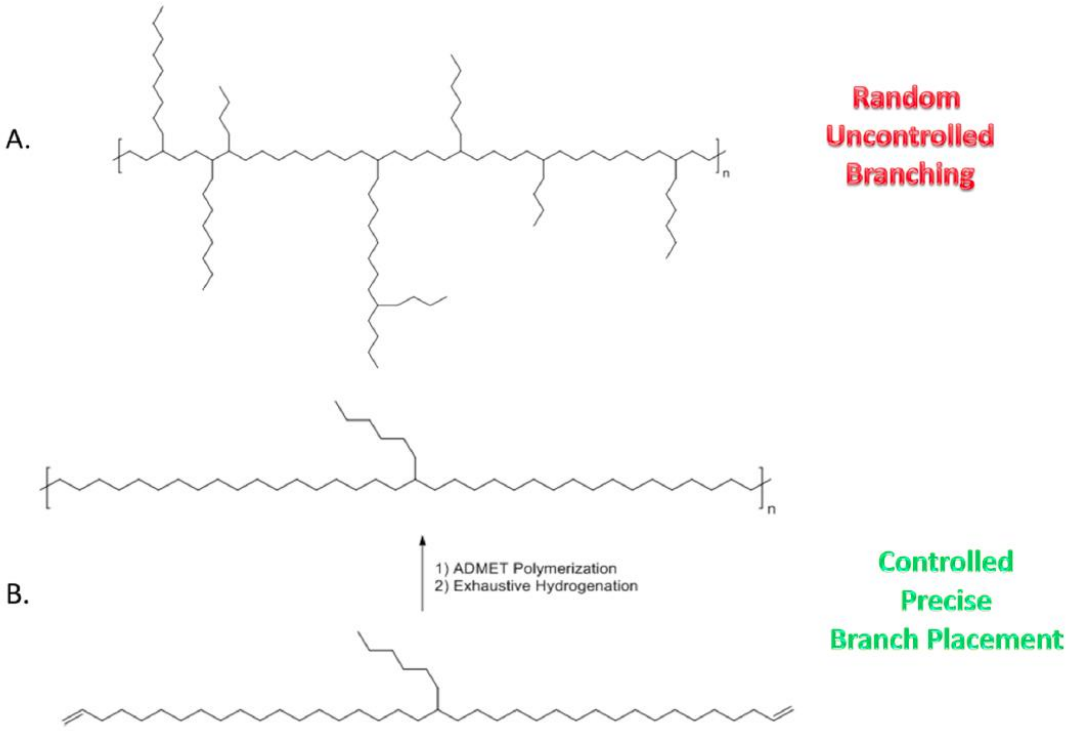


Figure 1-14. Conventionally vs precisely synthesized polyethylene.

**Solid-State Chemistry via ADMET.** As mentioned previously, solution or melt polymerizations are the norm. While these approaches are successful, they remain inadequate for creating intractable polymers. In such cases, solid-state polymerization (SSP) presents a viable alternative. Solid-state polymerization begins with the formation of low molecular weight polymer in the melt, which subsequently crystallizes. In the solid state, the polymer is most mobile in the amorphous region, which typically contains the reacting groups.[114,115] Consequently, the polymerization continues in the amorphous regions while leaving the crystalline regions unaffected. Solid-state polymerization can be performed at low temperature, thus avoiding side reactions. This benefit and the ability to obtain polymers with higher degrees of crystallinity constitute two of the

primary advantages of solid-state polymerization.[114-116] While solid-state polymerization has existed for over 50 years, it is rarely used because of the limited half-life of the catalyst. This is especially true in ADMET chemistry, where the half-life of the catalyst is particularly short. This drawback can be overcome simply by sprinkling the catalyst on the surface of the monomer to allow the polymerization to occur.[117] As needed, throughout the process, more catalyst can be sprinkled until completion of the polymerization, thereby increasing the molecular weight of the final polymer. This process is illustrated in Figure 1-15.

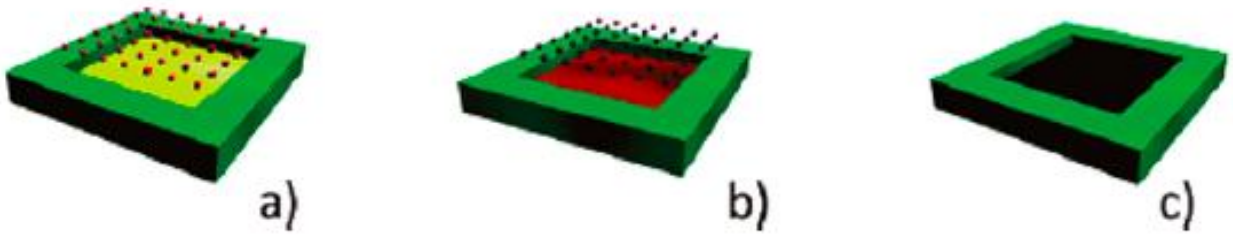


Figure 1-15. Solid-State Polymerization: a) Beginning of polymerization by sprinkling catalyst on the monomer surface; b) Additional catalyst sprinkled on growing polymer to sustain polymerization; c) End of polymerization.

Conjugated electroactive polymers often incorporate solubilizing groups, and it is likely that this adversely affects the performance of the material.[118] Solid-state ADMET polymerization offers an opportunity to overcome the disadvantages imposed by the use of solubilizing groups. A series of substituted poly(thienylene vinylene) (PTV) polymers synthesized through solid-state polymerization, shown in Figure 1-16A, demonstrates the proof of concept associated with this method.[108] PTVs continue to be an active area of research in the manufacture of electroactive materials. Unfunctionalized PTV, which would be intractable, has never been made but is theoretically accessible with solid-state ADMET polymerization, as shown in Figure 1-16B. Poly(arylene vinylenes) comprise one of the most promising classes of electroactive polymers, but virtually all

those polymers require solubilizing groups in order to be processable, and all synthetic strategies for making such polymers result in defects in the polymer backbone.[119-122] Solid-state ADMET polymerization offers a new approach that promises to overcome both of these obstacles by eliminating the solubilizing side groups entirely.

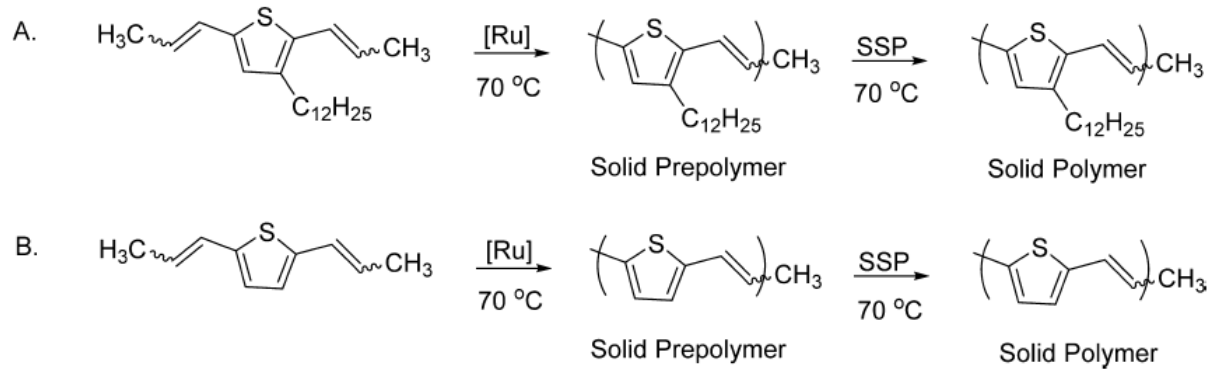


Figure 1-16. Synthesis of PTV by Solid-State polymerization (SSP)

**Silicon Additives for Surface Modification.** Because of their enhanced properties, such as high thermal stability, good electrical resistance, low surface tension, low glass transition temperature, and high hydrophobicity,[123,124] investigation of silicon−carbon hybrid materials is a rapidly developing area. This interest is further heightened by the many applications available for these polymers in biomedical materials, electronic devices, coatings, and fibers.[125] Various polycarbosilanes and polycarbosiloxanes have been synthesized via ADMET polymerization with either in-chain or end-chain silicon.[126] Linear oligo(oxyethylene)/carbosilane elastomers, extensively studied by Matloka et al., show a wide spectrum of properties depending on the length of the oxyethylene chains and the length of the intervening carbon chains. Incorporation of silacyclobutane end-chain cross-linkers to these telechelic materials can lead to thermally stable thermoset materials with improved properties when activated by high-temperature ring-opening reactions. This prior research on silicon

leads to a number of future opportunities.[127-129] An interesting possibility, so far not investigated with ADMET, is the use of siloxanes as pendant groups. Part of this dissertation will discuss siloxane branched polyethylene materials as modifiers of polyethylene surfaces. These materials could serve as industrial additives because of the differences in properties between polyethylene and polysiloxanes such as polarity, surface tension, and morphology.[130] Simple blending of polyethylene and polysiloxanes leads to phase separation.[131,132] Copolymerization leads to randomly placed siloxanes and therefore little to no control of the properties of the copolymer.[132,133]

Would precise placement of siloxane branches along the polymer chain allow us to overcome these problems? How would this affect the properties of the polymer obtained? Would it lead to well-defined structures? By finding the optimum pendant branch length and branch spacing, it may be possible to limit phase separation. These copolymers could include polyethylene run lengths in the backbone that may cocrystallize at the surface, thereby allowing polysiloxane branches to influence surface behavior, as shown in Figure 17.

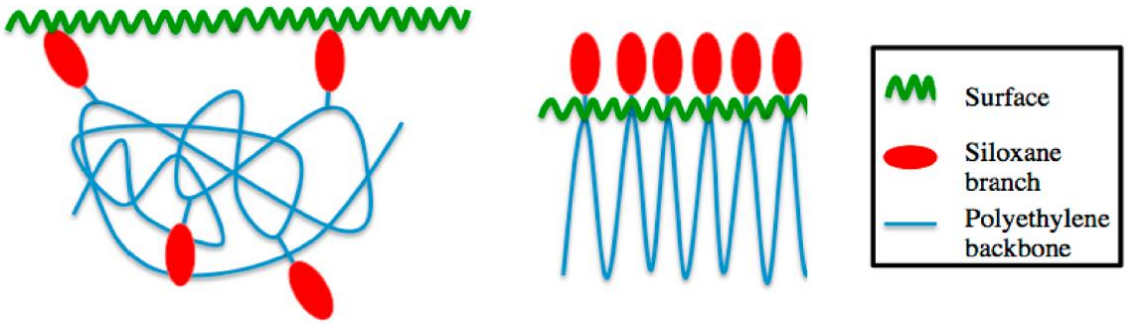


Figure 1-17. Random vs precise siloxane branches on polyethylene backbone.

These polymers would be useful additives for polymer extrusion where they can act as slip agents at the surface of the die, thereby reducing melt fracture in the finished material as explained in Section 1.3.[134]

**Fluorocarbon Additives for Surface Modification.** As already mentioned, fluorocarbons are known to act as slippery agents, reducing the defects observed during the extrusion of polyethylene.[40-42,135] Typical fluorocarbons however, present a number of technology disadvantages. Because of their small size, commercial fluorocarbons do not mix well with polyethylene. Consequently, they are used to coat the die of the extruder before the addition of polyethylene. This method is not efficient for large scale production, since it requires frequent interruption of the process to recoat the die. Another disadvantage of commercially available fluorocarbon additives for extrusion is their extremely high price. Using the same approach as for siloxane branched polyethylene, we would expect fluorocarbons additives to act similarly when mixed in with polyethylene being extruded. The technological application we propose allows the use of ADMET synthesized fluorinated polyethylenes as additives that will mix with polyethylene.

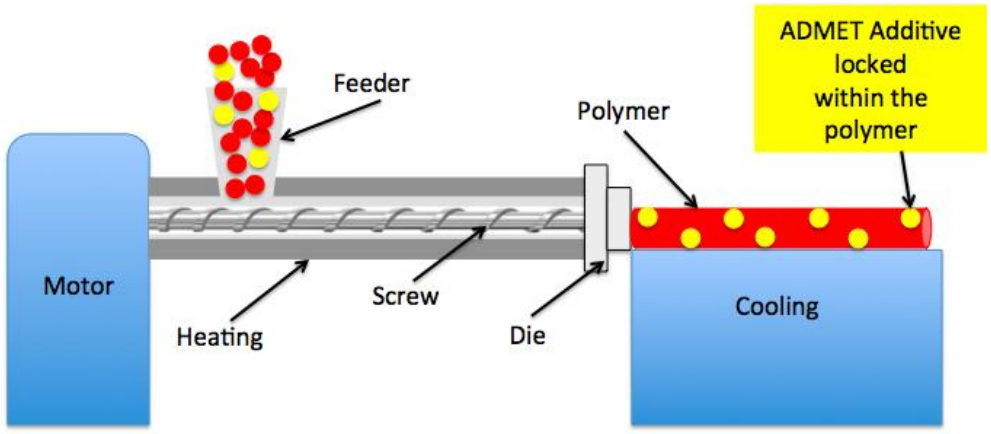


Figure 1-18. Extrusion process using fluorine branched polyethylene as an additive.

These polymers would be useful additives for polymer extrusion where they can act as slip agents at the surface of the die, thereby reducing melt fracture in the finished material as explained in Section 1.3.[134]

## 1.5 Dissertation Purpose

This dissertation describes the synthesis of siloxane precisely branched polyethylene via ADMET polymerization. The ultimate purpose of these polymers is for extrusion applications, but the synthetic challenges leading to those polymers are the focus of this dissertation. Chapter 2 discusses the various limitations and challenges that occurred and the steps that were taken to overcome them. The synthesis of the premonomers is also included in Chapter 2, and these premonomers form the core of the synthesis methods discussed in Chapters 3 and 4. The synthesis of siloxane branched polyethylene via Grignard reactions is examined in Chapter 3, while the synthesis of siloxane branched polyethylene via nucleophilic reactions is the focus of Chapter 4. In Chapter 5, a different approach is considered, and post polymerization functionalization is highlighted using hydrosilylation methods. Chapter 6 highlights the outcome of this project and various future opportunities, including the synthesis of polymers with dual fluorine/silicone branches.

# CHAPTER 2
# FUNCTIONAL POLYORGANOSILOXANES

## 2.1 Background

Polyorganosiloxanes, also referred to as silicones, are by far the most important hybrid polymer with an inorganic backbone and organic pendant group. At the beginning of the 20$^{th}$ century, Kipping and his coworkers confirmed the polymeric structure of siloxanes, but their focus remained in small molecules.[136] Commercial silicone products were delayed until 1940 because of a lack of convenient methods for monomer synthesis. In the later half of the 20$^{th}$ century applications of silicones expanded at a very rapid rate, and in 2003, commercial silicone products were available with world-wide sales reaching 10 billion dollars per year and growing.[137]

In the past 20 years, special attention has been given to siloxane-containing polymers because of the unique properties of the siloxane moieties, such as low glass transition temperature, low surface energy, hydrophobicity and high thermal and oxidative stability due to the flexibility of the Si-O backbone.[138-141] With the rising demand for materials with high performance and multiple functionalities, traditional polysiloxanes became insufficient,[142] and extensive research was directed towards silicon/carbon hybrid materials for applications in fields such as biomaterials, coatings, fibers, electronic devices, personal care, packaging and nanomaterials.[14,135,143] Table 2-1 shows the various silicone technologies available and their common industrial applications.

Table 2-1. Silicone technology and its industrial applications

| Silicone Technology | Industrial Application |
|---|---|
| Elastomers | Baby bottles nipples |
| Defoamers | Food - Beer |
| Coatings | Post-it - Cooking utensils - Mold release agents |
| Fluids and Lubricants | Greasing needles |
| Personal Care Products | Deodorants |
| Medical Products | Implants - Catheters - Pacemaker |

Commonly used methods to enhance polymers' physical and chemical properties and to modify their structures include blending and copolymerization. Polymer blending involves physically mixing two or more polymers, leading to a material that is modified on a macromolecular level and that possesses new properties.[130,144,145] Copolymerization on the other hand involves modifications at a micromolecular level, by reacting two or more monomers with each other, leading to a chemical linkage between them.[146,147]

Blending of polysiloxanes with organic polymers is ineffective because of the extremely non-polar nature of polysiloxanes, leading to immiscibility issues and macromolecular phase separation between siloxane and organic systems.[130,148] In some cases, a surfactant referred to as compatibilizer is mixed with the polysiloxane and the organic polymer in order to improve the adhesion between the two immiscible phases, thereby leading to more thermodynamically stable blends.[148,149] There are many drawbacks to this method, however, most notably the tendency of the compatibilizers to form micelles instead of stabilizing the interface.[150] Because of the disadvantages related to blending, research has been oriented towards chemically grafting polysiloxanes onto the organic polymers leading to copolymers. The formation of covalent linkages between the siloxane block and the organic block relies on the

successful and efficient introduction of reactive functional groups into the siloxane side chains.

## 2.2 Silicones with Reactive Functionalities

As mentioned above, the interest in polysiloxanes have been growing, and tremendous developments have been achieved. Unfortunately, the results of search of the literature via Scifinder (Figure 2-1), revealed a large disparity between the number of publications related to the synthesis of polysiloxanes versus the number of publications concentrating on the silicone functionalization. The low publication numbers related to silicon functionalization are surprising, in light of “Organosilicon Compounds”, published in 1960, in which Eaborn predicted the need for organosilicon polymers: “There will probably be important developments in the next decade in specialized uses of silicone-containing carbon-functional organic groups”,[151] and a similar statement in 1968 in “Chemistry and Technology of Silicones” by Noll: “ The most recent trend in monomer research is toward the organofunctional silanes. This appears particularly hopeful, since it would offer the possibility of a bridge between organosilicon chemistry and pure organic chemistry.”[152]

This low number of publications related to silicone functionalization is due to the relatively easy and well established synthetic methods for polysiloxanes, such as ring opening polymerization of cyclosiloxanes,[142] as well as condensation and hydrosilylation[148,153,154] of available silanes. Unfortunately, the development of novel copolymerization methods has been a major challenge.[155] Although it may not be 100% accurate, Figure 2-2 gives a good idea of the reactions that have been commonly used in the past 33 years for the development of hybrid organosilicones, with the most widely

applied methods being hydrosilylation and alcoholysis reactions.[1] These reactions will be discussed thoroughly in this dissertation.

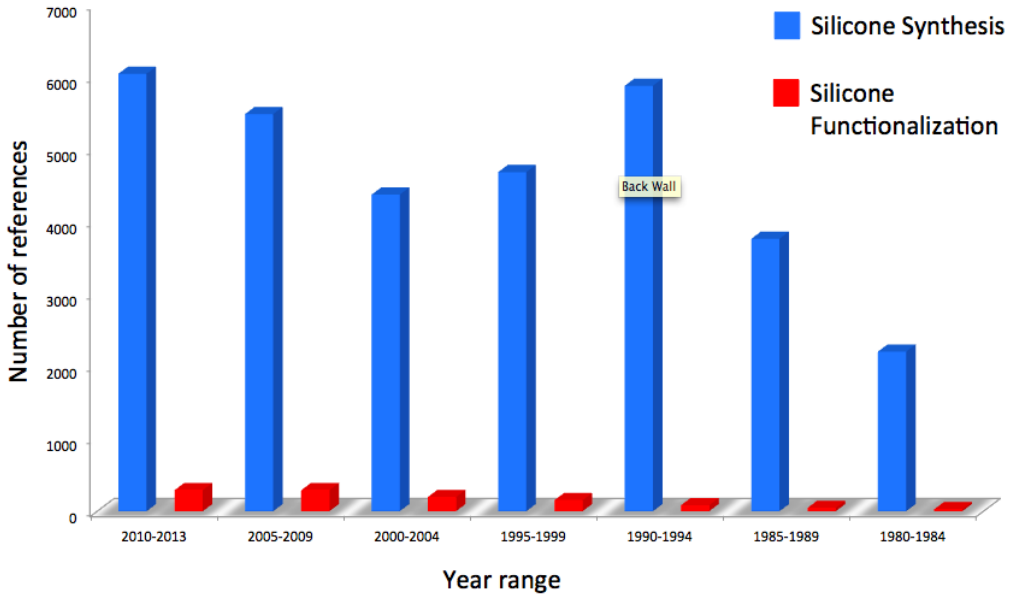


Figure 2-1. Silicone synthesis publications (blue) vs silicone functionalization publications (red) over the past 33 years (as of September 2013).

Recently, research attention has been focused on the development of efficient approaches for the synthesis of novel reactive α,ω-telechelic polysiloxanes[156] as starting materials of intermediates for the synthesis of copolymers for specialty applications. The choice of the terminal functional groups is the key factor that determines the reactivity of these monomers towards other reactants. The various available functional monomers and their utility are discussed in the following sub-sections.

[1] These numbers were obtained using the refine option in Scifinder for the publications gathered for Figure 2-1.

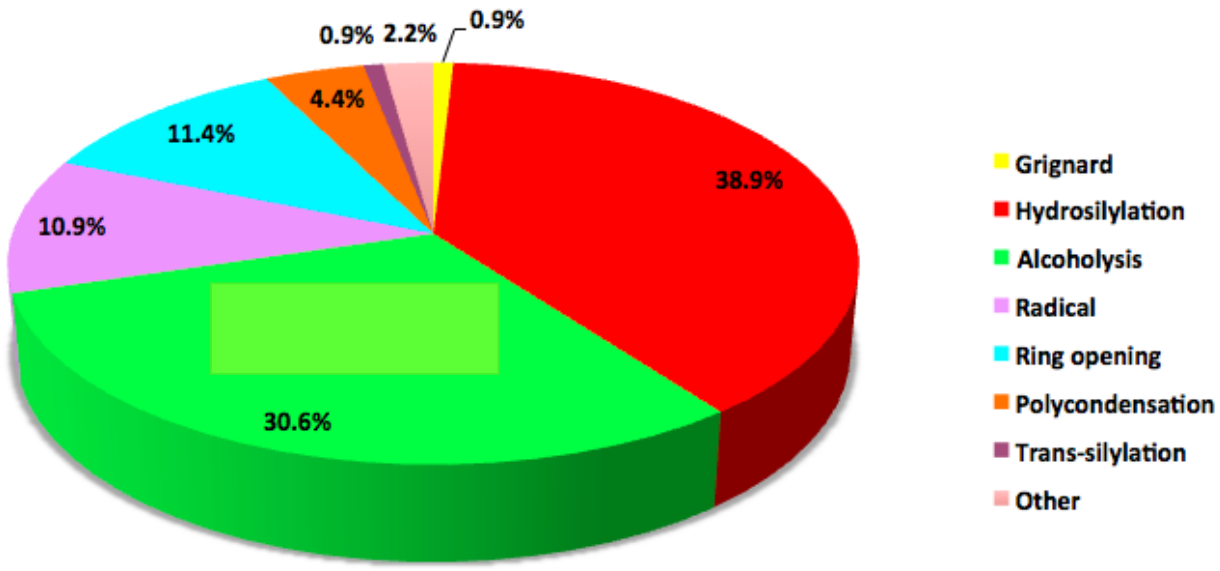


Figure 2-2. Reactions commonly used for the functionalization of silicones.

### 2.2.1 Functional Group Directly Bonded to Silicon

The first group of functionally terminated siloxanes that were made available were α,ω-difunctionally terminated with (Si-X) end groups, with X as the reactive moiety. The importance given to these compounds is due to their higher reactivity towards nucleophilic reagents in comparison to (C-X) functionally terminated compounds. This higher reactivity is due to the difference in electronegativity between silicon and carbon, which makes the Si-X bond more polar and more ionic than the C-X bond, allowing easier substitution at the silicon. Table 2-2 summarizes the various commercially available functionalized siloxanes and their applicable reactions.

Unfortunately, due to their high reactivity, many of these precursors are unstable in presence of moisture, alcohols or acids. Another drawback is that most of these siloxanes, when reacted with other monomers, will generally form a weak Si-O-C linkage, which can be easily broken in the presence of water or acid.

Table 2-2. Main α,ω-difunctionally terminated siloxanes and their synthetic uses

| Reactant | Reactive group | Type of Reaction | Catalyst |
|---|---|---|---|
| 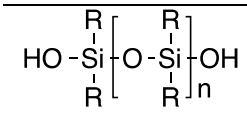 | -OH | Alcoholysis<br>Polycondensation | Pt, Tin carboxylates<br>Pyridine, imidazole |
| 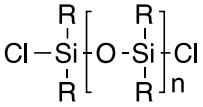 | -Cl | Polycondensation<br>Grignard | Copper, pyridine |
| 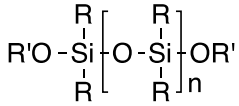 | -$OCH_3$, -$OC_2H_5$ | Grignard | Mg |
| 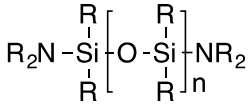 | -$NH_2$, -$N(CH_3)_2$ | Polycondensation | Pyridine, imidazole |
| 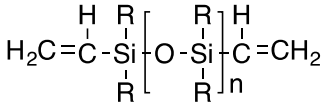 | -$CH=CH_2$ | Hydrosilylation<br>Peroxide activated cure | Pt<br>RO• |
| 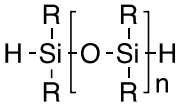 | -H | Hydrosilylation<br>Dehydrogenative Coupling | Pt,Rh, Pd…<br>Tin, Zinc or Iron salt catalysts |

To circumvent these issues a second group of functionally terminated silicones was developed and is discussed in the next paragraph.

### 2.2.2 Functional Groups Bonded to Carbon Linkages

To overcome the issues related to Si-X terminated siloxanes, precursors have been synthesized with organofunctional groups such as (Si-R-X), in which R is a hydrocarbon and X is the reactive group. A few examples of such reactive precursors is given in Table 2-3.

Table 2-3. α,ω-difunctionally terminated organosiloxanes; R can be alkyl, aryl or aralkyl.

| Precursor | X |
|---|---|
| 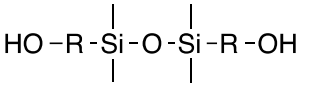 | -OH |
| 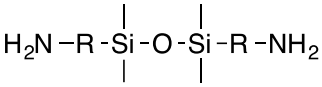 | -$NH_2$ |
| 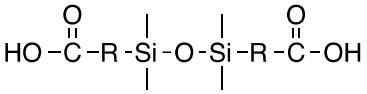 | -COOH |
| 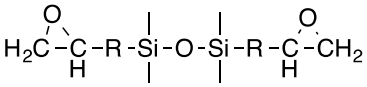 | 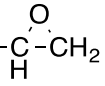 |
| 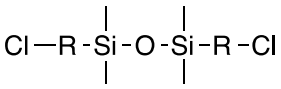 | -Cl |

Because the compounds shown in Table 2-3 are less reactive than their (Si-X) analogues, they are more resistant to moisture and undesired side reactions, leading to easier handling and longer shelf-life. In this dissertation, both types of precursors are used in order to establish the most suitable methods for the addition of the silicon branch to the α,ω-diene premonomers.

### 2.3 Synthetic Background of Diene Premonomers

The synthesis of precisely branched polyethylene depends on the ability of the Wagener group to synthesize symmetrical α,ω-dienes, since the symmetrical nature of the monomers controls the microstructure of the polymer.

The syntheses of alcohol and bromine functionalized diene precursors were developed by Baughman[157] and are commonly used within the group. These functionalized diene precursors are reacted with various functionalized siloxanes for the

preparation of the siloxane branched α,ω-dienes. The first step of this method is the synthesis of the alkenyl bromide in Figure 2-3 required for further reaction. The alkenyl bromide **(1-2)** can be obtained via bromination of the alcohol **(1-1)** with carbon tetrabromide and triphenyl phosphine. Purification of **(1-2)** is done via column and distillation. Isomerization of the alkene functionality is not acceptable, as it could lead to imprecisions in the polymer backbone. For this reason, it is important to use vacuum distillation, since this reduces the distillation temperatures, which could otherwise cause isomerization.

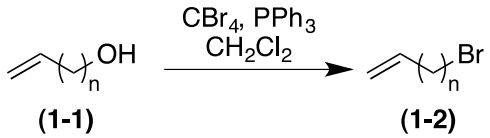


**(1-1)** **(1-2)**

Figure 2-3. Synthesis of alkenyl bromide.

Figure 2-4 shows the general synthetic scheme for the preparation of the primary alcohol and primary bromide premonomers. Alkenyl bromide **(1-2)** is reacted with deprotonated diethylmalonate via two consecutive $S_n2$ reactions, and the reaction is refluxed overnight. The reaction is closely monitored by thin layer chromatography (TLC), and excess sodium hydride (NaH) and alkenyl bromide are used to force the reaction to completion yielding only dialkylated malonate ester. NaH is slowly neutralized with water and the diester is saponified with excess potassium hydroxide (KOH) in a mixture of ethanol and water and refluxed overnight to yield a diacid. The diacid is then reacted with 1,1'-carbonyldiimidazole (CDI) at room temperature resulting in a clean and quantitative formation of the monoacid within 3 hours. The pure white solid monoacid is obtained by recrystallization from pentane. The acid is then reduced to the corresponding alcohol **(1-3)** using lithium aluminum hydride (LAH) in THF. If used

as premonomer, the pure alcohol **(1-3)** is obtained via column chromatography as a colorless oil; otherwise, it is brominated with carbon tetrabromide and triphenyl phosphine to produce premonomer **(1-4).** Premonomer **(1-4)** is purified via column chromatogragphy using n-hexanes.

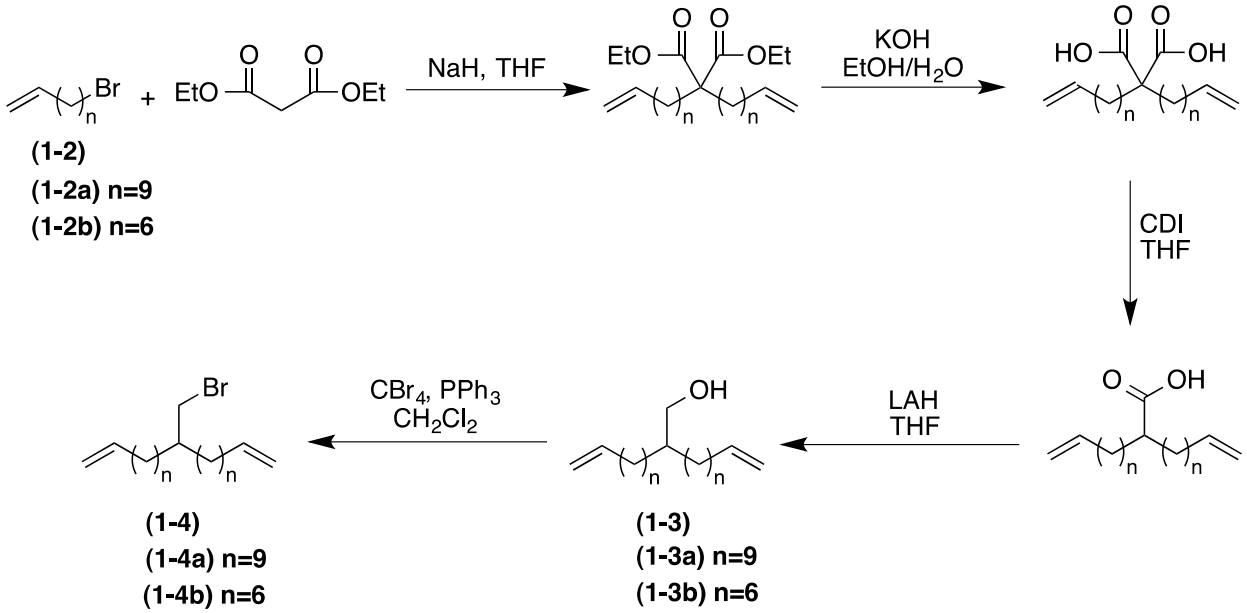


Figure 2-4. Alcohol and bromine diene premonomer synthesis.

These premonomers are further reacted in order obtain siloxane branched monomers, discussed throughout the dissertation.

## 2.4 Experimental

### 2.4.1 Materials and Instrumentation

All materials were purchased from Aldrich and used without further purification unless noted. Anhydrous solvents were obtained from an anhydrous solvent system. $^{1}H$ NMR and $^{13}C$ NMR were recorded in $CDCl_3$ on a Varian Mercury 300MHz spectrometer. $^{1}H$ and $^{13}C$ chemical shifts were referenced to residual signals from $CDCl_3$ ($^{1}H$=7.24 ppm and $^{13}C$=77.23 ppm). Elemental analyses were carried out by Atlantic Microlab, Inc.

### 2.4.2 Procedures

**11-Bromo-1-undecene (1-2a):** 10-Undecene-1-ol (100.00 g, 587 mmol) and carbon tetrabromide (214.63 g, 646 mmol) were dissolved in 500mL of dichloromethane in a 1L round-bottom flask equipped with a stir bar. After the mixture was chilled to 0°C, triphenylphosphine (169.42 g, 646 mmol) was slowly added on ice and the solution turned orange. The reaction was allowed to stir overnight at room temperature under argon. Dichloromethane was evaporated yielding a solid precipitate of triphenylphosphine oxide and the unpure product. The solid was removed by filtration, and the filtrate was passed through a silica plug to remove the remaining triphenylphosphine oxide. The collected product was a mixture of bromoform and the desired 11-bromo-1-undecene. The bromoform was removed by vacuum distillation. Yield: 93%; $^{1}$H NMR (300 MHz, $CDCl_3$): δ= 1.50-1.20 (m, 12H), 1.92-1.80 (m, 2H), 2.10-2.00 (m, 2H), 3.45-3.35 (t, 2H), 5.05-4.85 (m, 2H), 5.9-5.7 (m, 1H).

**2-(Undec-10-enyl)tridec-12-enoic acid:** To a flame dried 1L three-necked round-bottom flask equipped with a stir bar and addition funnel was added NaH (21.59 g, 540 mmol, 60% in oil) and 500 mL of THF. After 11-bromo-1-undecene (93 g, 401 mmol) was added to the white slurry, the reaction was allowed to stir on ice for 30 minutes. Then, diethyl malonate (29.17 g, 182 mmol) was added dropwise over 30 minutes. The reaction was allowed to stir for one hour at room temperature and at reflux for an additional day. The reaction was monitored by TLC using a 9:1 hexane: ethyl acetate as the mobile phase. More NaH and 11-bromo-1-undecene were added to the reaction, which was refluxed until the monoalkylated product had completely disappeared. The reaction was then cooled in an ice bath and slowly neutralized with 1M HCl. The reaction mixture was then extracted with ether, and the ether was removed

under reduced pressure. The recovered oil was then dissolved in a mixture of water (250 mL) and ethanol (125 mL). KOH (60.65 g, 1516 mmol) was added to the solution and the reaction was refluxed overnight. The reaction mixture was chilled in an ice bath, neutralized with concentrated HCl, and extracted with ether. The ether was removed under vacuum and the diacid crude was dissolved in a 500 mL round-bottom flask equipped with a stir bar and charged with 200 mL of dry THF. 1,1'-Carbonyldiimidazole (35.57 g, 219 mmol) was added to the reaction flask over the course of 30 minutes. Instant bubbles were observed due to the decarboxylation occurring. The reaction was allowed to stir at room temperature for 3 hours, after which 64 mL of an aqueous solution of NaOH (11.95 g, 298.64 mmol) was added in one portion and the reaction was allowed to stir for an hour at room temperature. The reaction was then concentrated under vacuum and 400 mL of a 2N HCl was added to the reaction residue. The solution was then extracted twice in $CH_2Cl_2$ and concentrated to yield 12.6 g of a white solid. Yield: 17.23%; $^{1}$H NMR (300 MHz, $CDCl_3$): δ= 5.82 (m, 2H), 4.98 (m, 4H), 2.08 (q, 4H), 2.06 (q, 4H), 1.63 (m, 4H), 1.55-1.20 (br, 28H), $^{13}$C NMR (75 MHz, $CDCl_3$): δ= 183.14, 139.44, 114.31, 45.75, 34.03, 32.37, 29.77, 29.75, 29.68, 29.34, 29.15, 27.58.

**2-(undec-10-enyl)tridec-12-en-1-ol (1-3a):** To a 500 mL three-necked round-bottom flask equipped with a stir bar was added 250 mL of THF to which was added $LiAlH_4$ (5.8 g, 137 mmol) via a powder funnel. The solid 9,9-acid (12.6 g, 35 mmol) was dissolved in a minimal amount of THF and added to the slurry on ice over 30 minutes. The reaction was placed under Ar and left to stir at room temperature for 24 hours. The reaction was quenched on ice with water and acidified with concentrated HCl, followed

by extraction with diethyl ether. The organic layer was washed with brine, then dried over $MagSO_4$ and concentrated to a light yellow oil. The product was purified by flash column chromatography using a 9:1 hexane: ethyl acetate mobile phase yielding 11.2 g of the desired primary alcohol. Yield: 92.41%; $^{1}H$ NMR (300 MHz, $CDCl_3$): δ= 5.80 (m, 2H), 4.98 (m, 4H), 3.54 (d, 2H), 2.02 (q, 4H), 1.4 (m, br, 33H). $^{13}C$ NMR (75 MHz, $CDCl_3$): δ= 139.21, 114.13, 65.61, 40.57, 33.88, 30.98, 30.14, 29.67, 29.57, 29.20, 28.99, 26.94, 15.25.

**12-(bromomethyl)tricosa-1,22-diene (1-4a):** The same bromination procedure was followed as outlined in the synthesis of 11-bromo-1-undecene. **(1-3a)** (11.2 g, 31.94 mmol) and carbon tetrabromide (11.65 g, 35.14 mmol) were dissolved in 250mL of dichloromethane in a 500 mL round-bottom flask equipped with a stir bar. The mixture was chilled to 0°C. Triphenylphosphine (9.22 g, 35.14 mmol) was slowly added on ice and the solution turned orange. The reaction was allowed to stir overnight at room temperature under argon. Dichloromethane was evaporated yielding a solid precipitate of triphenylphosphine oxide and the unpure product. The solid was removed by filtration, and the filtrate was passed through a silica plug to remove the remaining triphenylphosphine oxide. The collected product was a mixture of bromoform and the desired 12-(bromomethyl)tricosa-1,22-diene. The bromoform was removed via flash chromatography in hexanes and 11.5 g of the product **(1-4a)** was isolated. Yield: 87%; $^{1}H$ NMR (300 MHz, $CDCl_3$): δ= 5.80 (m, 2H), 4.98 (m, 4H), 3.45 (d, 2H), 2.06 (m, 4H), 1.55 (m, 1H), 1.33 (m, br, 32H). $^{13}C$ NMR (75 MHz, $CDCl_3$): δ= 139.26, 114.30, 39.97, 39.83, 34.08, 30.07, 29.87, 29.80, 29.37, 29.18, 26.84.

CHAPTER 3
SILICON BRANCHED POLYMERS WITH Si-C LINKAGES

## 3.1 Overview

Chlorosilicones constitute a major part of the reactive and commercially available silicones. The high reactivity of the Si-Cl bond makes it a suitable compound to undergo Grignard reactions. This increased reactivity is due to the significant difference in the length of the Si-Cl bond in comparison with the C-Cl bond as shown in Table 3-1.

Table 3-1. Comparison of Si-Cl and C-Cl bonds[158,159]

| Bond | Bond Strength (kJ/mol) | Bond Length (Å) |
|---|---|---|
| Si-Cl | 472 | 2.05 |
| C-Cl | 335 | 1.78 |

The advantage of using Grignard reactions for the synthesis of our monomers is that the terminal alkenes of the α,ω-diene precursor remain intact with no isomerization. However, there are several drawbacks linked to this method. Since most of the chlorosiloxanes available are bifunctional, the first challenge is the production of monosubstituted products while limiting the formation of disubstituted product, as shown in Figure 3-1.

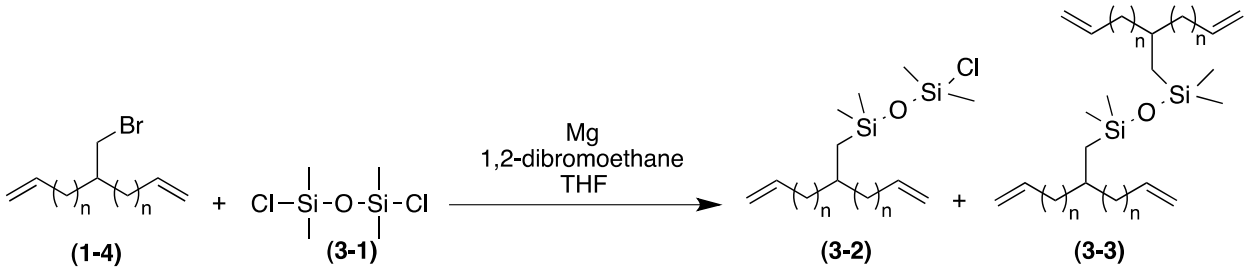


Figure 3-1. Grignard reaction with bifunctional siloxane.

The sequence of addition of reagents is a determining factor in limiting the production of the disubstituted product **(3-3)**. For full substitution of the chlorosiloxane, a "normal" addition is performed, in which the chlorosiloxane is added directly to the Grignard reagent. Since we are targeting the partial substituted product **(3-2)**, "reverse" addition is used, with the Grignard added to the chlorosiloxane solution.[160]

The second challenge involves purification of the products and the removal of undesired corrosive and hydrolytically sensitive by-products.[160] On the monosubstituted desired product **(3-2),** the Si-Cl bond can undergo hydrolysis in the presence of water or moisture producing corrosive HCl and crosslinking with another monomer as shown in Figure 3-2.

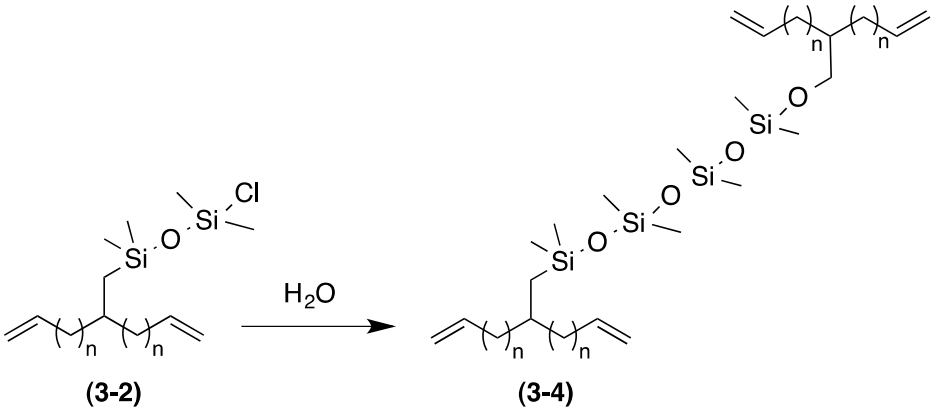


Figure 3-2. Hydrolysis of the reactive monosubstituted monomer **(3-2)**.

Another important factor to consider during Grignard reactions is the miscibility of the Grignard reagent with the substrate solution. To favor the monosubstituted product **(3-2)**, the reaction of the chlorosiloxane with the Grignard reagent must be slow. The rate can controlled by adjusting the concentration of the Grignard solution.[161]

Understanding the substitution reactions of the Si-Cl bonds and the proper reaction conditions is the first step to successfully synthesizing the siloxane branched diene monomers.

## 3.2 Results and Discussion

### 3.2.1 Grignard model study

Since the synthesis of diene bromide **(1-4)** described in Chapter 2 requires several steps, the reaction was modeled by using structurally similar 11-bromo-1-undecene **(3-5)**, with 1,3-dichloro-1,1,3,3-tetramethyldisiloxane **(3-1)**. This model reaction is illustrated in Figure 3-3.

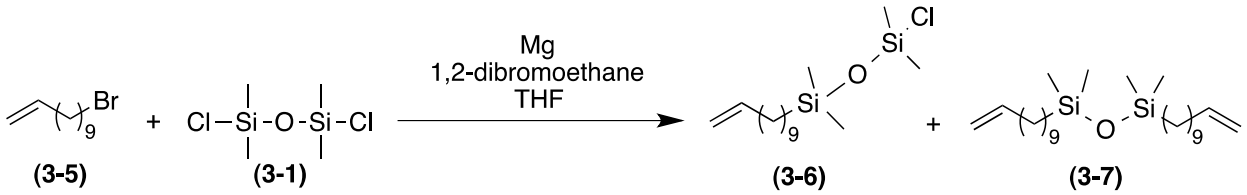


Figure 3-3. Model Grignard reaction.

The magnesium turnings were stored in the oven overnight to avoid moisture, and 1,2-dibromoethane was used to clean the surface of the magnesium and activate it via a process called entrainment.[162,163] The reverse addition method was used for these reactions in order to limit formation of the undesired product **(3-7)**. Once the Grignard reagent was formed, it was added dropwise to a round-bottom flask containing a solution of chlorosiloxane in excess **(3-1)**.

Even though **(3-1)** was used in excess, both the monosubstituted **(3-6)** and the disubstituted **(3-7)** products were formed. Instead of showing two sharp peaks for $Si(CH_3)_2Cl$ observed in **(3-6)** and $Si(CH_3)_2O$ common to both compounds **(3-6)** and **(3-7)**, these peaks overlapped on the $^1H$ NMR spectrums and a broad peak was observed

between 0.05ppm and 0.2ppm. The presence of both compounds was confirmed by $^{13}C$ NMR, with three different signals for the carbons bonded to the silicon as shown in Figure 3-4.

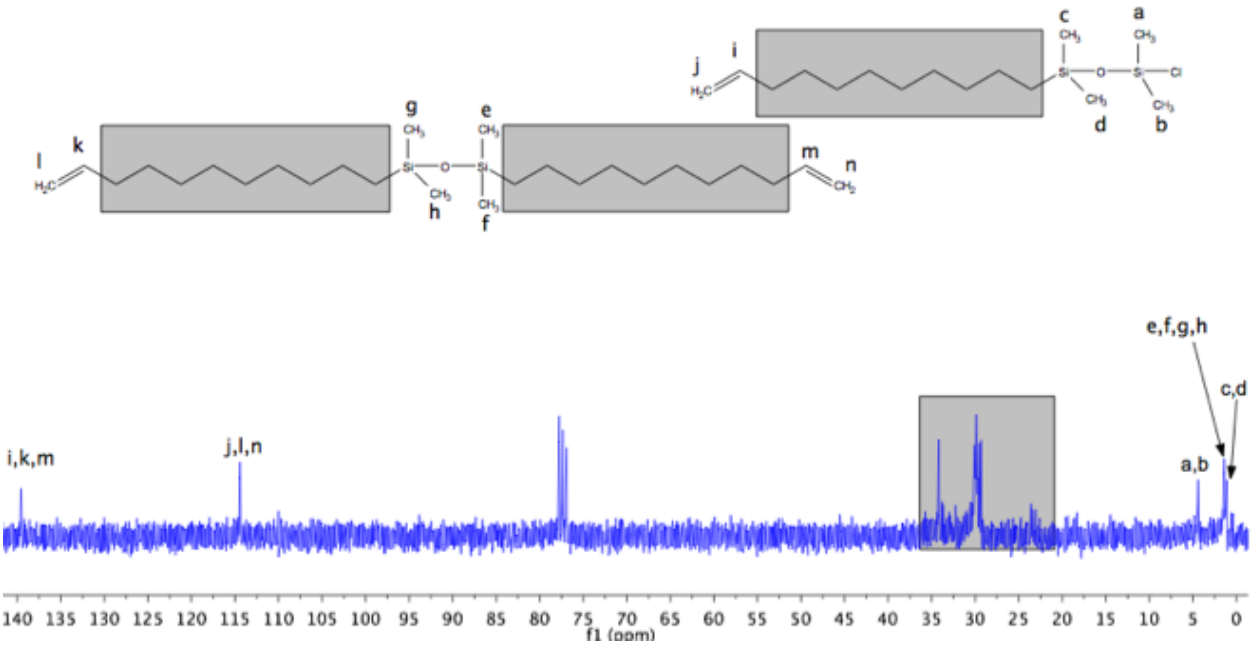


Figure 3-4. $^{13}C$ NMR of monosubstituted **(3-6)** and disubstituted **(3-7)** 1,3-dichloro-1,1,3,3-tetramethyldisiloxane.

Separation of compounds **(3-6)** and **(3-7)** was attempted, but the tethered chlorosiloxane end group of **(3-6)** lead to further reactions that could not be controlled, making the isolation of the monosubstituted **(3-6)** impossible. Therefore, an alternative method for the addition of the siloxane branch was pursued.

### 3.2.2 Step addition of the siloxane branch

Since the expected challenges related to using bifunctional siloxanes occurred, we reverted to using the step addition reaction shown in Figure 3-5, which would allow control of the length of the siloxane branch. The first step involves reacting an excess Grignard with dichloromethylsilane to form a stable carbon-silicon bond. The hydrogen

terminated silane monomer **(3-9)** shown in Figure 3-5 can be further oxidized to the corresponding Si-OH. The resulting silanol functionalized monomer **(3-10)** shown in Figure 3-5 can then be used for a selective Si-OH/Cl coupling. These two steps can be repeated to achieve the required branch length and terminated by coupling with a chlorotrimethylsilane or with another functional silane. Although this step-wise method has been described by Masamune[164] for saturated organosilicons, it has never been used with unsaturated compounds. This method has the advantage of leading to a disubstituted product by using an excess of magnesium and 11-bromo-1-undecene **(3-5).** Therefore little purification of the final product would be required allowing a direct addition of the substrate to the reaction.

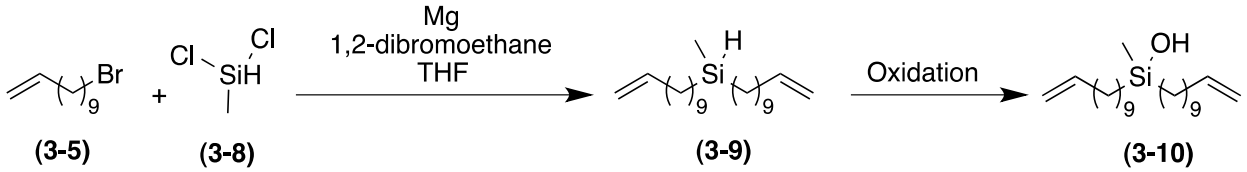


**(3-5)** **(3-8)** **(3-9)** **(3-10)**

Figure 3-5. Stepwise addition of the siloxane branch.

The 11-bromo-1-undecene **(3-5)** was reacted with a solution of Mg and 1,2-dibromoethane in THF to form a Grignard reagent. Dichloromethylsilane **(3-8)** was then added to the solution, and the substitution reaction took place to form compound **(3-9).** The NMR showed the presence of impurities that were removed by distillation in the Kugelrohr at 120°C under vacuum ($10^{-3}$Torr).

Pure compound **(3-9)** was then oxidized by three different methods in the attempt to synthesize compound **(3-10)**. These methods previously published are shown in Figure 3-6.[164-167]

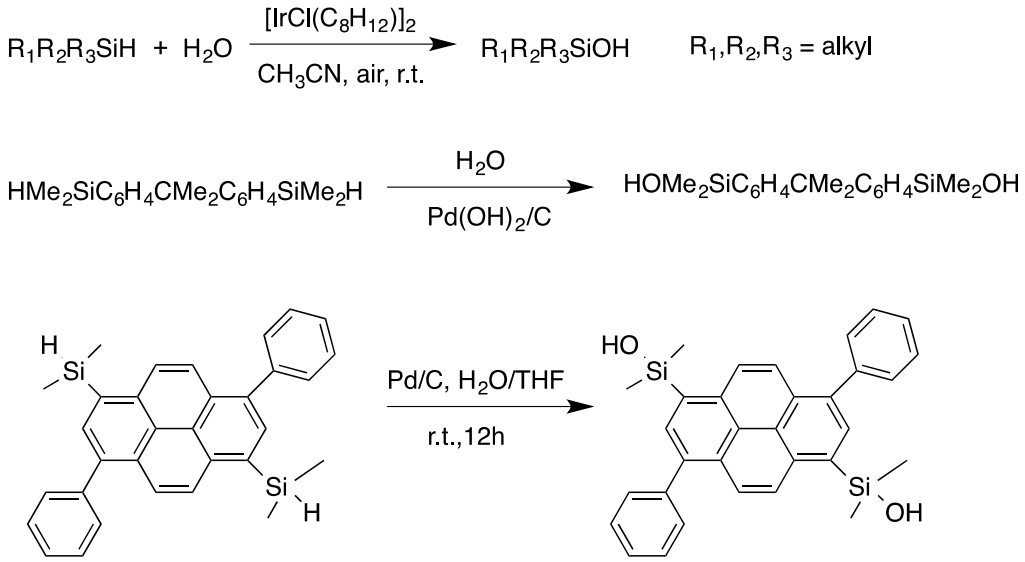


Figure 3-6. Oxidation reactions.[164-167]

The reaction conditions were slightly modified from the published conditions in order to solubilize the diene **(3-10)**. The conditions and yields are shown in Table 3-2.

Table 3-2. Oxidation of silane

| Catalyst | Mol% | Solvent | Yield (**3-10**)[a] |
|---|---|---|---|
| $[IrCl(C_8H_{12})]_2$ | 1 | $CH_3CN$, $H_2O$ | 17% |
| $Pd(OH)_2/C$ | 1 | THF, $H_2O$ | 0% |
| Pd/C | 5 | THF, $H_2O$ | 0% |

a. The yield was determined via $^1H$ NMR.

**Iridium catalyzed oxidation:** The silane pre-monomer **(3-9)** (1 eq.) was dissolved in acetonitrile (10 mL), to which was added the Iridium catalyst (0.01eq.) and water (2eq.). The reaction was stirred under air for 2 h at room temperature. The organic layer was extracted from the water and evaporated. The $^1H$ NMR peak at 3.6ppm in Figure 3-7 confirmed the presence of the starting material **(3-9)**. This peak integrated to 0.85 relative to the internal hydrogens of the diene, therefore allowing us to

determine the yield of the reaction. The Iridium catalyzed oxidation of **(3-9)** yielded 17% of the silanol **(3-10)**.

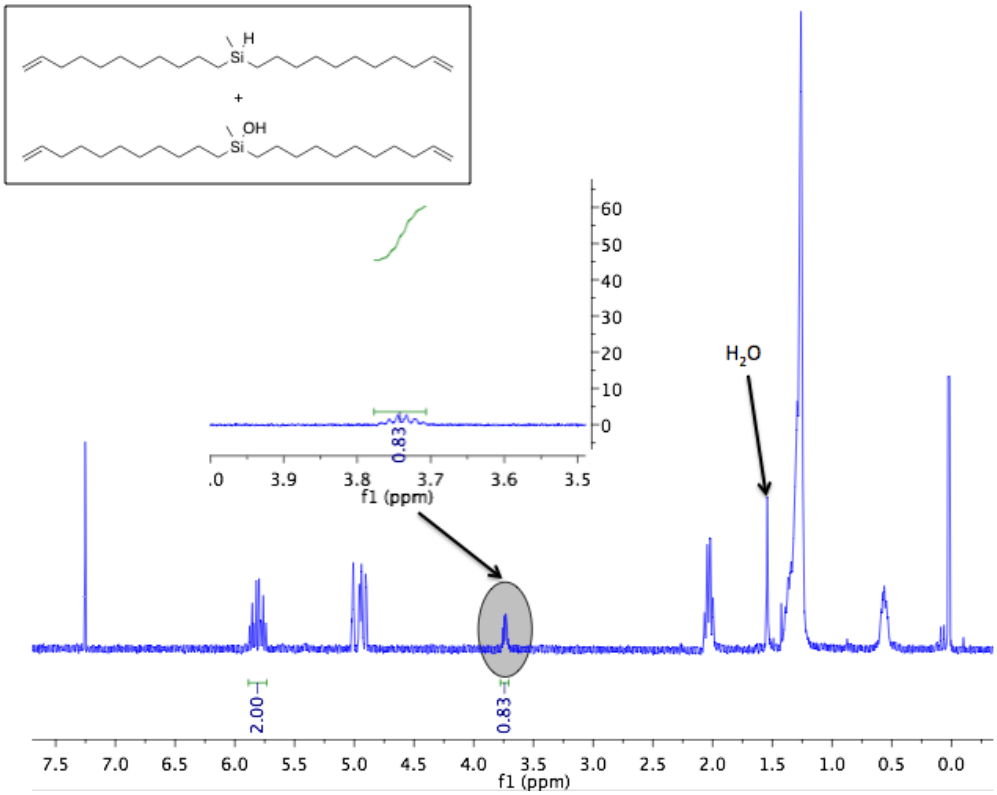


Figure 3-7. $^{1}$H NMR of Iridium catalyzed oxidation.

The presence of both **(3-9)** and **(3-10)** was observed in the IR spectrum shown in Figure 3-8, and the synthesis of **(3-10)** was confirmed by Mass Spectrometry as well. Attempts to isolate the silanol product via distillation led to crosslinking and with the sample changing from a clear oil to a viscous yellow product.

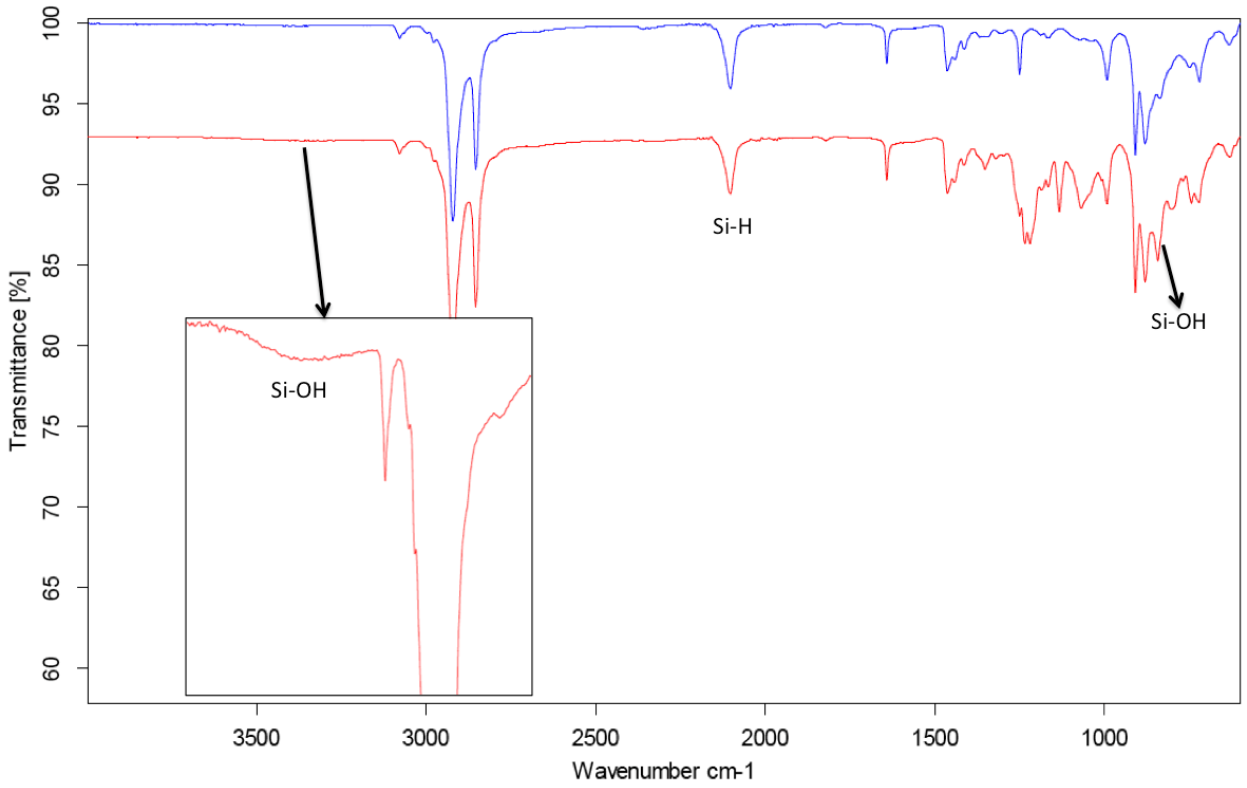


Figure 3-8. FT-IR of **(3-9)** (blue) and the product (red) of the Iridium oxidation.

**Pearlman's catalyzed oxidation:** Pearlman's catalyst ($Pd(OH)_2/C$) has been used for the oxidation of silanes. The silane pre-monomer **(3-9)** was slowly added to an ice-cooled suspension of Pearlman's catalyst (20 mg) in THF (50 mL) and water (5 mL). Evolution of hydrogen was observed, and the reaction mixture was stirred at room temperature for 1 hour after the hydrogen evolution had ceased. The catalyst was removed by filtration and the solvent was removed under reduced pressure. Then a regular work up in ether was performed yielding a clear oil. The silane hydrogen peak of compound **(3-9)** observed at 3.6 ppm completely disappeared by $^1H$ NMR. However, even though mild conditions were used (limited amount of hydrogen and no heat), partial reduction of the terminal double bond was observed at 5.9ppm and 5.1ppm, and

a triplet appeared at 0.85ppm, which is representative of methyl hydrogens. The formation of **(3-10)** was not observed using mass spectrometry.

**Palladium-on-activated-charcoal catalyzed oxidation:** Another method for the oxidation of silanes is by using palladium-on-activated-charcoal (Pd/C). The silane pre-monomer **(3-9)** was dissolved in 20mL of THF and was added to a mixture of 5% palladium-on-charcoal in a mixture of THF (5mL) and water (13mL) at room temperature. The reaction mixture was stirred for 12 h at room temperature, after which the catalyst was removed by filtration through Celite. The filtrate was concentrated under reduced pressure prior to completing a regular work up. In this case, in addition to the disappearance of the silane hydrogen peak at 3.6 ppm, the complete disappearance of the terminal double bonds was observed as well. This observation is not surprising, as there have been records of silanes used as sources of hydrogen for the reduction of alkynes and alkenes in presence of palladium-on-charcoal catalyst at room temperature; an example is shown in Figure 3-9.[168] The hydrogen required for the reduction of the double bonds is produced in situ by addition of the silane to the palladium catalyst, with subsequent rapid and efficient reduction of the double bond. The reaction times reported for this process are much faster than those for the oxidation reactions, making the reduction likely to occur.

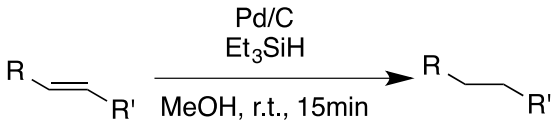


Figure 3-9. Alkene reduction with triethylsilane.[168]

Since the oxidation attempts on the silane **(3-9)** were unsuccessful, the stepwise addition of the silicone branch was abandoned, and other routes were investigated.

### 3.2.3 Grignard addition using monofunctional siloxane

Because none of the methods mentioned earlier were successful for the synthesis of the the α,ω-diene monomer, other options were explored. Trimethylchlorosilane, which is a monofunctional readily available chlorosilane, was reacted in the presence of a Grignard diene as shown in Figure 3-9.


**(1-4a)** **(3-11)** **(3-12)**

Figure 3-10. Grignard reaction using monofunctional chlorotrimethylsilane

The first attempt to synthesize **(3-12)** was performed by reacting **(1-4a)** with Mg and 1,2-dibromoethane in THF to form the Grignard reagent. After allowing the reaction to reflux overnight, an excess of **(3-11)** was added dropwise to the reaction flask at 0°C. After all the chlorosilane was added, the reaction was heated and allowed to reflux overnight. The reaction was washed several times with hexanes and the salts were removed by Celite filtration. Proton NMR of the product obtained showed the presence of **(3-12)** in addition to impurities. One of the impurities was identified as the methyl branched diene indicated by the presence of the methyl hydrogen peaks at around 0.85 ppm. Thus, we can conclude that the reaction did not go to completion, and compound **(3-13)** shown in Figure 3-11 was formed.

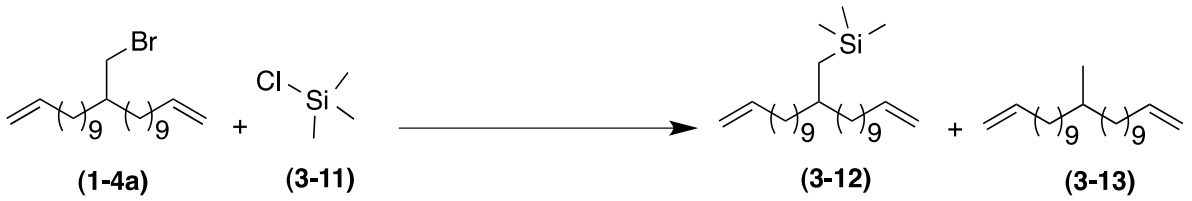


Figure 3-11. Grignard reaction products

The second impurity had a low boiling point under vacuum and was isolated via distillation in the Kugelrohr. Its $^{1}H$ NMR is shown in Figure 3-12.

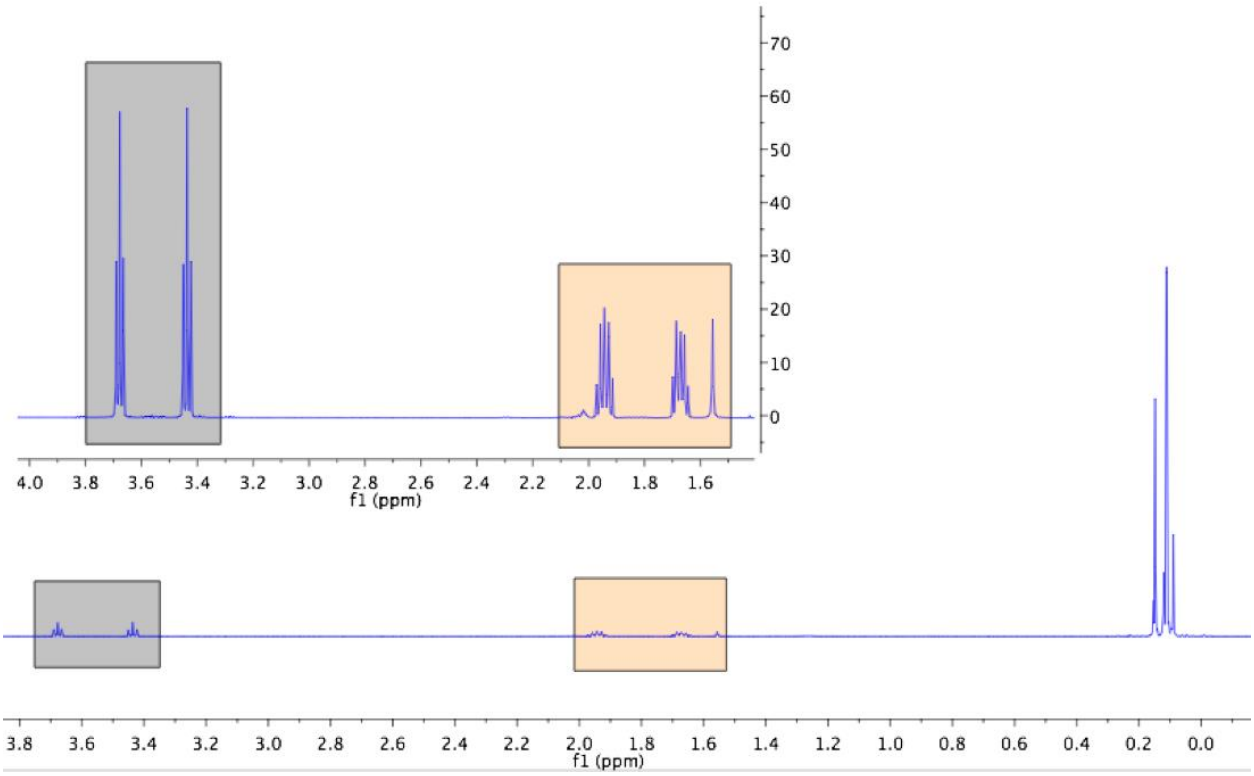


Figure 3-12. $^{1}H$ NMR of impurity

The peaks at around 3.4 ppm and 3.7 ppm are those of hydrogens adjacent to oxygens. However, since two different shifts are observed, there must be two types of oxygens in the molecule. The peaks at around 2.0 ppm and 1.7 ppm also confirm this conclusion.

A 2D Gradient Heteronuclear Multiple-Bond Correlation (gHMBC) NMR experiment shown in Figure 3-13 allowed us to better understand that the source of this impurity was due to a reaction involving THF. HMBC experiments allow the detection of carbon-to-hydrogen connectivity over 2-4 bonds, indicated that the impurity was formed from the reaction of the chlorosilane with THF. This can be explained by the presence of excess Mg and the direct addition of the trimethylchlorosilane**(3-1)** to the Grignard solution, which led to formation of the $(CH_3)_3SiMgCl$ Grignard which then further reacts with THF.

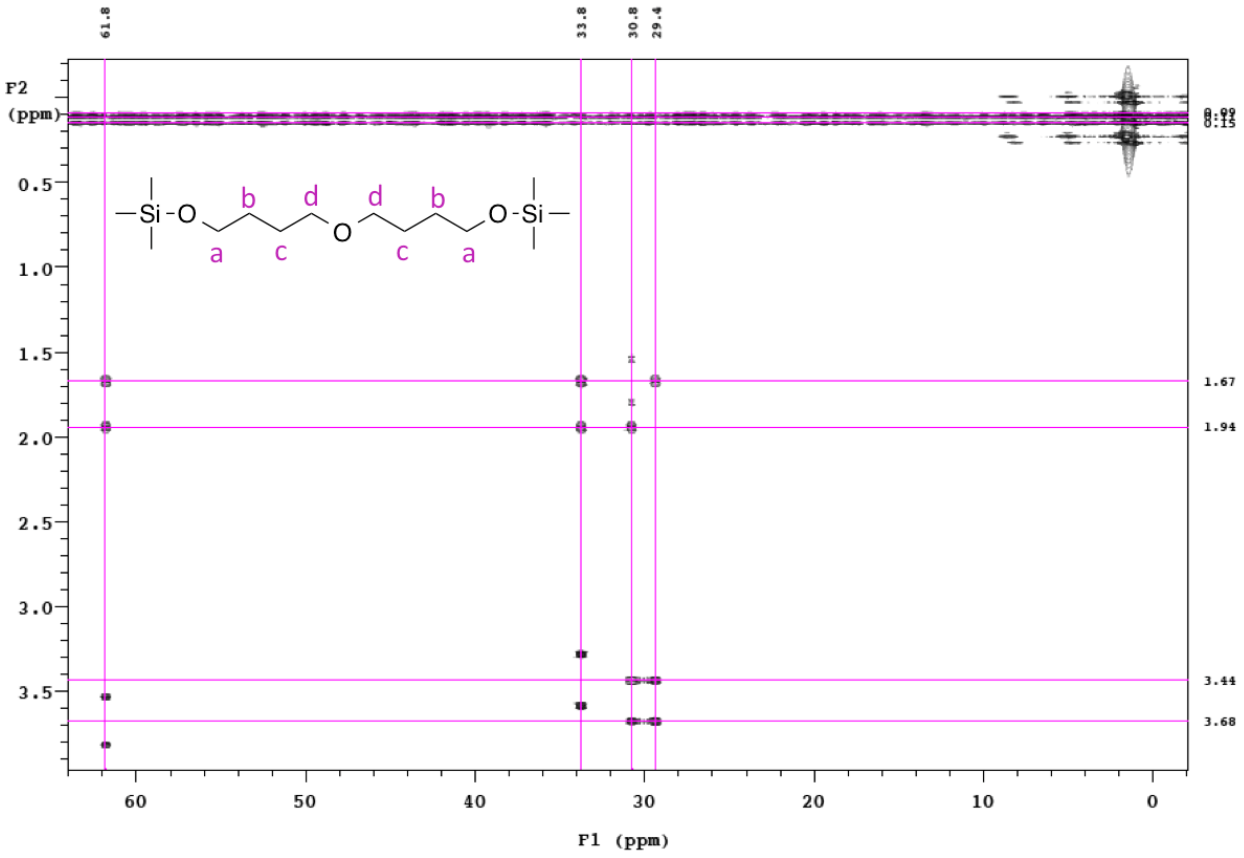


Figure 3-13. gHMBC spectra showing connectivity between C and H: a) H=3.68 ppm and C=61.8 ppm, b) H=1.67 ppm, and C=30.8 ppm, c) H=1.94 ppm and C= 29.4 ppm, d) H=3.44 ppm and C=33.8 ppm

All though very few mechanistic studies have been reported for Grignard reactions with chlorosilicons, references were found for the reaction of chlorosilanes

with THF.[148,169] In fact, reactions between THF and dichlorosilanes have been used to form functionalized organosilicons, as illustrated in Figure 3-14.

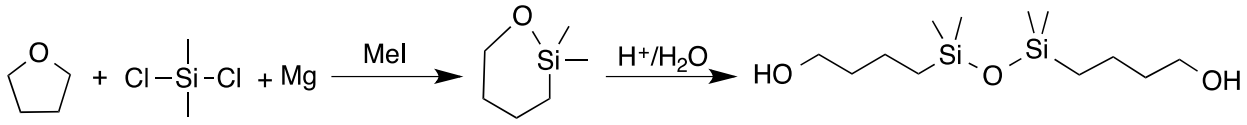


Figure 3-14. Synthesis of 1,3-Bis(4-hydroxybutyltetramethyl)disiloxane via Grignard.[169]

In order to avoid this problem in future reactions, the Grignard intermediate was transferred into a separate flask by cannula, leaving the excess Mg in the reaction flask.

**Grignard reaction optimization:** Even though Grignard reactions involving chlorosilanes are essential for the synthesis of specialty organosilicones, there has been very little investigation of the reaction and the optimum reaction conditions. Therefore, the reaction was conducted using various conditions in an attempt to obtain the required product **(3-12)** in high yields, while trying to control the various side reactions that occur during this process. The various conditions attempted are shown in Table 3-3.

All the reactions were carried out in dry solvents and all glassware was flame dried and purged with argon. The two most common solvents for Grignard reagents, tetrahydrofuran (THF) and diethyl ether were used, even though THF has several advantages over diethyl ether such as lower fire-hazard risk and higher boiling point, allowing use of elevated temperatures. Since one of our objectives was to react the Grignard reagent entirely, therefore limiting the production of compound **(3-13)**, the starting material **(1-4a)** shown in Figure 3-11 was used as the limiting reagent. Two different methods were used for the formation of the reactive magnesium: activation of

the Mg surface using 1,2-dibromoethane, and the formation of the magnesium in-situ via the redox reaction between potassium metal and magnesium chloride.

Table 3-3. Grignard reaction condition

| Entry | Catalyst (eq) | **(1-4a)** | TMSCl | Solvent (Grignard Molarity) | Ratio[a] (**3-12:3-13)** |
|---|---|---|---|---|---|
| (a) | Mg (4.0eq) 1,2-dibromoethane (1.1eq) | 1.0eq | 1.2eq | THF (0.5M) | 0:100 |
| (b) | Mg (4.0eq) 1,2-dibromoethane (1.1eq) | 1.0eq | 1.2eq | THF (1M) | 13:87 |
| (c) | Mg (4.0eq) 1,2-dibromoethane (1.1eq) | 1.0eq | 2.0eq | THF (0.5M) | 0: 100 |
| (d) | Mg (4.0eq) 1,2-dibromoethane (1.1eq) | 1.0eq | 2.0eq | THF (1M) | 11:89 |
| (e) | Mg (4.0eq) 1,2-dibromoethane (1.1eq) | 1.0eq | 2.0eq | Ether (0.5M) | 0:100 |
| (f) | Mg (4.0eq) 1,2-dibromoethane (1.1eq) | 1.0eq | 2.0eq | Ether (1M) | 0:100 |
| (g) | $K^0$ (3.9eq) $MgCl_2$ (2.0eq) | 1.0eq | 1.5eq | THF (0.5M) | <1:>99 |
| (h) | $K^0$ (3.9eq) $MgCl_2$ (2.0eq) | 1.0eq | 2.0 eq | THF (1M) | <1:>99 |

a. The yield was determined via $^1H$ NMR.

In order to avoid the reaction between the chlorosilane and THF, the Grignard reagent was transferred via cannula into a separate dry flask prior to the addition of the chlorosilane. Because the concentration of the Grignard solution has been shown to have an impact on the kinetics of the reaction, two concentrations were used: 1 and 2 Molar. The Grignard reagent was allowed to reflux overnight, and then for another 24 hours after the addition of the chlorosilane.

Regardless of the method used to activate the magnesium, the formation of the Grignard reagent was almost quantitative, and there was very little residual **(1-4a)** found in some cases. This was confirmed by observing the disappearance of the hydrogens alpha to the bromine, which appears as a doublet at 3.45 ppm by $^{1}$H NMR. When 2 equivalents of TMSCl were used for the reaction, we observed the formation of impurities as shown in Figure 3-15, due to the reaction of TMSCl with the solvent. The formation of the target compound **(3-12)** was limited regardless of the conditions used, and the major product observed was **(3-13)**. These two compounds can be differentiated from each other by their hydrogen shifts, at around 0.85 ppm for **(3-13)** and 0.5 ppm for **(3-12)**. These poor yields can be attributed to the bulky and relatively long diene chains surrounding the reactive functionality, which hinders the reaction with the chlorosilane. In fact, the yields reported in the literature for Grignard reactions are relatively low (60% and below), even for less bulky compounds. When higher yields were reported, the Grignard reagent was used in great excess, which cannot be done in our case. Figure 3-15 is a compilation of the various products obtained for some of the entries in Table 3-3.

Isolation of the target product **(3-12)** was not possible. In fact, the most common method for the purification of organosilicones is via distillation. This method could not be used with our monomers, as it led to crosslinking of the products and the formation of a viscous compound, even when performed under high vacuum. Several attempts to separate **(3-12)** and **(3-13)** via column chromatography were also unsuccessful. Therefore the synthesis of the monomers via Grignard reaction was no longer pursued.

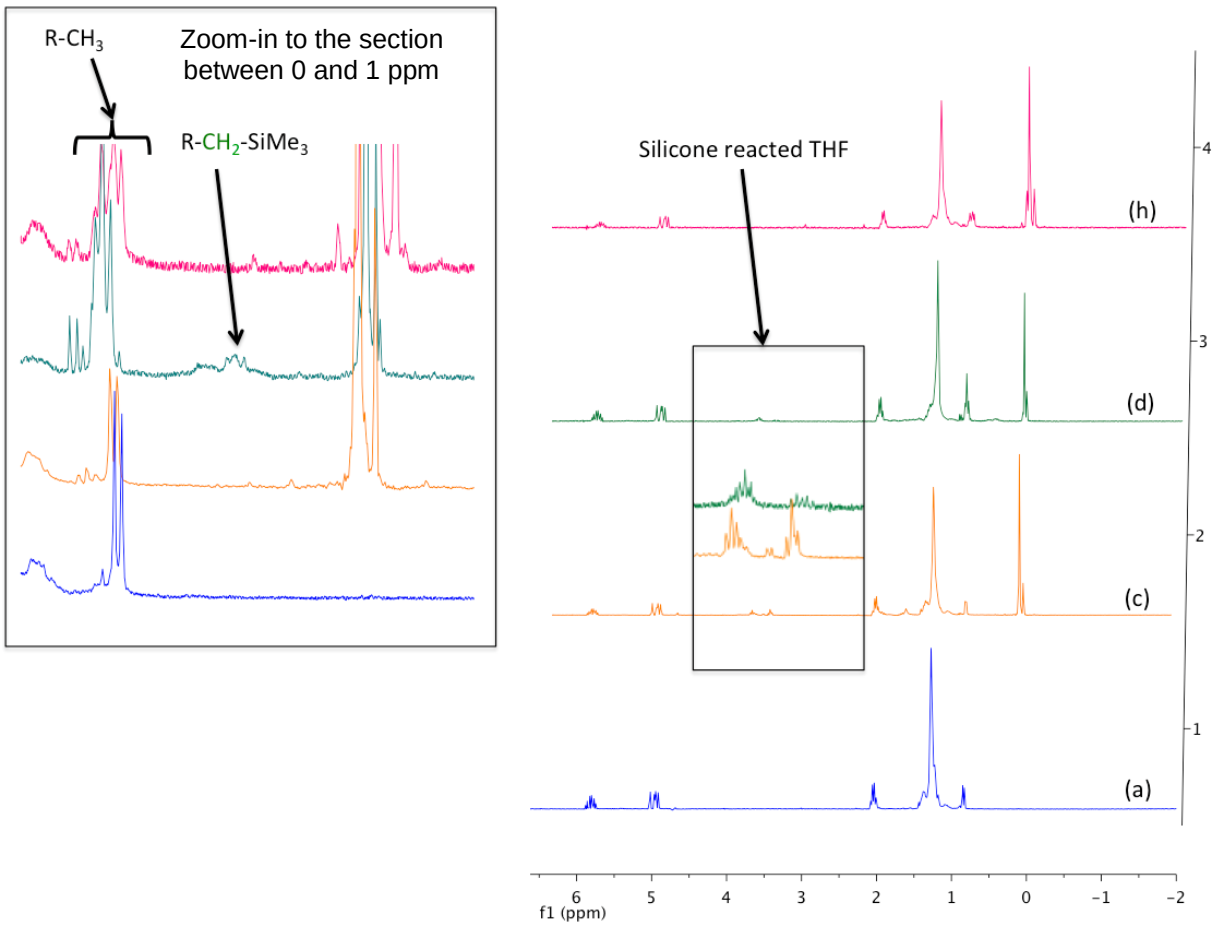


Figure 3-15. $^{1}$H NMR of Grignard reaction products: (a) formation of **(3-13)**, (c) formation of the ring opened THF along with **(3-13)**, (d) formation of the ring opened THF, **(3-12)** and **(3-13),** and (h) formation of **(3-13)** and minimal amount of **(3-12)**.

## 3.3 Conclusion

While Grignard reactions are commonly used for the synthesis of organosilicones, the conditions leading to nearly quantitative yields are not yet established when it comes to chlorosilicones. Of the approximately 2500 reactions listed on Scifinder between an alkylbromide and trimethylchlorosilanes in presence of magnesium, only 0.8% report yields above 60%. Alkoxysilicones, on the other hand, have shown much better yields when used as substrates for Grignard reactions. Currently, there are no alkoxysilicones commercially available that will suit our needs.

However, every year, many new functional organosilicones are being commercialized. Though this method for the functionalization of the diene monomer is being aborted for now, it should be re-attempted when a greater variety of functional silicones or even functionalizable precursors become commercially available.

## 3.4 Experimental

### 3.4.1 Materials and Instrumentation

All silicon materials were purchased from Gelest and distilled over $CaH_2$ prior to use. All other reagents, including catalysts, were purchased from Aldrich and used without further purification unless noted. Anhydrous solvents were obtained from an anhydrous solvent system. $^{1}H$ NMR and $^{13}C$ NMR were recorded in $CDCl_3$ on a Varian Mercury 300MHz spectrometer. $^{1}H$ and $^{13}C$ chemical shifts were referenced to residual signals from $CDCl_3$ ($^{1}H$=7.24 ppm and $^{13}C$=77.23 ppm). Mass spectrograms were carried out on a Thermo Scientific DSQ MS using the chemical ionization mode. Thin layer chromatography (TLC) was used to monitor all reactions and was performed on plastic backed neutral alumina plates. Column chromatography was performed using neutral alumina. Thermogravimetric analysis (TGA) was performed on TA Instruments TGA Q1000 Series using dynamic scans under nitrogen. Differential scanning calorimetry (DSC) analysis was performed using a TA Instruments Q1000 series equipped with a controlled cooling accessory (refrigerated cooling system) at 10°C/min. All samples were prepared in hermetically sealed pans (4-7 mg/sample) and were referenced to an empty pan. Melting temperatures were taken as the peak of the melting transition, glass transition temperatures as the mid point of a step change in heat capacity. Thermal experiments were conducted as follows: samples were heated through the melt to erase thermal history, followed by cooling at 10°C/min to -80°C, and

then heated through the melt at 10°C/min. Data reported reflects this second heating scan. FT-IR data was gathered from a Bruker Vertex 80v using a Pike GladiATR stage and the data was processed using the OPUS 6.5 software.

### 3.4.2 Procedures

**1-chloro-1,1,3,3-tetramethyl-3-(undec-10-en-1-yl)disiloxane (3-6):** A flame-dried three-neck round bottom flask equipped with a stir bar was charged with 20mL of THF and Mg (1.68g, 69.1 mmol) under argon. The flask was chilled in an ice bath, and 1,2-Dibromoethane (3.24g, 17.2 mmol) was added to the solution and stirred at RT for 30 minutes. Compound **(3-5)** (4g, 17.2 mmol) was then added dropwise and refluxed overnight under argon. A separate three-neck round bottom flask equipped with a condenser, addition funnel and a stir bar was flame dried under vacuum. After purging the flask with argon, a solution of **(3-1)** (5.6g, 27.6 mmol) in THF was added to the flask. The cooled Grignard solution was transferred to an addition funnel and added dropwise to the dichlorosilicone solution over 1 h. The solution was refluxed overnight and the formation of a white precipitate was observed. The reaction was then cooled and hexane was added to the reaction. The product was separated from the magnesium salts by filtration over Celite and the solvents were evaporated in vacuo. Purification of **(3-6)** was not possible due to crosslinking via the reactive chlorosilane end groups.

**Methyldi(undec-10-en-1-yl)silane (3-9):** A flame-dried three-neck round bottom flask equipped with a stir bar was charged with 20mL of THF and Mg (4.16g, 171.6 mmol) under argon. The flask was chilled in an ice bath, and 1,2-Dibromoethane (8.06g, 42.9 mmol) was added to the solution and stirred at RT for 30 minutes. Compound **(3-5)** (10.00g, 42.9 mmol) was then added dropwise and the mixture was refluxed overnight under argon. The reaction was cooled to room temperature and dichloromethylsilane **(3-**

**12)** (2.24g, 19.48 mmol) was added dropwise over an hour, after which the reaction was refluxed overnight under argon. The reaction was then cooled and hexane was added to the reaction. The product was separated from the magnesium chloride salts by filtration over celite and the solvents were evaporated under vacuum. The target compound **(3-10)** was isolated by distillation in a Kugelrohr under pressure to afford 4.3g of **(3-13)**. (Yield = 63.2%) $^{1}$H NMR (300 MHz, $CDCl_3$): δ(ppm) 5.91-5.73 (m, 2H), 5.09-4.84 (m, 4H), 3.68 (m, 1H), 2.04 (q, *J* = 6.9 Hz, 4H), 1.26 (s, 32H), 0.63-0.51 (m, 4H), 0.12 (s, 3H). $^{13}$C NMR (75 MHz, $CDCl_3$): δ(ppm) 139.22, 114.04, 33.81, 31.89, 29.67, 29.61, 29.57, 29.50, 29.32, 29.15, 28.94, 22.67, 14.10, 1.55. FT-IR: 3077, 2920, 2852, 2103, 1642, 1540, 1459.7, 1252, 1180, 993, 908, 879, 721cm$^{-1}$. HRMS Actual $[M-H]^+$=349.3296 Theory $[M-H]^+$=349.3291

**Iridium catalyzed methyldi(undec-10-en-1-yl)silanol (3-10):** To a solution of **(3-9)** (1.00 g, 2.85 mmol) in acetonitrile (10 mL) was added $[IrCl(C_8H_{12})]_2$ (0.02 g, 0.029 mmol) and deionized water (0.1 g, 5.7 mmol). The reaction mixture was stirred under air for 24 h at room temperature. Extraction of the organic layer in diethyl ether followed by evaporation of the solvents under vacuum afforded **(3-10)** (17%) and residual starting material **(3-9)** (83%). $^{1}$H NMR (300 MHz, $CDCl_3$): δ(ppm) 5.90-5.73 (m, 2H), 5.05-4.86 (m, 4H), 3.70 (m, 0.83H), 2.04 (q, *J* = 11.6 Hz, 4H), 1.25 (s, 32H), 0.60-0.52 (m, 4H), 0.12 (s, 3H). $^{13}$C NMR (75 MHz, $CDCl_3$): δ(ppm) 139.22, 114.04, 33.81, 31.89, 29.67, 29.61, 29.57, 29.50, 29.32, 29.15, 28.94, 26.67, 22.83, 14.10, 4.67, 1.55. FT-IR: 3400, 3077, 2920, 2852, 2103, 1642, 1540, 1459.7, 1252,1180, 1150, 1100, 993, 908, 879, 721cm$^{-1}$. GC-CI-MS: Actual $[M+NH4]^+$ = 384.3672 Theoretical $[M+NH4]^+$ = 384.3656

**Pearlman catalyzed methyldi(undec-10-en-1-yl)silanol (3-10):** To an ice-cooled suspension of Pearlman's catalyst (20 mg) in THF (50 mL) and water (2.5 mL) was slowly added a solution of **10** (1.00 g, 2.85 mmol) in THF (15 mL). Evolution of hydrogen evolution was observed, and as soon as it had ceased, the reaction mixture was stirred at room temperature for 24 hours. The catalyst was removed by filtration, the solvent was removed at 30 °C under reduced pressure, and the organic layer was extracted with diethyl ether. The organic layer was washed with brine and dried over magnesium sulfate prior to removal of the solvents under vacuum. The expected product **(3-10)** was not observed, and partial hydrogenation of the double bond was observed.

**Palladium-on-charcoal catalyzed methyldi(undec-10-en-1-yl)silanol (3-10):** To a mixture of 5% palladium on charcoal (0.01 g) in THF (12 mL) and water (0.012 g, 0.70 mmol) was added a THF solution (20 mL) of **(3-9)** (1.00g, 2.85 mmol). After the reaction mixture was stirred for 24 h, it was filtered using Celite. The filtrate was concentrated under reduced pressure and the organic layer was extracted into diethyl ether. The organic layer was washed with brine and dried over magnesium sulfate prior to removal of the solvents under vacuum. The expected product **(3-10)** was not formed, and complete hydrogenation of the double bonds was observed.

**General procedure for the Grignard synthesis of (3-12) using Mg and 1,2-dibromoethane:** A 50-mL three-neck flask equipped with a condenser and stir bar was flame dried under vacuum. The apparatus was then flushed with argon and 4 equiv. of Mg turnings were added to the flask along with dry THF. Then, 1.1 equiv. of 1,2-dibromoethane was added dropwise to the magnesium, leading to bubbling due to the

formation of ethylene. The mixture was stirred at room temperature for an hour, followed by dropwise addition of 1 equiv. of (**1-4a),** and the reaction mixture and refluxed for 24 hours. The reaction was then cooled to room temperature and the Grignard solution was transferred via cannula into a 50-mL dry round-bottom flask equipped with an addition funnel and a condenser. The required amount of trimethylchlorosilane (1.2 equiv., 1.5 equiv. or 2.0 equiv.) was added dropwise to the reaction flask over 1 hr. The reaction was allowed to stir at room temperature for an hour and then refluxed overnight. The reaction was cooled to room temperature and hexane was added to the reaction flask. The magnesium chloride salts were removed by Celite filtration. The organic solvents were removed under vacuum giving a crude yellow liquid product. The product could not be purified via distillation, silica gel column chromatography or alumina column chromatography. NMR of the crude sample allowed the determination of the various products obtained.

**General procedure for the Grignard synthesis of (3-12) using K and magnesium chloride:** In a flame-dried round-bottom flask were introduced THF, 2 equiv. of magnesium chloride and 3.9 equiv. of potassium metal. The mixture was refluxed for 1 hour or until the potassium metal was fully reacted. The dark gray mixture was cooled to room temperature, and THF (5 mL) was used to rinse the walls of the flask prior to the addition of **(1-4a)**. The reaction was allowed to proceed for an hour at room temperature and then was refluxed overnight. The reaction was cooled to 0°C, and the proper amount of trimethyl chlorosilane (1.2 equiv., 1.5 equiv. or 2.0 equiv.) was added dropwise. The reaction was allowed to proceed for an hour at room temperature and then refluxed overnight. The reaction was cooled to room temperature and hexane was added to the reaction flask. The magnesium chloride salts were removed by filtration through Celite. The organic solvents were removed under vacuum giving a crude yellow

liquid product. The product could not be purified via distillation, silica gel column chromatography or alumina column chromatography. NMR of the crude sample allowed the determination of the mixture of products obtained.

CHAPTER 4
SILICON BRANCHED POLYMERS WITH O-C LINKAGE

## 4.1 Overview

Silyl groups are some of the most commonly used protective groups in organic chemistry, due to their facile reaction with alcohol functionalities, as well as the ease in which they can be cleaved. In small molecules, Si-O-C linkages can be easily hydrolyzed, but this is not always the case with long chain molecules or polymers. In fact, the nature of the chain connected to these linkages will affect their stability in the presence of water. If the organic chain is hydrophilic, hydrolysis will occur rapidly to break the Si-O-C linkage. However, if the organic chain is hydrophobic, such as polyethylene, it will prevent hydrolysis of the reversible Si-O-C linkage, which can be stable for more than a decade. Since chlorosiloxane materials are readily available, and their nucleophilic reactions with alcohol functionalities are well known and studied, we decided to synthesize precisely branched polyethylene with the Si-O-C linkages and study their properties.

## 4.2 Results and discussion

### 4.2.1 Monomer synthesis

The monomers with Si-O-C linkage were synthesized via a nucleophilic substitution reaction of the alcohol **(4-1)** with an excess of commercially available chlorosiloxanes, as illustrated in Figure 4-1.

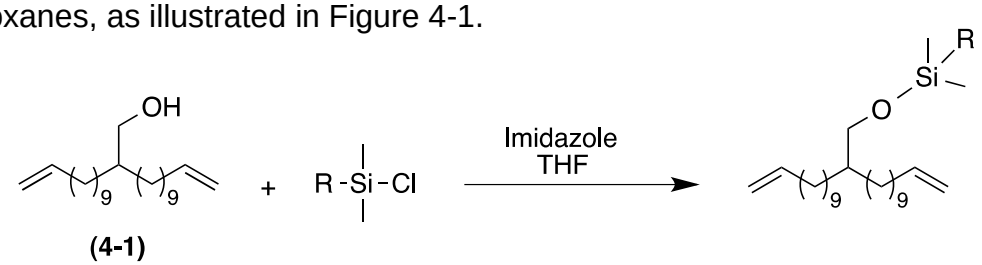


**(4-1)**

Figure 4-1. Nucleophilic reaction leading to the Si-O-C linkage

The reactive chlorosiloxanes used as well as the series of monomers with siloxane branches of various sizes are shown in Table 4-1, and a general synthetic procedure is described below.

Table 4-1. Chlorosiloxane substrate used and monomer synthesized

| Chlorosilicone | Monomer |
|---|---|
| 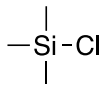 **(4-2)** | 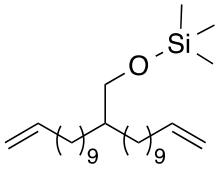 **(4-6)** |
| 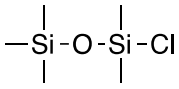 **(4-3)** | 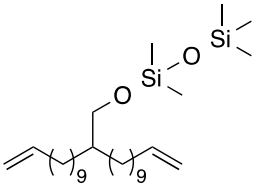 **(4-7)** |
| 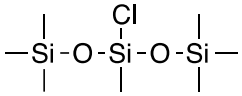 **(4-4)** | 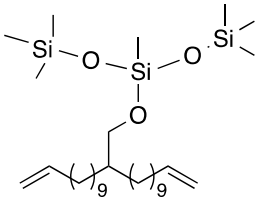 **(4-8)** |
| 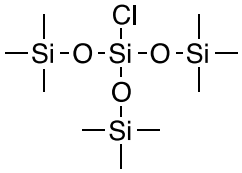 **(4-5)** | 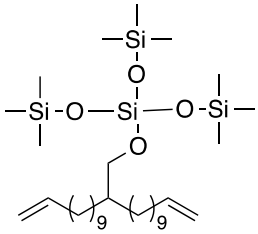 **(4-9)** |

An excess of chlorosilicone was added to a solution of primary alcohol **(4-1)** and 1H-imidazole in THF at 0°C. The reaction was then allowed to proceed at room temperature overnight. In order to avoid hydrolysis of the Si-O-C linkages, the reaction

was not quenched with water. Instead, THF was evaporated under vacuum, and the monomer and the imidazolium chloride salt formed during the reaction were dissolved in a minimal amount of hexanes and passed through an alumina plug, to afford the pure monomers as a clear oil.

The monomers were characterized using $^{1}$H NMR, $^{13}$C NMR, FT-IR and Mass Spectrometry. An example of the FT-IR spectrum of the alcohol **(4-1)** in comparison with the siloxane functionalized **(4-9)** is shown in Figure 4-2.

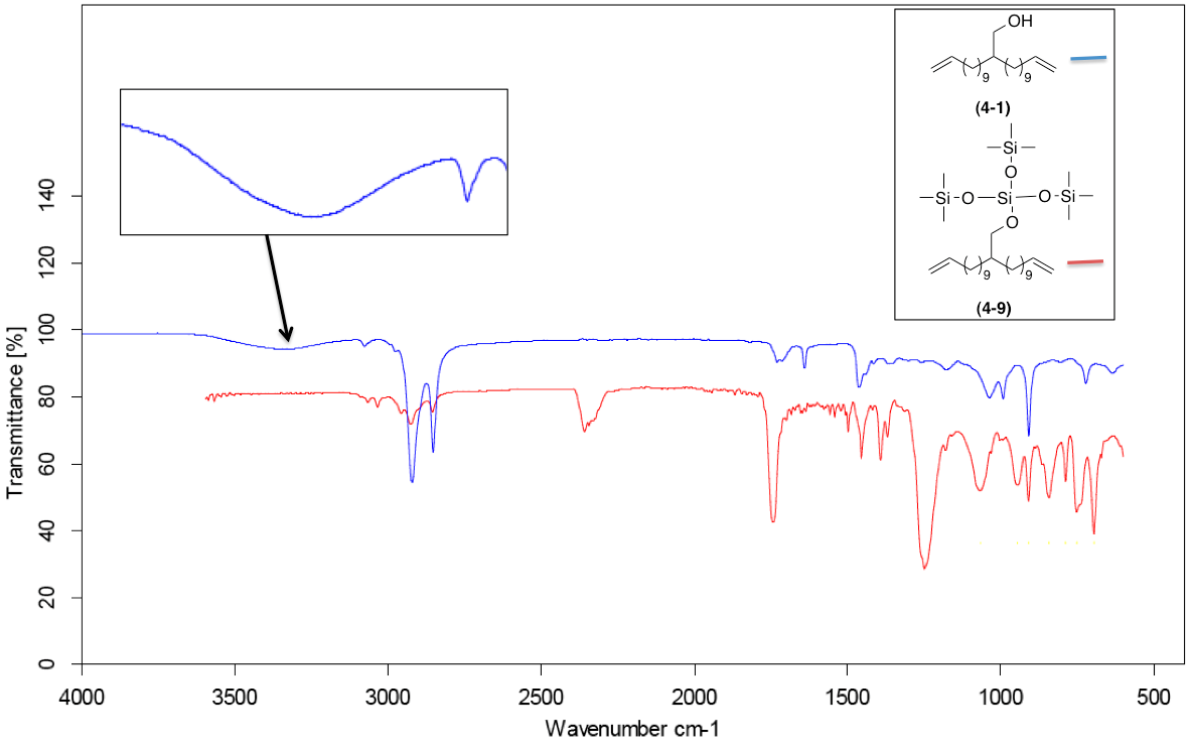


Figure 4-2. FT-IR comparison of compounds **(4-1)** (blue) and **(4-9)** (red)**.**

FT-IR constitutes a good method to determine the complete disappearance of the alcohol **(4-1)** as the OH stretch peak appears as a strong broad peak between 3200 $cm^{-1}$ and 3600 $cm^{-1}$. The absence of signal in this region, also confirms that no hydrolysis of the siloxane end groups has occurred. In addition to the disappearance of

the OH peak, the IR spectra of monomer **(4-9)** shows the appearance of new peaks that are identified as the silicones peaks. The strong sharp band at 1250 $cm^{-1}$ is representative of Si-$CH_3$ groups. The presence of this peak confirms there has been no or limited crosslinking of the monomer, and supports the conclusion that the ends groups have not been hydrolyzed. We can also see the presence of a strong peak at 1100 $cm^{-1}$ that is representative of the siloxane linkage Si-O-Si.

In addition to using IR to identify loss of the alcohol functionality, the $^1H$ NMR clearly shows that the hydrogens on the $CH_2$ alpha to the oxygen shifts downfield when the O-H of **(4-1)** is replaced by silane moieties **(4-6, 4-7, 4-8 and 4-9).** Figure 4-3 shows the superimposed $^1H$ NMR spectra of **(4-1)** and **(4-9)**.

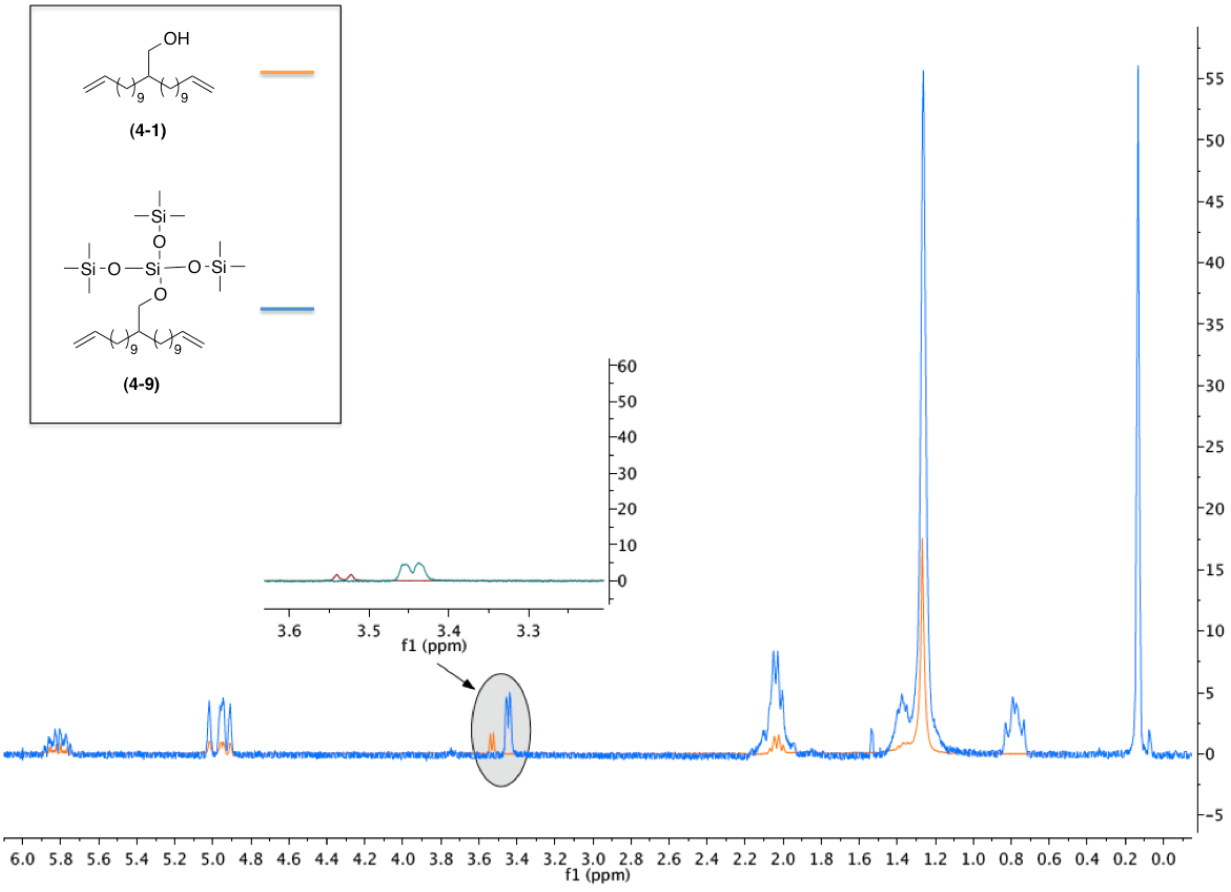


Figure 4-3. $^1H$ NMR spectra of alcohol **(4-1)** (orange) and monomer **(4-9)** (blue).

### 4.2.3 ADMET polymerization

Polymers were synthesized using 2.5g of the monomers presented in Table 4-1 in 1mL of dibenzyl carbonate at 55°C, using 1mol % of 2nd generation Grubbs' catalyst shown in Figure 4-4. Thirty minutes after the addition of the catalyst, the formation of a viscous polymer was observed, and within 3 hours, stirring of the polymer was almost impossible, and the polymer precipitated from the solution. To insure that all the monomer had reacted, additional catalyst was added 24 hours later, and stirring was induced manually using a strong magnet on the outside of the flask, to move the stir bar. The polymerization was allowed to continue for another 24 hours after which a mixture of ethyl vinyl ether and toluene was used to quench the polymerization. The polymers were insoluble in toluene even when heated. A variety of solvents and solvent mixtures were used in attempts to solubilize the polymer, but none was successful. Therefore, the polymers were allowed to sit in the toluene/ethyl vinyl ether mixture for 24 hours in order to dissolve as much of the unreacted monomers and catalyst as possible. The polymer was then removed by filtration and dried under vacuum.

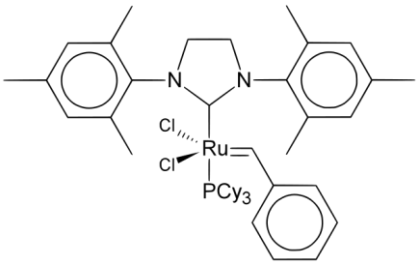


Figure 4-4. Grubbs' 2nd generation catalyst.

Due to the insolubility of the polymers, their hydrogenation could not be achieved, and only the moderately elastic unsaturated polymers shown in Figure 4-5 were produced.

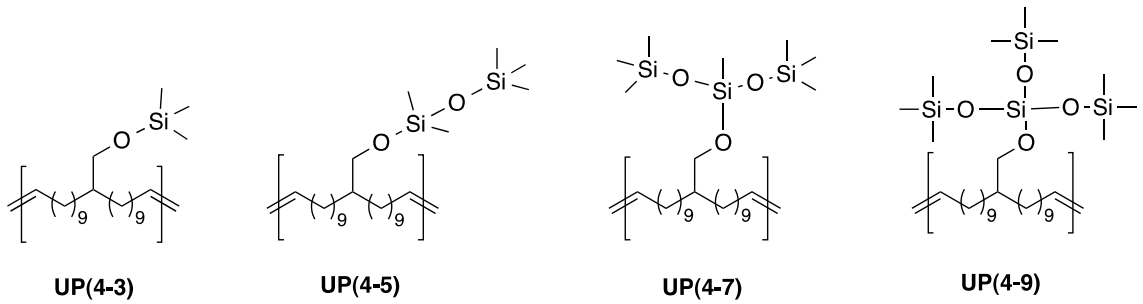


Figure 4-5. Structures of the unsaturated polymers.

The standard spectroscopic measurments ($^{1}$H NMR, $^{13}$C NMR) and molecular weight determination by gel-permeation chromatography (GPC) could not be performed. The structures of the polymers were analyzed by FT-IR and their thermal properties were measured using DSC and TGA.

### 4.2.4 Structural analysis

Since none of the standard techniques could be used to analyze the polymers, FT-IR was used to compare the structures of the monomers and the unsaturated polymers. Figure 4-6 compares the IR spectra of **(4-5)** and **UP(4-5)**. Similarities between both IRs are observed, mainly for the peaks corresponding to the siloxane branch. Indeed, no change is observed for the peaks at 1260 $cm^{-1}$ relative to the $(CH_3)_3$-Si-O, which means no or limited crosslinking has occurred during the polymerization. No change is noted either for the Si-O-Si and $(CH_3)_2$-Si-O peaks which appear respectively at 1100 $cm^{-1}$ and 800 $cm^{-1}$ in both the monomer and the unsaturated polymer. The IR spectra usually allows us to observe shifts in the alkene peaks at low frequency, indicating the reduction of the terminal double bonds and an increase in the internal olefin. These peaks overlap with the siloxane related peaks, which are stronger peaks, therefore, these changes cannot be noted. Finally, the peak observed in the 2300 $cm^{-1}$ region of the monomer, is due to presence of solvent.

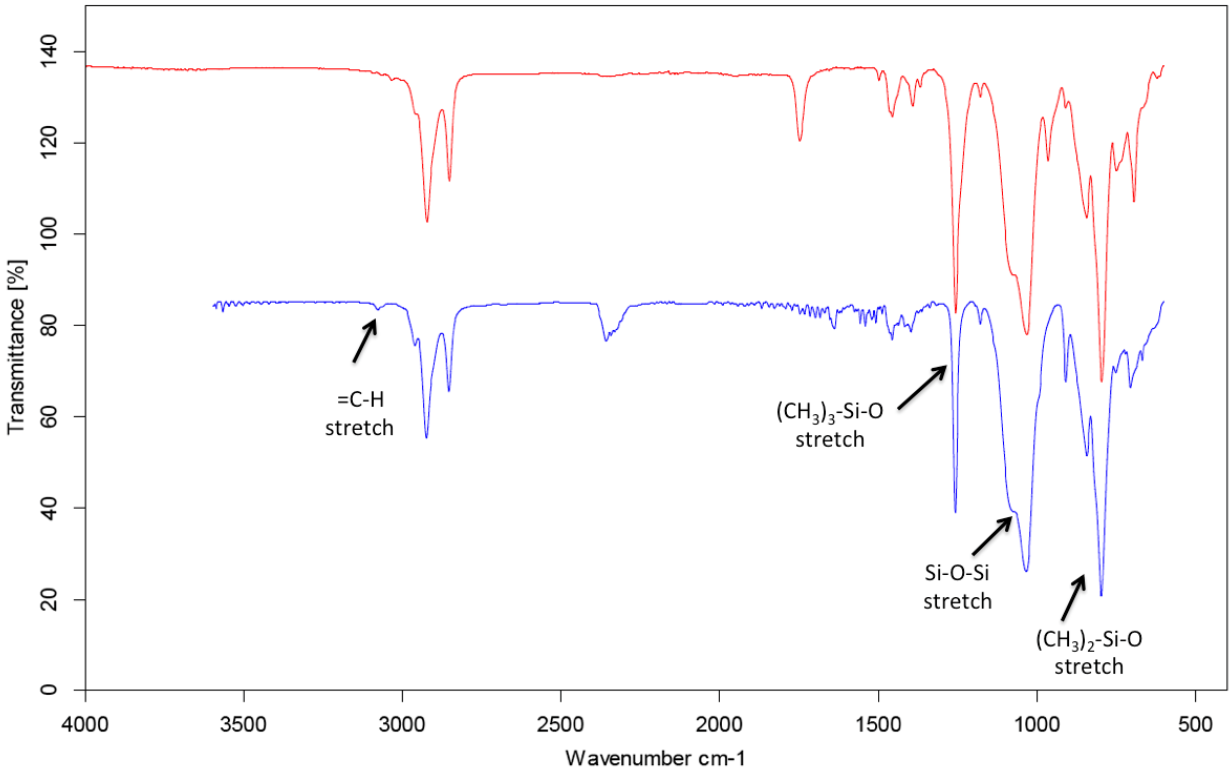


Figure 4-6. IR of **UP(4-5)** (red) and **(4-5)** monomer.

### 4.2.5 Degradation and Thermal Analysis

Thermal gravimetric analysis (TGA) and differential scanning calorimetry (DSC) were performed on each of the unsaturated polymers in Figure 4-5. The thermal degradation of these polymers is shown in the TGA thermograms in Figure 4-7. These were measured in an inert atmosphere, as percentage of weight loss versus temperature in the 0°C-500°C range. The thermal stability of these polymers is of importance, since in practical applications they will be heated in order to prepare the pellets used for extrusion processes.

All polymers showed an initial weight loss, followed by a second sharp weight drop at a higher temperature. The first weight loss corresponds to the cleavage of part or all of the siloxane branch. The percent weight losses observed experimentally were 86% for **UP(4-3)** and 84% for **UP(4-5)** which corresponds to the cleavage of the

trimethylsilane end group. On the other hand, the weight loss percentages observed for **UP(4-7)** and **UP(4-9)** corresponds to the cleavage of the entire branch with a 62% weight loss for **UP(4-7)** and 54% weight loss for **UP(4-9)**. The second weight loss drop occurs at higher temperatures, and corresponds to the degradation of the unsaturated polyethylene backbone.

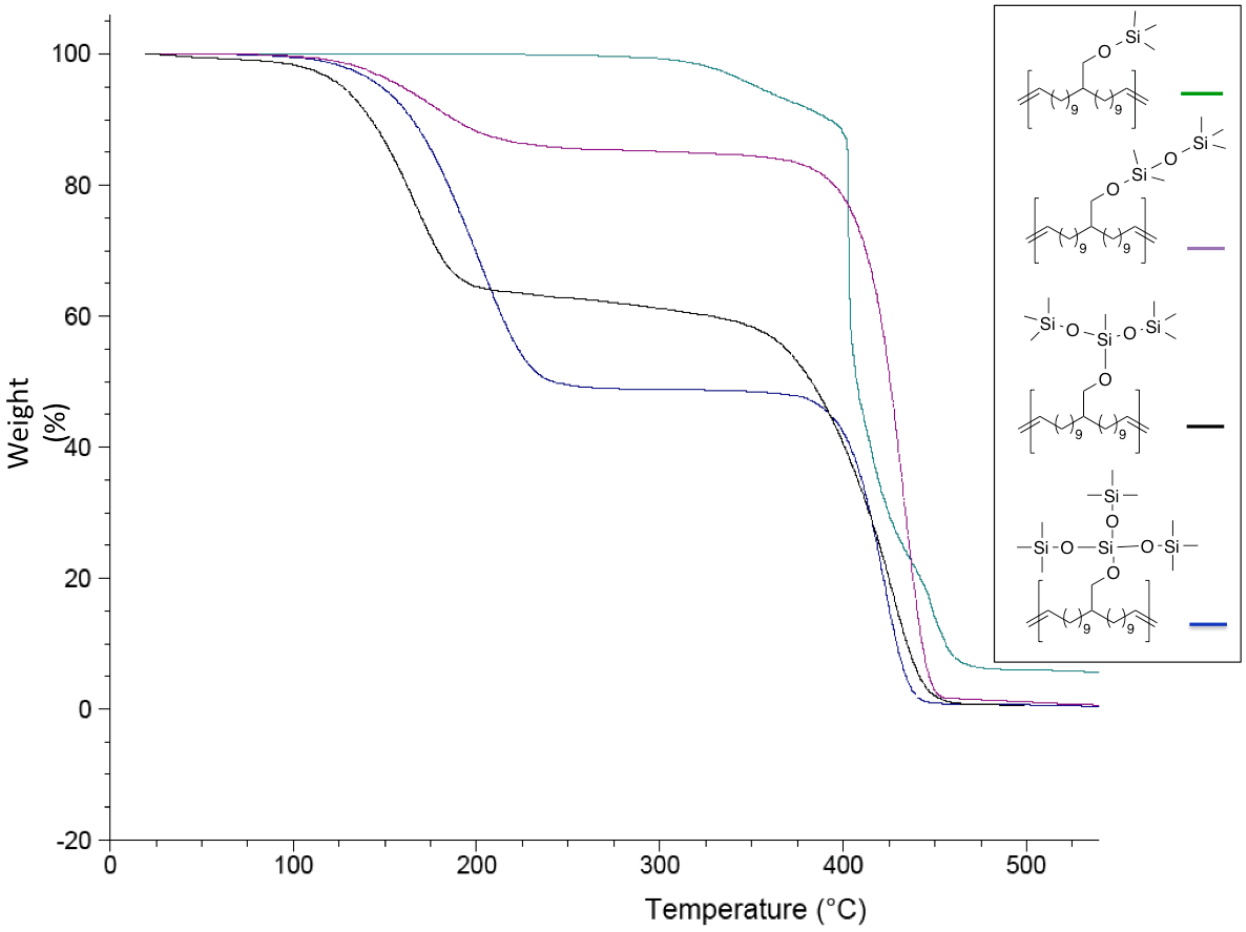


Figure 4-7. TGA traces of the unsaturated polymers in $N_2$(g).

Due to the type of branching present on these polymers, crosslinking was the first plausible explanation for the insolubility of the polymers. However, it is clear from the thermograms that no to minimal crosslinking occurred. The thermograms of silicon crosslinked polymers that have been previously studied in our group show only one

sharp weight loss at higher temperatures (>350°C), instead of the two weight losses observed in this study.[170]

The thermal behavior of the unsaturated polymers was performed by differential scanning calorimetry (DSC) and detailed characteristics of the thermal transitions are summarized in Table 4-2. Values of glass transition temperatures ($T_g$) were obtained at the mid-point of the transition and the melting temperatures ($T_m$) were taken as the temperature at the peak of the melting transition temperature in the second heating scan. The crystallization temperature ($T_c$) was taken as the temperature at the peak of the crystallization transition in the second cooling scan. The data were collected by scanning samples from -80°C to the temperature recorded at 5% weight loss in the TGA thermogram. The rate of cooling and heating was 10°C/min and values were recorded for the second heating and cooling ramps.

Table 4-2. Thermal analysis of the unsaturated polymers.

| | DSC | | | TGA |
|---|---|---|---|---|
| Polymer | $T_g$ (°C)[a] | $T_m$ (°C)[b] | $T_c$ (°C)[c] | $T_1$ (°C)[d] |
| **UP(4-3)** | -65 | - | - | 250 |
| **UP(4-5)** | -71 | 29 | - | 125 |
| **UP(4-7)** | - | -10<br>22 | -12 | 150 |
| **UP(4-9)** | - | 28 | - | 155 |

a. transition mid-point; b. temperature at maximum of melting peak;
c. temperature of minimum of recrystallization peak; d. recorded at 5% total mass loss under nitrogen gas.

The DSC traces for the unsaturated polymers are shown in Figure 4-8 – 4-11. Thermograms of **UP(4-3)** and **UP(4-5)** display glass transition temperatures at -65°C

and -71°C respectively, while no glass transition temperature was recorded for **UP(4-7)** and **UP(4-9)**. These results are to be predicted, as we expect the glass transition temperatures of the polymers to decrease as their siloxane content increases. In fact the $T_g$ of poly(dimethylsiloxane) (PDMS), -125°C, is the lowest recorded for commonly used polymers.[137] This very low $T_g$ reflects the high dynamic flexibility of the siloxane chains due to the long Si-O bond length (1.63Å), the large Si-O-Si (145º) and O-Si-O (110º) bond angles and the lack of substituents on the oxygen atoms. Therefore, even though no $T_g$ was recorded for **UP(4-7)** and **UP(4-9)** we would expect to see one if we had the capability to conduct those thermograms at lower temperature. Unfortunately, the lowest temperature that can be reached with the instruments available in the lab is -80°C.

The flexibility of PDMS is also at the origin of its low melting temperature, (-40°C) and the lack of crystallinity.[137] The addition of a rigid polymer, such as high density polyethylene, would be expected to lead to a higher melting temperature due to the increased stiffness. **UP(4-3)** is an amorphous polymer with no melting peak. **UP(4-5)**, **UP(4-7)** and **UP(4-9)** all exhibit sharp melting peaks, with two melting peaks for **UP(4-9)** suggesting the presence of two types of crystals. We would expect the melting temperatures to decrease as the size of the siloxane branch increases, but, no correlation was observed. Variation in molecular weight and molecular weight distribution, which were not measured for our polymers, have been the cause for variation of physical and chemical properties of similar polymers, and this could account for the lack of correlation in our polymers. Both **UP(4-7)** and **UP(4-9)** show a cold crystallization peak, and only **UP(4-7)** displays a crystallization peak.

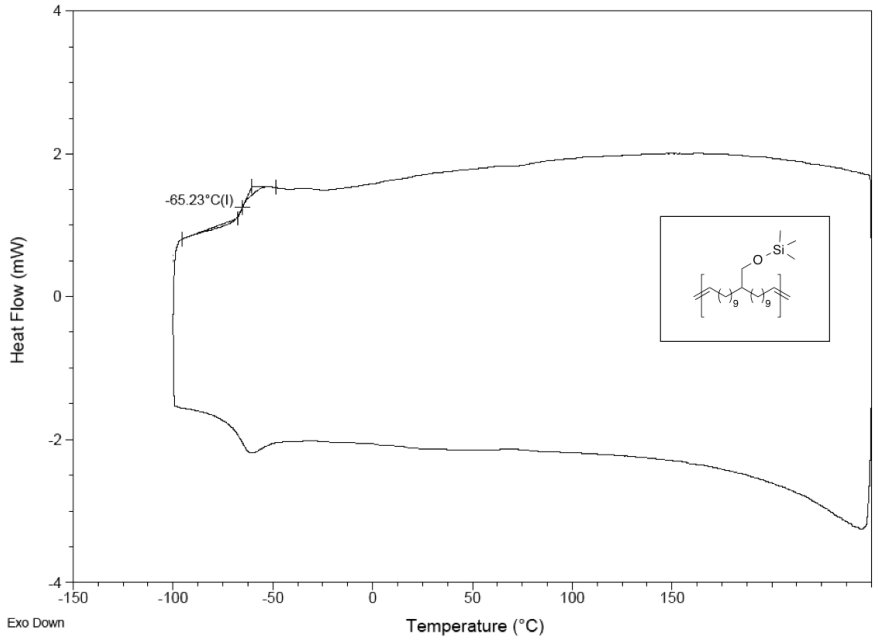


Figure 4-8. DSC traces of **UP(4-3)**.

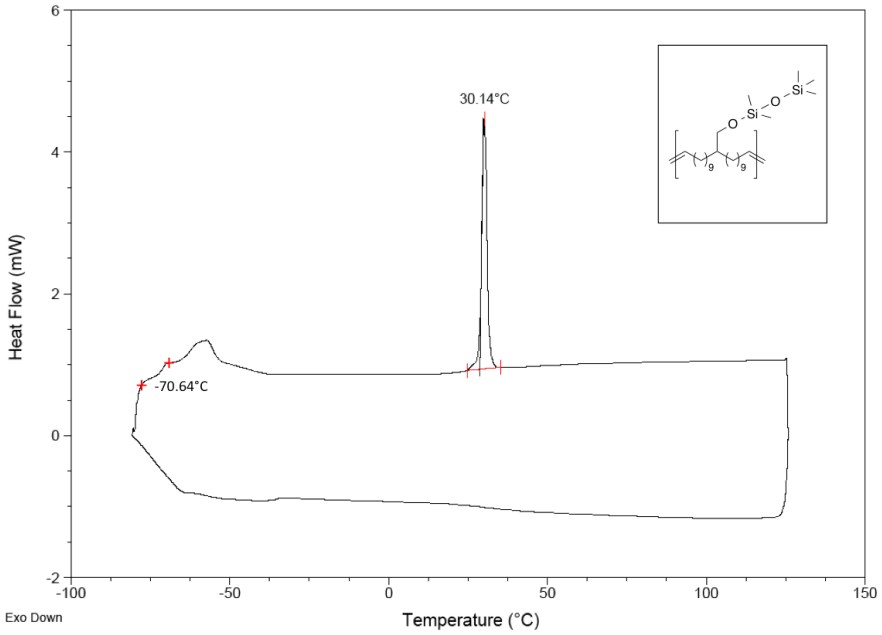


Figure 4-9. DSC traces of **UP(4-5)**.

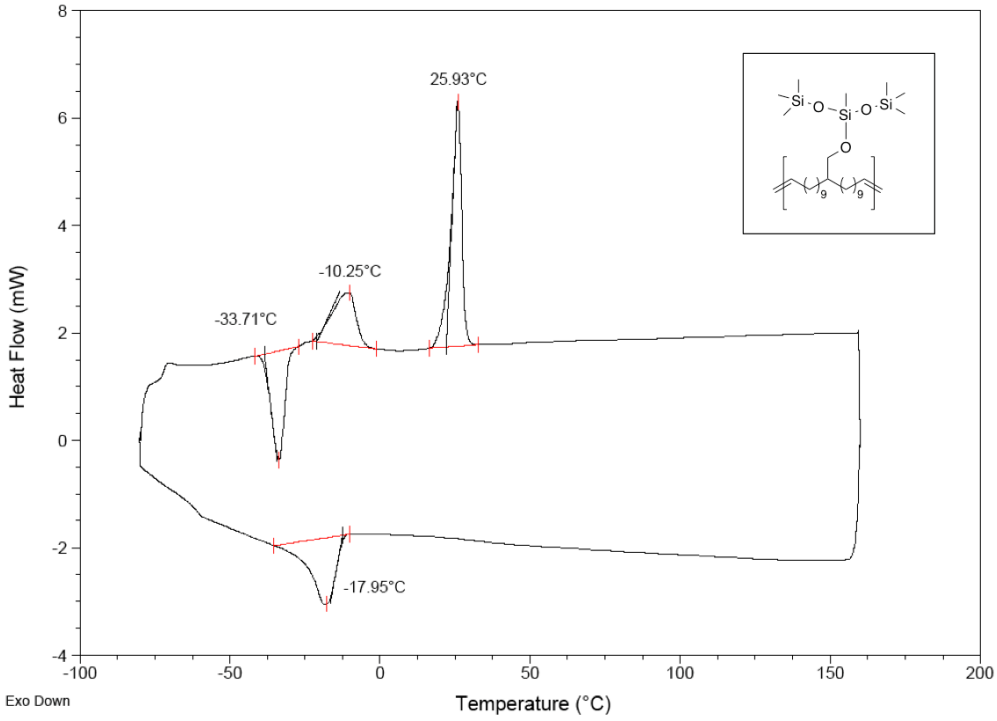


Figure 4-10. DSC traces of **UP(4-7)**.

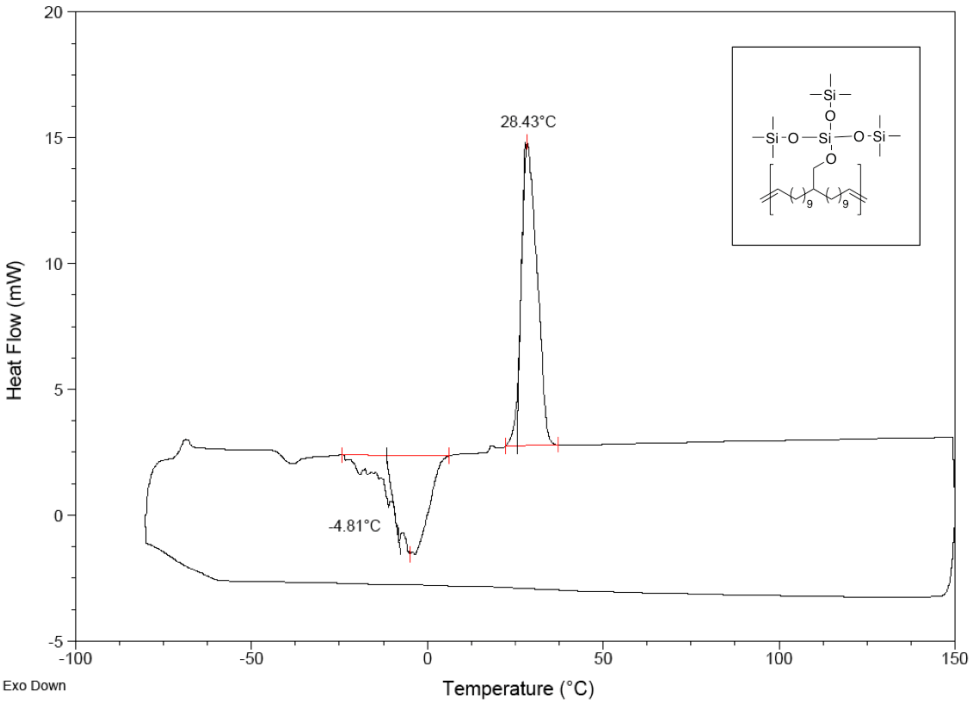


Figure 4-11. DSC traces of **UP(4-9)**.

### 4.2.6 Solid-state NMR

In order to rule out potential crosslinking of the polymer, solid-state NMR was performed on monomer **(4-9)** and polymer **UP(4-9)**. The experiments were done in the Max-Planck Institute of Polymer Research by Dr. Robert Graf. All solid state NMR measurements were performed at 25 kHz MAS spinning frequency, 700.21 MHz $^{1}H$ Larmor frequency, 100 kHz rf nutation frequency on all frequency channels. For $^{13}C$ and $^{29}Si$ NMR measurements, 50 kHz $^{1}H$ high power decoupling was applied using the SPINAL64 scheme.

$^{1}H$ and $^{29}Si$ solid-state NMR measurements of both the monomer **(4-9)** and the polymer **UP(4-9)** showed the expected protons attached to the silicon bound methyl groups and the aliphatic backbone. The integrals confirm the structure of the polymer and that crosslinking is non-existant.

## 4.4 Conclusions

This Chapter discussed the attachment of the siloxane branch on the diene monomer via a C-O-Si linkage. A variety of monomers and polymers with different siloxane size branches were synthesized. Partial characterization of the polymers was achieved due to insolubility problems. Crosslinking can be attributed as the reason for this insolubility, however, the combination of FT-IR and TGA shows that if crosslinking has occurred, it is minimal. Confimation of no-crosslinking was obtained for **UP(4-9)** via solid-state NMR. Although this method would be expected to yield unstable and easily hydrolyzed compounds, the thermogravimetric analysis proved otherwise. The melting temperatures and glass temperatures obtained for the polymers were as expected. The incorporation of a soft siloxane branch onto high density polyethylene reduced both the melting temperature and the glass transition temperature. Due to their lack of solubility,

these polymers still require further characterization, and the key focus will be to study their rheological behavior when mixed with high density polyethylene. Because the main purpose of this project is to prepare materials for industrial applications, the many steps leading to the synthesis of these polymers and low yields need to be addressed. Chapter 5 will explore alternative and more efficient synthesis methods.

## 4.5 Experimental

### 4.5.1 Materials and Instrumentation

All chlorosiloxanes were purchased from Gelest and distilled over $CaH_2$ prior to use. All other materials were purchased from Aldrich and used without further purification unless noted. Grubbs 1$^{st}$ generation catalyst, bis(tricyclohexylphosphine)benzylidineruthenium (IV) dichloride (G1), was kindly provided by Materia, Inc. Anhydrous solvents were obtained from an anhydrous solvent system. All $^{1}H$ NMR and $^{13}C$ NMR were obtained on a Varian Mercury 300MHz spectrometer and recorded in $CDCl_3$. $^{1}H$ NMR and $^{13}C$ NMR shifts were referenced to residual signals from $CDCl_3$ ($^{1}H$ = 7.24 ppm and $^{13}C$ = 77,23 ppm). Mass spectrograms were carried out on a Thermo Scientific DSQ MS using the chemical ionization mode. Thin layer chromatography (TLC) was used to monitor all reactions and was performed on plastic backed neutral alumina plates. Column chromatography was performed using neutral alumina. Thermogravimetric analysis (TGA) was performed on TA Instruments TGA Q1000 Series instrument using dynamic scans under nitrogen. Differential scanning calorimetry (DSC) analysis was performed using a TA Instruments Q1000 series DSC equipped with a controlled cooling accessory (refrigerated cooling system) at 10°C/min. All samples were prepared in hermetically sealed pans (4-7 mg/sample) and were referenced to an empty pan. Melting temperatures were taken as the peak of

the melting transition, glass transition temperatures as the mid point of a step change in heat capacity. Thermal experiments were conducted as follows: samples were heated through the melt to erase thermal history, followed by cooling at 10°C/min to -80°C, and then heating through the melt at 10°C/min. Data reported reflects this second heating scan. FT-IR data was gathered from a Bruker Vertex 80v using a Pike GladiATR stage and the data were processed using the OPUS 6.5 software.

### 4.5.2 Procedures

#### 4.5.2.1 Monomer Synthesis

**Trimethyl(2-(undec-10-en-1-yl)tridec-12-en-1-yl)oxy)silane (4-3):** A dry 250 mL round bottom flask was charged with 50 mL of dry THF, 1H-Imidaole (1.35g, 19.75 mmol) and primary alcohol **(4-1)** (3g, 8.23 mmol). The reaction vessel was lowered into an ice bath and allowed to stir under argon for 30 minutes. Chlorotrimethylsilane (1.07g, 9.88 mmol) was dripped in slowly at 0°C and the reaction was left on ice for 2 hours, before allowing it to stir overnight at room temperature. The reaction was monitored by TLC until **(4-1)** completely disappeared. The solvent was reduced to a minimum under vacuum and the imidazolium chloride salts formed were removed by filtration. The monomer was purified by neutral alumina column chromatography using hexane as the eluent. After purification, 3.23g of compound **(4-3)** was collected as a clear oil (Yield= 93%). $^{1}$H NMR (300MHz, $CDCl_3$): $\delta$(ppm) 5.78-5.95 (m, 2H), 4.89-5.05 (m, 4H), 3.43 (d, J=7.2 Hz, 2H), 2.05 (d, J=7.1 Hz, 4H), 1.35 (m, 32H), 0.11 (s, 9H); $^{13}$C NMR (75MHz, $CDCl_3$): $\delta$(ppm) 139.0, 114.3, 66.1, 40.5, 34.0, 31.1, 30.3, 29.8, 29.7, 29.3, 29.2, 27.1, -0.2; FT-IR: 3077, 2925, 2854, 1641, 1466, 1250, 1091, 992, 909, 877, 840, 745 $cm^{-1}$.

**1,1,1,3,3-pentamethyl-3-((2-(undec-10-en-1-yl)tridec-12-en-1-yl)oxy)disiloxane(4-5):** The same procedure described for the synthesis of **(4-3)** was used for the synthesis of **(4-5)** using 1-chloro-1,1,3,3,3-pentamethyldisiloxane (1.83g, 9.88 mmol)**.** After purification, 3.46g of compound **(4-5)** was collected as a clear oil (Yield= 85%). $^{1}$H NMR (300 MHz, $CDCl_3$): δ(ppm) 5.92-5.72 (m, 2H), 5.06-4.88 (m, 4H), 3.56-3.45 (d, 2H), 2.04 (q, *J* = 7.0 Hz, 4H), 1.52-1.15 (m, 32H), 0.12 (s, 15H). $^{13}$C NMR (75 MHz, $CDCl_3$): δ(ppm) 139.24, 114.04, 65.49, 40.06, 33.81, 30.98, 30.12, 29.66, 29.63, 29.51, 29.45, 29.15, 28.95, 26.88, 1.56, 1.51. FT-IR: 3072, 2924, 2854, 1641, 1459, 1258, 1034, 909, 844, 797, 705 $cm^{-1}$. HRMS Actual $[M-H]^+$=495.4589 Theory $[M-H]^+$=459.4132.

**3-((2-allylpent-4-en-1-yl)oxy)-1,1,1,3,5,5,5-heptamethyltrisiloxane (4-7):** The same procedure described for the synthesis of **(4-3)** was used for the synthesis of **(4-7)** using 3-chloro-1,1,1,3,5,5,5-heptamethyltrisiloxane (2.54g, 9.88 mmol)**.** After purification, 4.32g of compound **(4-7)** was collected as a clear oil (Yield= 91.5%).$^{1}$H NMR (300 MHz, $CDCl_3$): 5.86-5.74 (m, 2H), 5.05-4.88 (m, 4H), 3.45 (d, *J* = 5.2 Hz, 2H), 2.08 (q, 4H), 1.30-1.23 (m, 32H), 0.13 (s, 18H), 0.09 (s, 3H). $^{13}$C NMR (75 MHz, $CDCl_3$): 139.23, 114.03, 65.62, 40.35, 33.79, 30.94, 30.05, 29.61, 29.59, 29.48, 29.13, 28.93, 26.85, 25.11, 1.52, 1.43. FT-IR: 3086, 2926, 2855, 1644, 1540, 1460, 1352, 1250, 1214, 1131,1068, 904, 880, 842, 794, 742, 688 $cm^{-1}$.

**Tris(trimethylsilyl) (2-(undec-10-en-1-yl)tridec-12-en-1-yl) silicate (4-9):** The same procedure described for the synthesis of **(4-3)** was used for the synthesis of **(4-9)** using 3-chloro-1,1,1,5,5,5-hexamethyl-3-((trimethylsilyl)oxy)trisiloxane (3.27g, 9.88 mmol)**.** After purification, 5.00g of compound **(4-9)** was collected as a clear oil (Yield=

94%).$^{1}$H NMR (300 MHz, $CDCl_3$): 5.89-5.71 (m, 2H), 5.05-4.88 (m, 4H), 3.52 (d, 2H), 2.04 (q, *J* = 7.1 Hz, 4H), 1.53-1.06 (m, 32H), 0.11 (s, 27H). $^{13}$C NMR (75 MHz, $CDCl_3$): δ(ppm) 139.24, 114.04, 65.49, 40.06, 33.82, 30.99, 30.12, 29.66, 29.63, 29.51, 29.15, 28.95, 26.89,1.56. FT-IR: 3034, 2925, 2854, 1642, 1455, 1250, 1067, 909, 842, 788, 751 $cm^{-1}$. GC-CI-MS: Actual $[M+NH4]^+$ = 662.4833 Theoretical $[M+NH4]^+$ = 662.4846

#### 4.5.2.2 Polymer Synthesis

##### General Metathesis Conditions

All monomers and dibenzylcarbonate were degassed for 24 hours before polymerization. The monomer and solvent mixture was injected into a 100 mL dried Schlenk tube equipped with a stir bar under argon. The second generation Grubbs' catalyst (1mol %) was added to the Schlenk tube, and the mixture was allowed to stir for 30 min at 50°C with slow exposure to moderate vacuum, yielding slow bubbling of ethylene. The viscosity increased quickly, allowing the polymer to precipitate from the solution within 3 hours and slowing the stirring. After 24 hours, additional catalyst was added to the polymerization to ensure maximum possible couplings. Due to the viscosity of the polymer, proper mixing of the polymer with the remaining solution was performed manually, using an external magnet to move the stir bar. The reaction was allowed to go on for another 24 hours, after which, it was quenched in toluene with a few drops of ethyl vinyl ether. Since the polymers were insoluble in toluene, even at high temperature, the polymer was allowed to sit in the solution for 24 hours in order to ensure that as much as possible of the catalyst and monomer were removed. The solvents were evaporated under vacuum, yielding highly elastic yellow polymers.

**UP(4-3) synthesis:** 3g of **(4-3)** was reacted in 1mL of dibenzylcarbonate with 1mol % of **(G2)** for 24 hours at 50°C under vacuum. An additional 1mol % of **(G2)** was added to the reaction allowing it to react for another 24 hours.

FT-IR: 2945, 2854, 1250, 968, 840, 753, 722 $cm^{-1}$. DSC results: $T_g$ (glass transition) = -65.2°C

**UP(4-5) synthesis:** 3.2g of **(4-5)** was reacted in 1mL of dibenzylcarbonate with 1mol % of **(G2)** for 24 hours at 50°C under vacuum. An additional 1mol % of **(G2)** was added to the reaction allowing it to react for another 24 hours.

FT-IR: 2922, 2852, 1748 (solvent), 1456, 1392, 1257, 1032, 966, 845, 796, 749, 695 $cm^{-1}$. DSC results: $T_g$ (glass transition) = -71.0°C, $T_m$ (melting peak) = 28.7°C

**UP(4-7) synthesis:** 4g of **(4-7)** was reacted in 1mL of dibenzylcarbonate with 1mol % of **(G2)** for 24 hours at 50°C under vacuum. An additional 1mol % of **(G2)** was added to the reaction allowing it to react for another 24 hours. FT-IR: 2924, 2853, 1459, 1251, 1054, 966, 838, 753, 691 $cm^{-1}$. DSC results: $T_m$ (melting peak) = -10.0°C and 21.6°C, $T_c$ (recrystallization peak) = -12.5°C

**UP(4-9) synthesis:** 4.5g of **(4-9)** was reacted in 1mL of dibenzylcarbonate with 1mol % of **(G2)** for 24 hours at 50°C under vacuum. An additional 1mol % of **(G2)** was added to the reaction allowing it to react for another 24 hours. FT-IR: 2920, 2850, 1502, 1458, 1392, 1258, 1077, 964, 909, 791, 738, 696 $cm^{-1}$. DSC results: $T_m$ (melting peak) = 28.4°C

CHAPTER 5
SILOXANE FUNCTIONALIZED POLYETHYLENE VIA HYDROSILYLATION

## 5.1 Overview

Hydrosilylation (or hydrosilation), which involves an insertion/addition reaction, is the most practical and popular method used for the synthesis of organosilicon compounds.[171] It involves the addition of a silicon hydride (Si-H) to unsaturated bonds such as alkenes or alkynes in the presence of a transition metal complex catalyst, as illustrated in Figure 5-1.

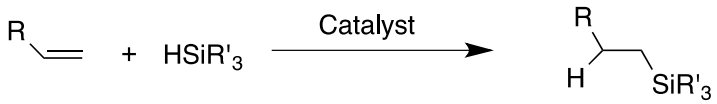


Figure 5-1. Alkene hydrosilylation.

The various advantages of hydrosilylation reactions include high yields, short reaction times, negligible side products, mild reaction conditions and a variety of compatible commercially available silicones.[171] Even though many catalysts have been developed for this application, the platinum-based Speier and Karstedt catalysts remain the most widely used hyrdosilylation catalysts due to their high activity.[172]

Though not as popular, hydrosilylation can also occur between Si-H and C=O to form Si-O-C linkages as shown in Figure 5-2. Ruthenium-, rhodium- and palladium-based catalysts are mainly used for this reaction.[173-175] These reactions occur under completely neutral conditions and do not require any product purification, which is important since the Si-O-C bonds are susceptible to acid- or base-catalyzed reactions. Another advantage for this method is the production of an Si-O-C functionality which is connected to a secondary carbon. Compared to Si-O-C linkages to primary carbons, connection to a secondary carbon leads to higher stability towards hydrolysis.[176]

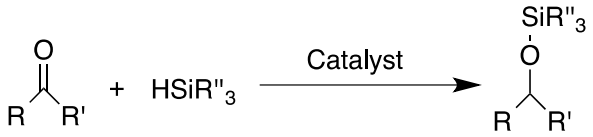


Figure 5-2. Ketone hydrosilylation.

This chapter will discuss the use of hydrosilylation reactions with a variety of catalysts to produce siloxane branched polyethylene using readily available silicones. This study includes pre-polymerization functionalization as well as post-polymerization functionalization.

## 5.2 Results and discussion

### 5.2.1 Pre-polymerization functionalization

As mentioned previsously, hydrosilylation reactions usually occur between a silicone and an alkene. If hydrosilylation is used directly with the α,ω-diene precursor shown in Figure 5-3, the silicone will react with the terminal alkenes resulting in a final product that can no longer be able to undergo ADMET polymerization. Therefore, an indirect attachment method was explored.

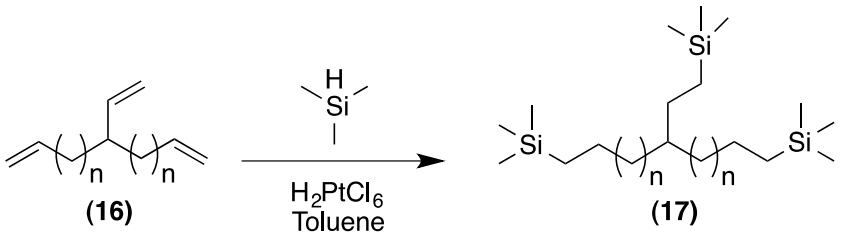


Figure 5-3. Hydrosilylation reaction of an α,ω-diene precursor.

In a recent study, siloxanes have been used as solubilizing side chains for conjugated polymers.[177] Alkene side chains were added onto an isoindogo molecule via base-promoted N-alkylation, which were then reacted with 1,1,1,3,5,5,5-heptamethyltrisiloxane, as shown in Figure 5-4.

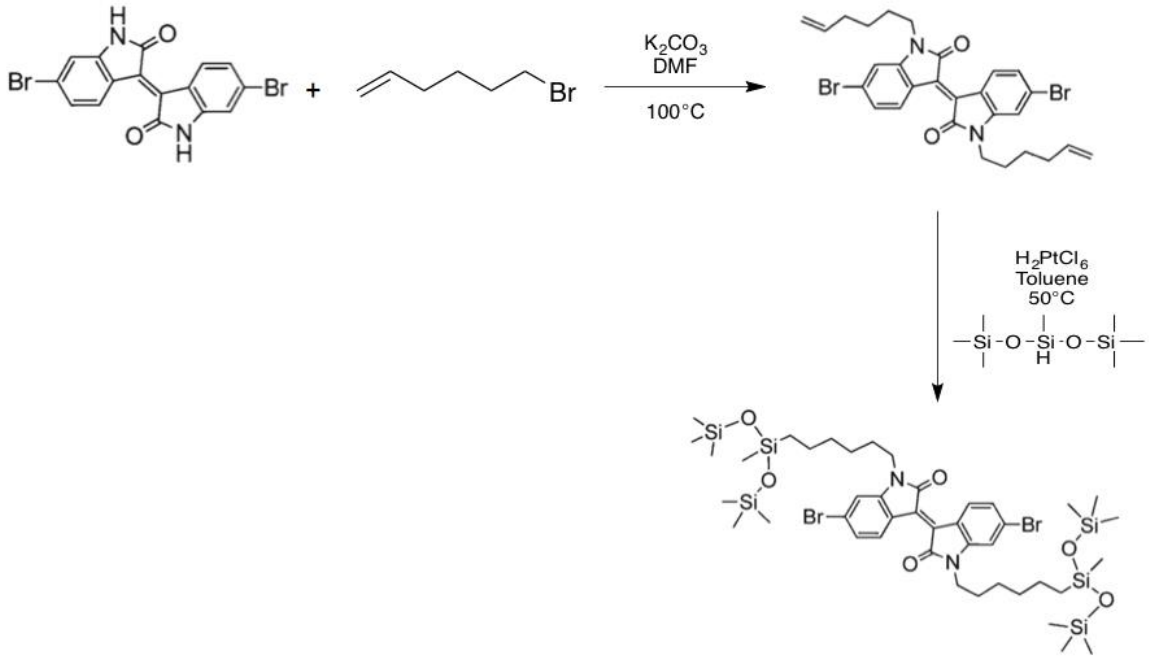


Figure 5-4. N-alkylation and hydrosilylation of core isoindigo molecule for transistor applications.

Inspired by this method, the hydrosilylation of allyl bromide **(5-1)** illustrated in Figure 5-5 was attempted with 1,1,1,3,5,5,5-heptamethyltrisiloxane using the conditions of Bao and coworkers. Allyl bromide was picked because of its bifunctionality; the allyl group can first undergo hydrosilylation leaving the bromine to undergo a Grignard reaction for attachment to the diene precursor as shown in Figure 5-5.

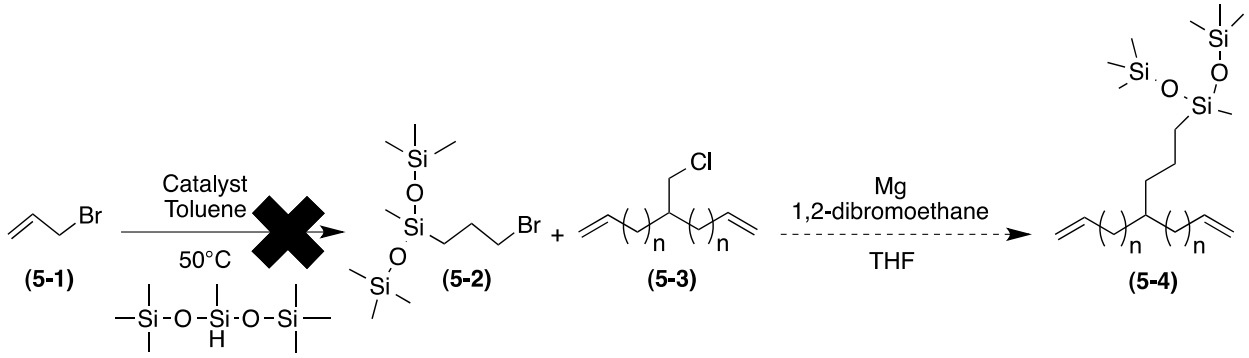


Figure 5-5. Unsuccessful hydrosilylation of allyl bromide.

The hydrosilylation was unsuccessful using chloroplatinic acid catalyst ($H_2PtCl_6$) and no product was formed. The reaction was then attempted with two other hydrosilylation catalysts, Karstedt's catalyst and Grubbs' catalyst, with no success for either. The starting material was intact in all three cases. The non-reactivity of the allyl bromide **(5-1)** towards the silicone hydride using three different catalysts could be explained by the proximity of the alkene and the bromine, which hinders the access of the catalyst to the reactive alkene. Using an alkene bromide with longer spacing between the two functionalities would lead to much longer branches and therefore was not explored.

### 5.2.2 Post-polymerization functionalization

#### 5.2.2.1 Post-polymerization functionalization of unsaturated polyethylene

High density polyethylene can be modeled through ADMET polymerization of 1,9-decadiene followed by hydrogenation, as shown in Figure 5-6.[178]

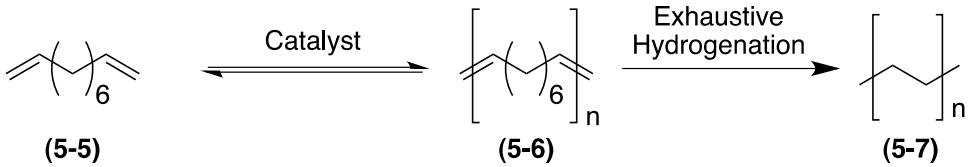


Figure 5-6. ADMET synthesis of high density polyethylene.

Instead of undergoing exhaustive hydrogenation, the unsaturated polymer **(5-6)** can undergo hydrosilylation, leading to branching within the polymer as shown in Figure 5-7. This method would not yield precisely branched polyethylene due to two possible reaction sites for each unsaturation, leading to possible distances between the branches of 6,7 or 8 methylene units. Using this functionalization method would allow us to determine if the differences in spacing between the branches would affect extrusion

capabilities in comparison with siloxane branches precisely placed on the polyethylene backbone.

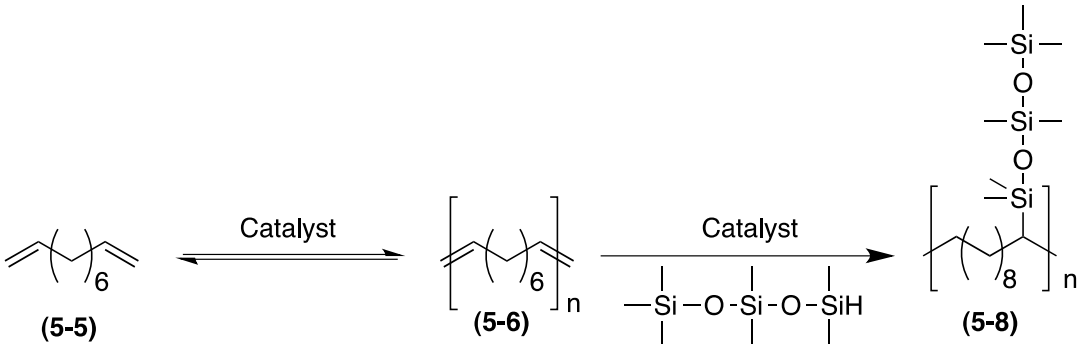


Figure 5-7. Hydrosilylation of unsaturated polyethylene.

Even though hydrosilylation can occur at room temperature, the reactions were conducted at 45°C in THF in order to solubilize the unsaturated polyethylene **(5-6)**. Two catalysts were used under the same reaction conditions: Speier's platinum catalyst and palladium-on-carbon. Disappearance of the double bond was monitored by $^{1}$H NMR and the reaction was complete after 64 hours. The polymers were precipitated in cold methanol, and then filtered to yield a gray powder. The polymers obtained were similar in shape and consistency to ADMET high density polyethylene as illustrated in Figure 5-8, rather than the elastic looking siloxane branched polyethylene synthesized in Chapter 4.

Figure 5-8. **UP(4-9)** (left), high density polyethylene (middle) and **(5-8)** (right).

Because the pure polymers were insoluble in all solvents, their structures could not be assessed by NMR. The FT-IR spectra in Figure 5-9 of the unsaturated polyethylene **(5-6)** and the products obtained from the reaction, allowed us to have a better understanding of the reaction that occurred.

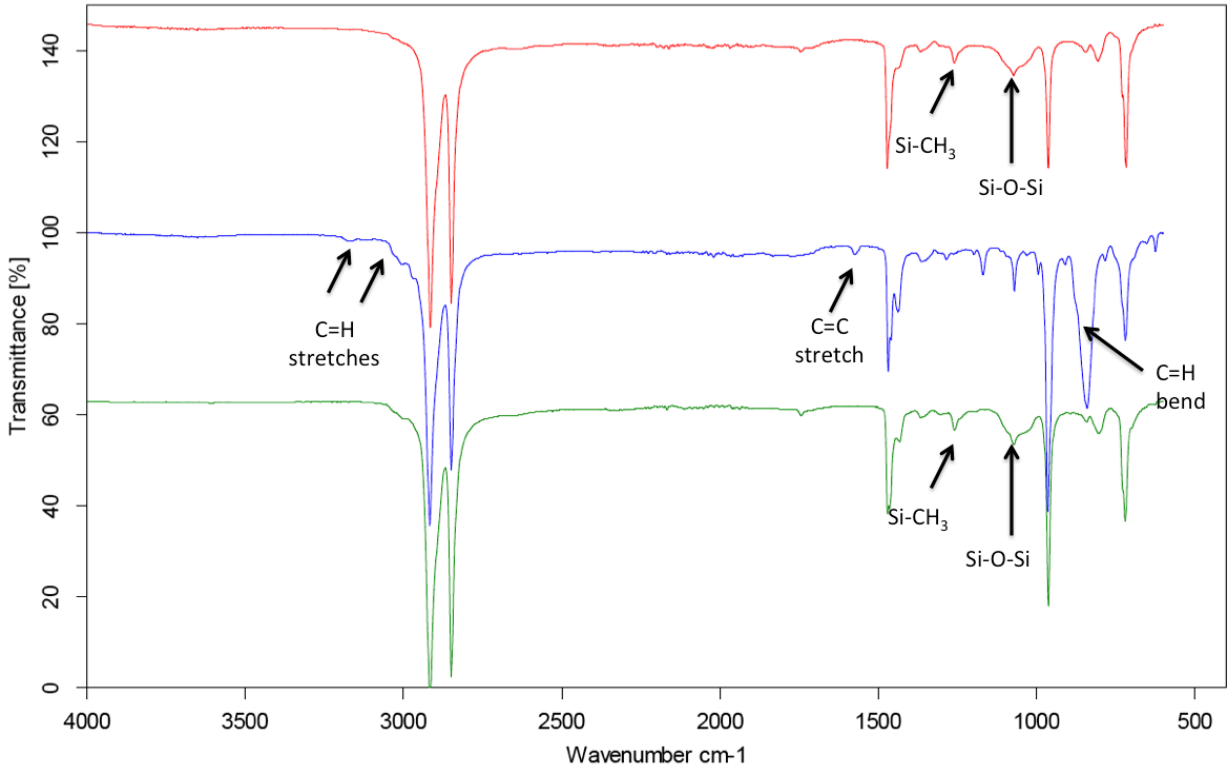


Figure 5-9. FT-IR comparison of compounds **(5-6)** (blue), and palladium catalyzed **Pd(5-8)** (red), and Speier's catalyzed **Pt(5-8)** (green)**.**

The disappearance of the alkene peaks seen in the unsaturated polymer **(5-6)** at 3100 $cm^{-1}$, 1660 $cm^{-1}$ and 841 $cm^{-1}$ confirms that the unsaturations have completely reacted. The very weak silicon peaks, which are usually very sharp, are noteworthy, especially the $Si\text{-}CH_3$ peak at 1250 $cm^{-1}$. This observation led us to conclude that even though the hydrosilylation reaction did occur, the main reaction was the hydrogenation of the polymer. This explains as well the difference in shape noticed between these polymers and the siloxane polymers from Chapter 4.

The thermal degradation behavior of these polymers is shown in the TGA thermograms in Figure 5-10. These were measured in an inert atmosphere ($N_2$), as percentage of weight loss versus temperature in the 0°C-500°C range. The thermograms for the unsaturated polyethylene **(5-6)** and high density polyethylene **(5-7)** are included for comparison.

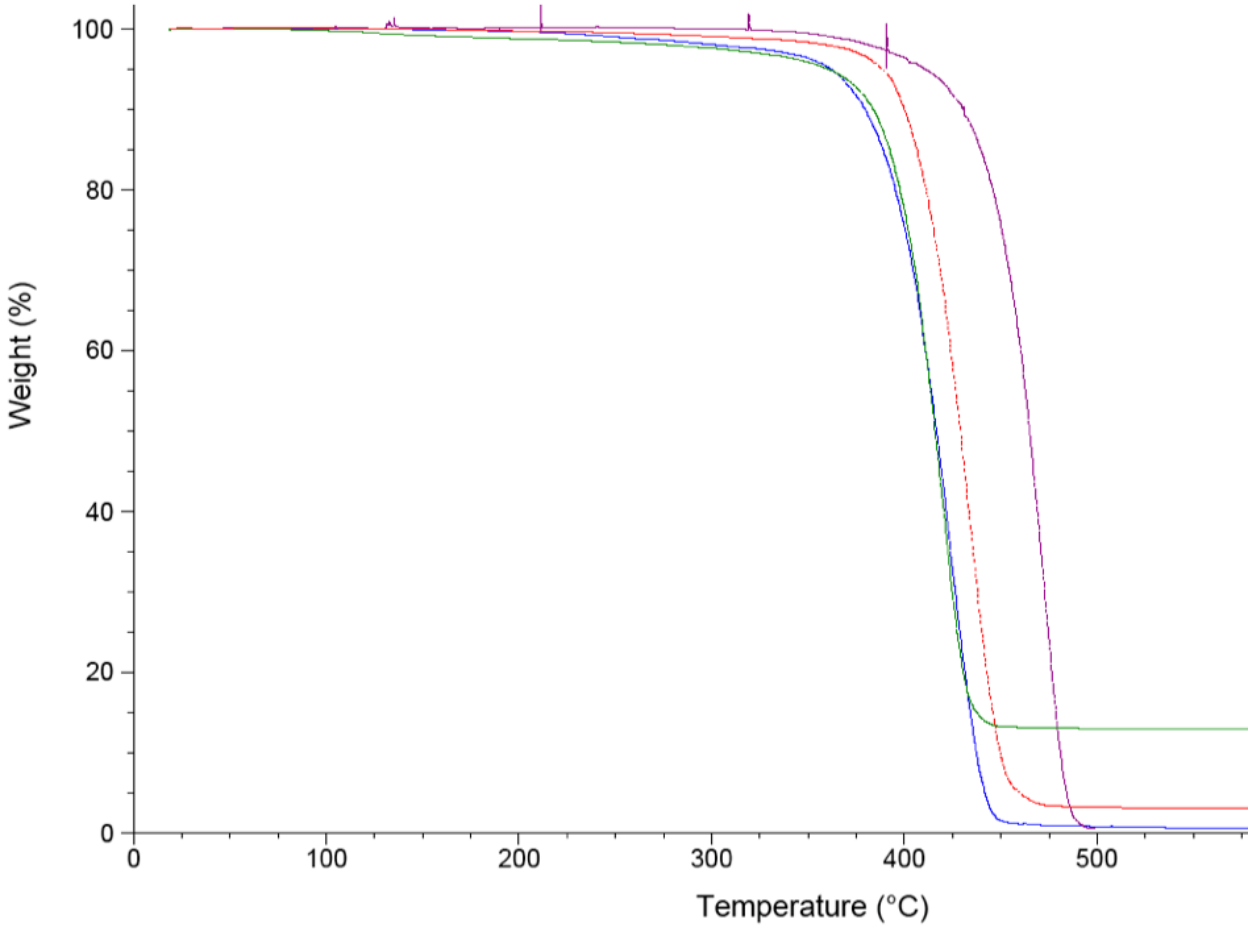


Figure 5-10. TGA thermograms of unsaturated polyethylene **(5-6)** (blue), palladium catalyzed **Pd(5-8)** (red), Speier's catalyzed **Pt(5-8)** (green) and ADMET PE **(5-7).**

We can see in these thermograms that all polymers are stable up to high temperatures with the palladium catalyzed **Pd(5-8)** polymer being a little more stable than Speier's catalyzed **Pt(5-8)**. Both siloxane functionalized polymers show one weight loss temperature, as opposed to the two weight losses noted for the polymers

synthesized in Chapter 4. This confirms the limited functionalization of the polymers observed in the IR spectra.

The thermal behavior of the polymers was also analyzed by differential scanning calorimetry (DSC), and the melting temperatures ($T_m$) were recorded as the temperature at the peak of the melting transition temperature in the second heating scan. The data were collected by scanning samples from -80°C to the temperature recorded at 5% weight loss in the TGA thermogram. The rate of cooling and heating was 10°C/min and values were recorded for the second heating and cooling ramps.

Table 5-1. Thermal analysis of the unsaturated polymers.

| Polymer | $T_m$ (°C)[a] |
|---|---|
| **(5-6)** | 70.7 |
| **Pd(5-8)** | 82.3 |
| **Pt(5-8)** | 111.4 |
| **(5-7)** | 130.1 |

a. Temperature at maximum of melting peak;

The DSC heating traces for polymers **(5-6), Pd(5-8)** and **Pt(5-8)** are shown in Figure 5-11. Thermograms of all three polymers show a melting temperature, with **Pd(5-8)** and **Pt(5-8)** showing broad melting peaks. This broad melting peak confirms the irregularity of the siloxane branches on the polymer backbone. The melting temperature recorded for **Pt(5-8)** is considerably higher than that of **Pd(5-8)** and suggests that **Pd(5-8)** has a greater number of flexible siloxane branches in comparison to **Pt(5-8)** which leads to a lower melting temperature. No glass transition was observed for any of the

polymers, indicating that the number of siloxane branches present on these polymers is not sufficient to affect their thermal behavior.

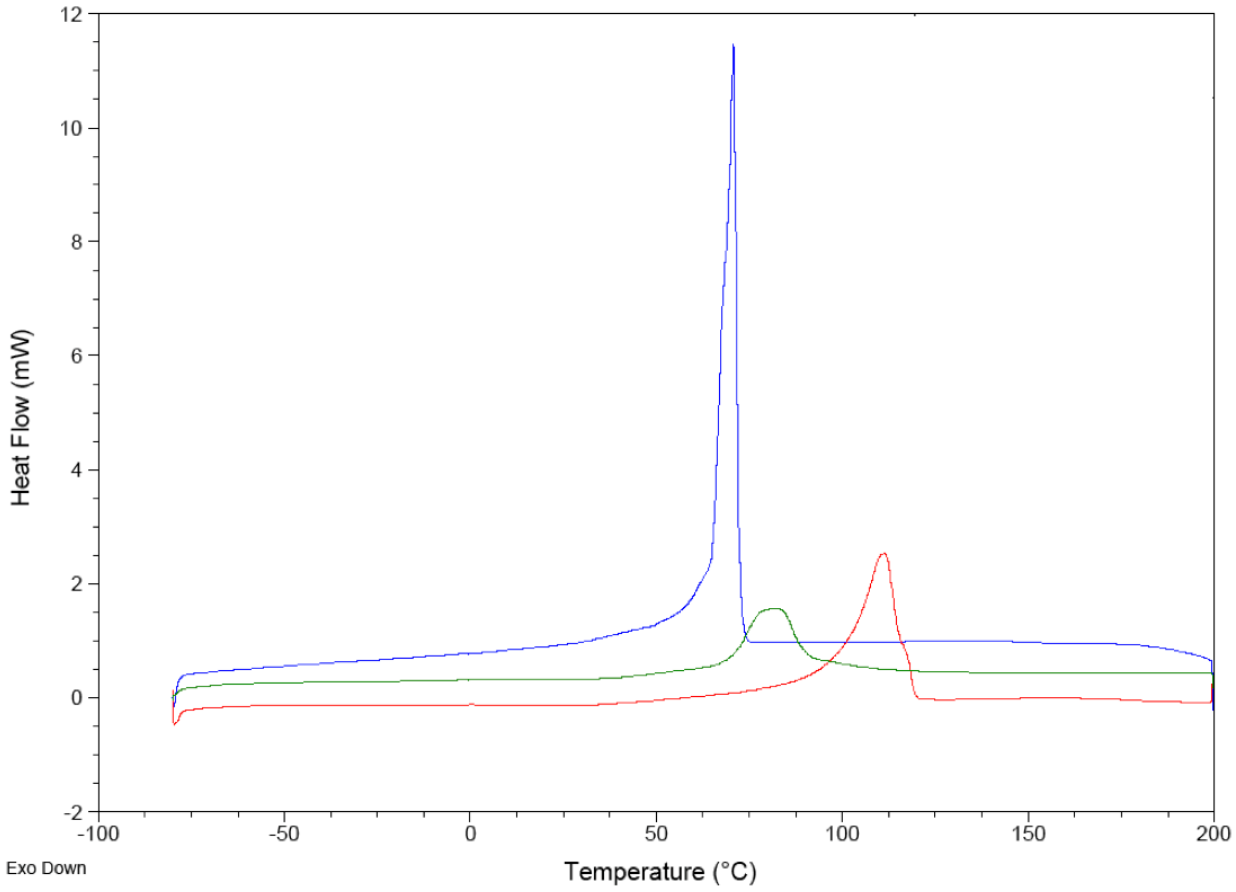


Figure 5-11. DSC heating thermograms of unsaturated polyethylene **(5-6)** (blue), Palladium catalyzed **Pd(5-8)** (red), Speier's catalyzed **Pt(5-8)** (green).

### 5.2.2.2 Post-polymerization functionalization leading to C-O-Si linkages

As discussed earlier, hydrosilylation reactions have been used with ketones to produce C-O-Si linkages in high yields. The synthesis of an α,ω-diene with a ketone branch can be easily obtained in three steps as shown in Figure 5-12.

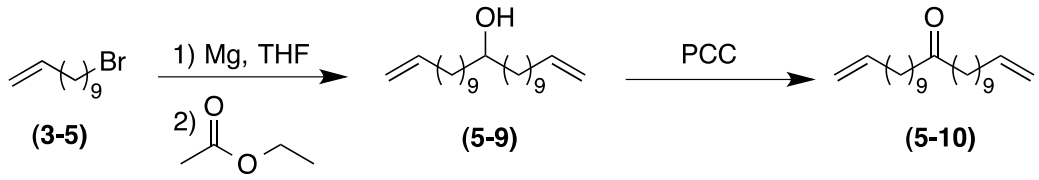


Figure 5-12. Synthesis of tricosa-1,22-dien-12-one **(5-10)**.

The 9-spacer bromide **(3-5)** is reacted with Mg to form a Grignard reagent followed by the addition of ethyl formate to form the secondary alcohol **(5-9),** which is then reacted with pyridinium chlorochromate (PCC) to produce the 9,9-ketone **(5-10)**. Since the catalysts used for the hydrosilylation of ketones are also reactive with alkenes, the ketone **(5-10)** was polymerized with Grubbs' 2nd generation catalyst and hydrogenated prior to performing the hydrosilylation reaction as shown in Figure 5-13.

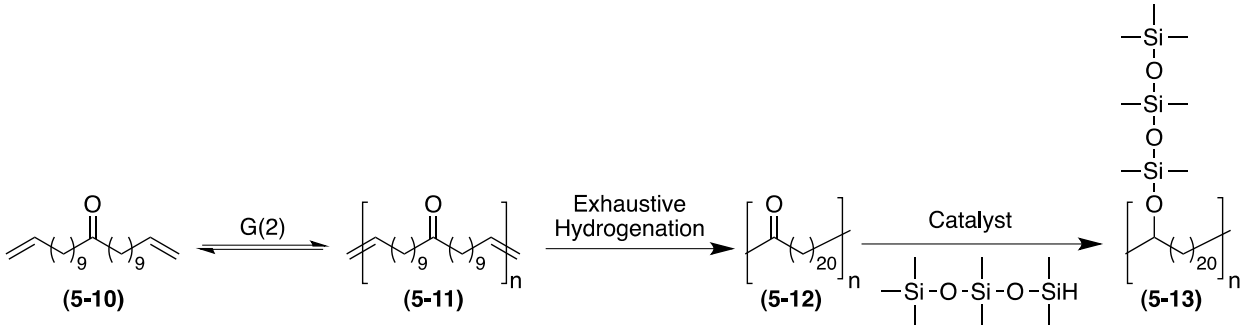


Figure 5-13. Post-polymerization hydrosilylation of ketone.

The ketone polymer in the form of a white solid was dissolved in a minimal amount of dry toluene at 60°C prior to the addition of 1.2mol% of the palladium-on-carbon catalyst and the siloxane. After the reaction was allowed to proceed for 24 hours, the solvent was evaporated under vacuum and the polymer was precipitated in methanol. The polymer was filtered from the solution and dried under vacuum overnight. The FT-IR spectrum of the polymer, Figure 5-14, showed partial reduction of the ketone into the alcohol rather than the expected hydrosilylation reaction product. The carbonyl

peak at 1747 $cm^{-1}$ was still present in the spectra in addition to a new peak at 3300 $cm^{1}$, which is representative of the alcohol. A peak was observed at 1263 $cm^{-1}$, which can be attributed to either the C-O stretch of the alcohol or the presence of the $(CH_3)_2$-Si-O- functionality. For the $(CH_3)_2$-Si-O- group, a second weaker peak is expected at approximately 800 $cm^{-1}$, which we can clearly see. Therefore, we can confirm that, in addition to the reduction of the ketone to the alcohol, partial hydrosilylation of the polymer occurred.

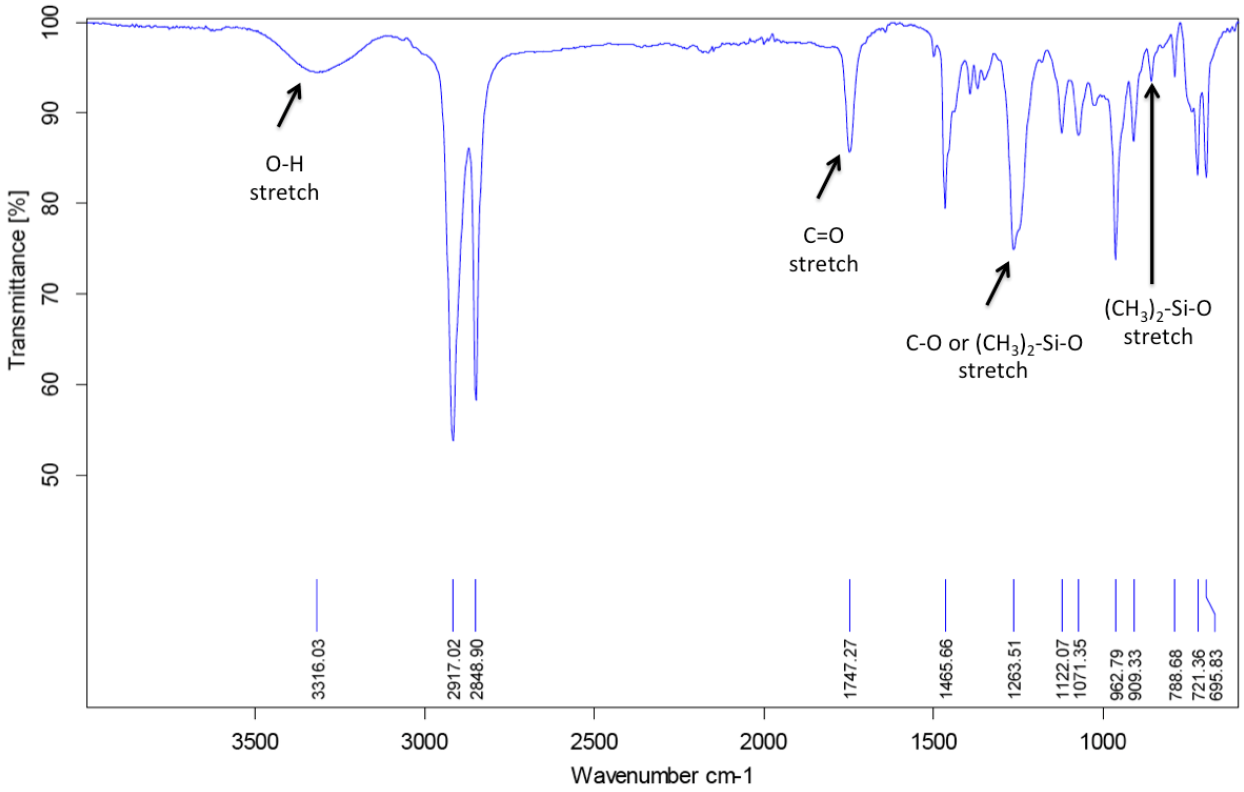


Figure 5-14. FT-IR spectrum for post-polymerization hydrosilylation of ketone.

The minimal incorporation of siloxane branches did not affect the thermal behavior of the polymers, and no difference was noted in either the TGA or DSC data obtained for the polymers.

### 5.2.2.3 Dehydrogenative coupling with alcohol

**Post-polymerization:**

Although hydrosilylation is the most widely applied reaction for preparation of silicones, its use has been limited by difficulties in the preparation of required 1-alkenylated organic precursor. Therefore, alternative reactions between alcohols and Si-H have been investigated, as shown in Figure 5-15.

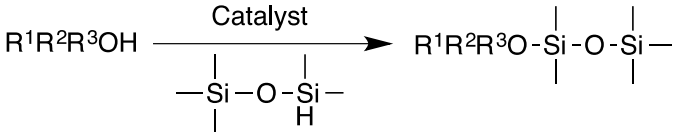


Figure 5-15. Dehydrogenative coupling of silicones and alcohol.

Palladium-on-carbon and tris(pentafluorophenyl)borane catalysts were successfully used for this dehydrogenative coupling with hydrogen gas as the only by-product.[176] As part of the present project, this reaction was performed with the polymerized and hydrogenated secondary alcohol **(5-9),** as shown in Figure 5-16.

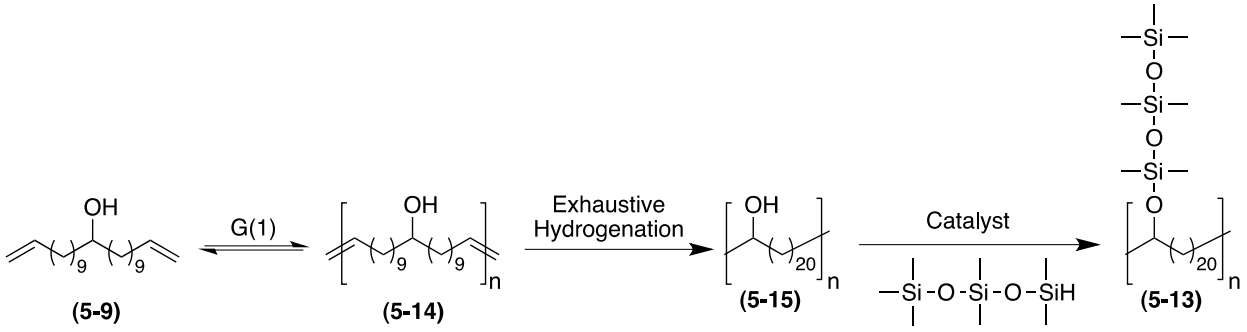


Figure 5-16. Synthetic route to post-polymerization dehydrogenative coupling of 1,1,1,3,3,5,5-heptamethyldisiloxane and ADMET secondary polyol.

The secondary alcohol was selected because the trends in reaction rates and yields for these reactions were found to be opposite to those of conventional reactions, with sterically bulky alcohols being silylated much faster than less hindered primary

alcohols. In addition to that, the product formed was expected to be more resistant to hydrolysis in comparison to its primary analogue.

The saturated alcohol polymer **(5-15)** is soluble only in a mixture of methanol/toluene (5/95). As an alcohol, methanol can also undergo the coupling reaction to produce the side product shown in Figure 5-17. However, this side reaction is not an issue if an excess of 1,1,1,3,3,5,5-heptamethyldisiloxane is used, for two reasons: (1) as a primary alcohol, methanol would be expected to be less reactive to the dehydrogenative recation than the secondary polymer polyol; and (2) the byproduct obtained is liquid and soluble in a variety of solvents, while the polymer itself is solid and insoluble.

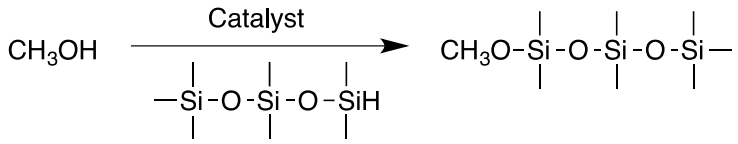


Figure 5-17. Methanol dehydrogenative coupling by-product.

Polymer **(5-15)** was dissolved in a mixture of methanol/toluene (5/95) at 60°C under argon. The catalyst was added to the reaction mixture followed by the drop-wise addition of 1,1,1,3,3,5,5-heptamethyldisiloxane. Hydrogen bubbling was observed instantly and the reaction was allowed to proceed for 24 hours. While still warm, the polymer was precipitated in cold methanol, followed by vacuum filtration to afford a white polymer. The FT-IR spectrum, Figure 5-18, showed that no reaction had occurred and that the alcohol polymer was still intact in both cases with no representative peaks of siloxane. The vigorous bubbling that was observed can be attributed to the methanol reacting with the 1,1,1,3,3,5,5-heptamethyldisiloxane (Figure 5-17).

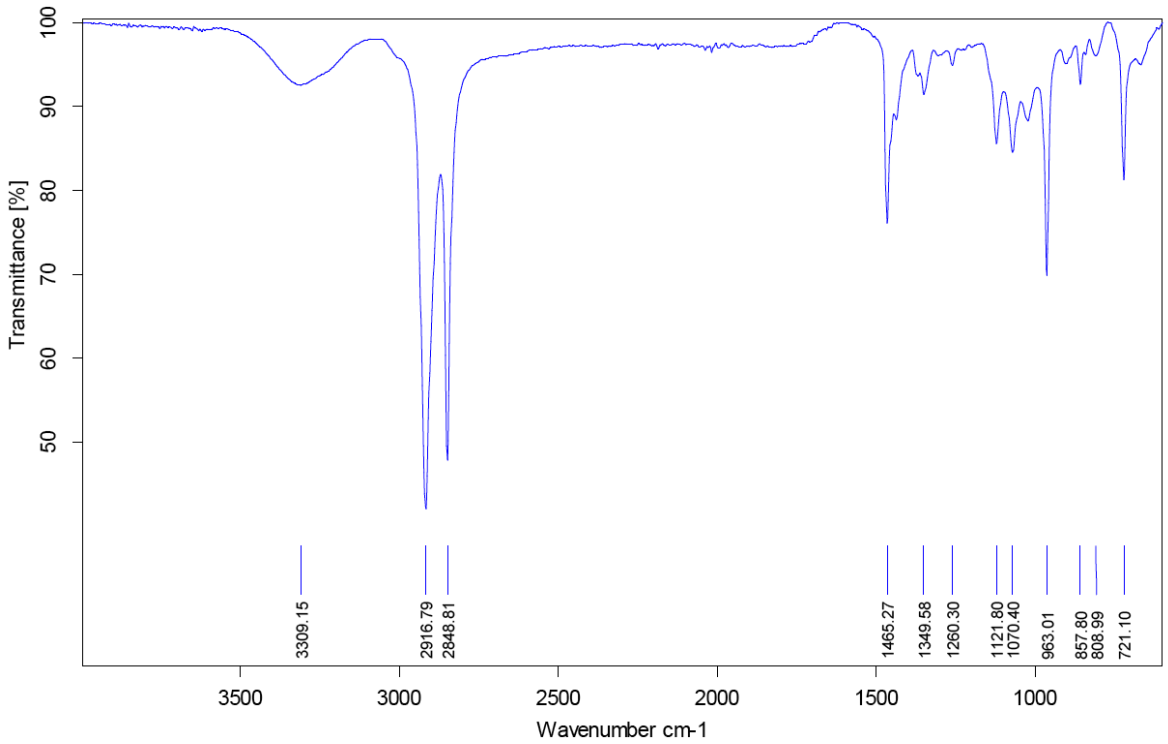


Figure 5-18. FT-IR spectrum of alcohol dehydrogenative coupling product showing no presence of siloxane peaks.

Palladium-on-carbon catalyst is known to be used for hydrogenation reactions, but tris(pentafluorophenyl)borane is a mild catalyst that has shown no reactivity towards alkenes and alkynes. Therefore, the dehydrogenative coupling reaction with tris(pentafluorophenyl)borane as the catalyst was attempted prior to polymerization using tricosa-1,22-dien-12-ol **(5-9)**.

**Pre-polymerization:**

The pre-polymerization dehydrogenative coupling reaction between tricosa-1,22-dien-12-ol **(5-9)** and 1,1,1,3,3,5,5-heptamethyldisiloxane in presence of tris(pentafluorophenyl)borane is shown in Figure 5-19.

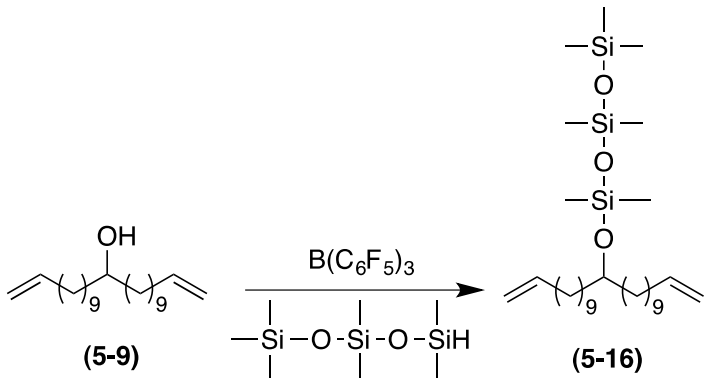


Figure 5-19. Pre-polymerization dehydrogenative coupling of tricosa-1,22-dien-12-ol **(5-9)** with 1,1,1,3,3,5,5-heptamethyldisiloxane.

The solid monomer **(5-9)** was dissolved in a minimal amount of dry toluene, to which was added 1mol% of tris(pentafluorophenyl)borane. Then, 1,1,1,3,3,5,5-heptamethyldisiloxane was added drop-wise to the reaction and instant vigorous bubbling was observed. The reaction was allowed to stir under argon for 24 hours at room tempreature. The catalyst was removed by filtration, and the solvent was evaporated under vacuum to produce compound **(5-16)** with no further purification. Proton NMR comparison (Figure 5-20) of the starting compound **(5-9)** and the product **(5-16)** indicates that the reaction was complete because of the complete disappearance of the hydroxyl proton at 1.59 ppm, as well as the chemical shift observed for the hydrogen alpha to the hydroxyl from 3.6 ppm for the free alcohol to 3.75 ppm for the silicone functionalized alcohol. Two chemical shifts can be observed for the methyls connected to the Si atoms at 0.05 ppm for the RO-$SiMe_3$ hydrogens and at 0.1 ppm for the RO-$SiMe_2$-OR' hydrogens. The superimposed spectrum are shown in Figure 5-20.

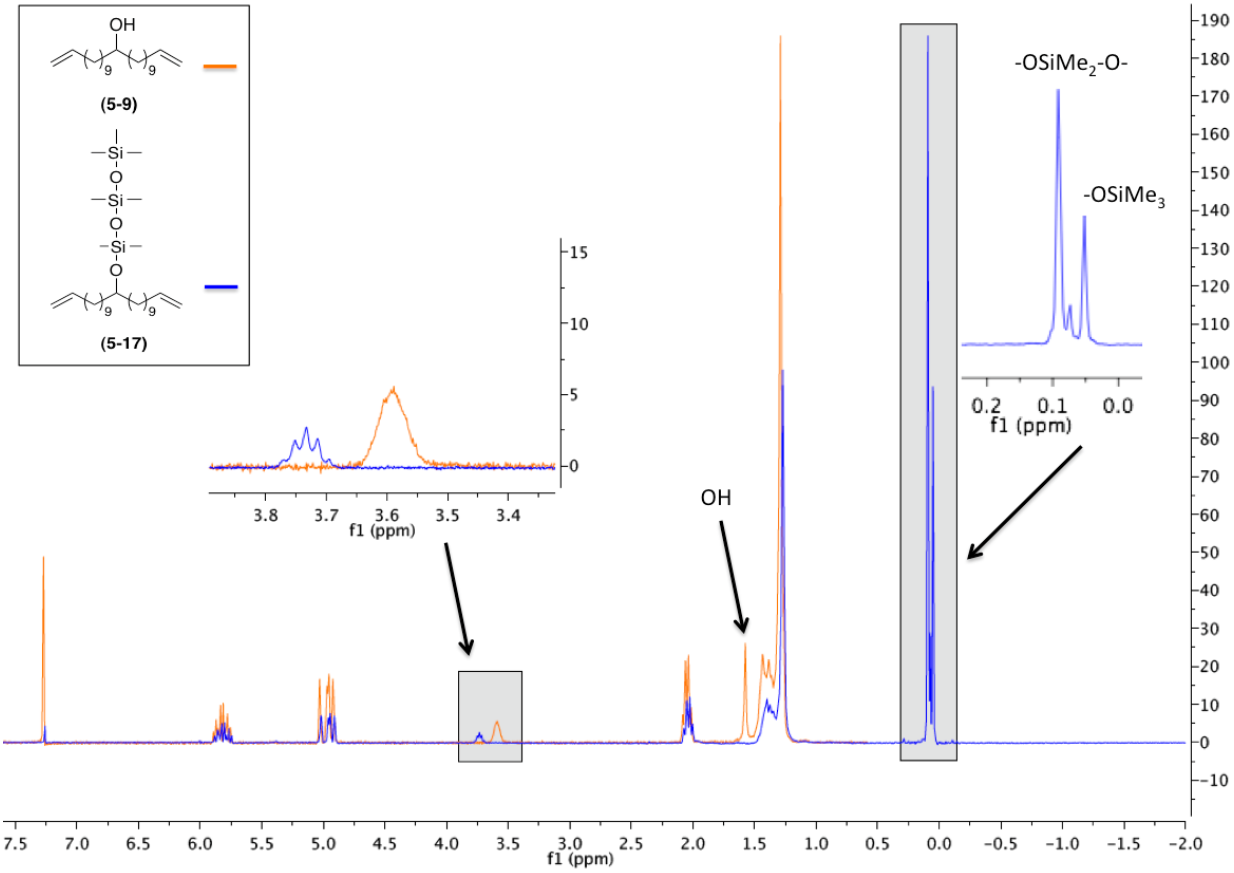


Figure 5-20. $^{1}$H NMR of **(5-9)** (orange) and **(5-16)** (blue).

The FT-IR spectrum of the product **(5-16)** in comparison to the starting material **(5-9)** shown in Figure 5-21 supports the observations made from the proton NMR. The disappearance of the OH stretch at 3300 $cm^{-1}$ and the absence of the Si-H peak in the region of 2800-2080 $cm^{-1}$ confirm that both starting materials have completely reacted. The peak corresponding to the $(CH_3)_3$-Si-O- stretch is clearly observed, therefore confirming that no crosslinking has occurred. Finally the IR spectrum of the monomer **(5-16)** shows bands representative of both the siloxane Si-O-Si in the 1130-1000 $cm^{-1}$ region and the $(CH_3)_2$-Si-O- stretch in the 800 $cm^{-1}$ region.

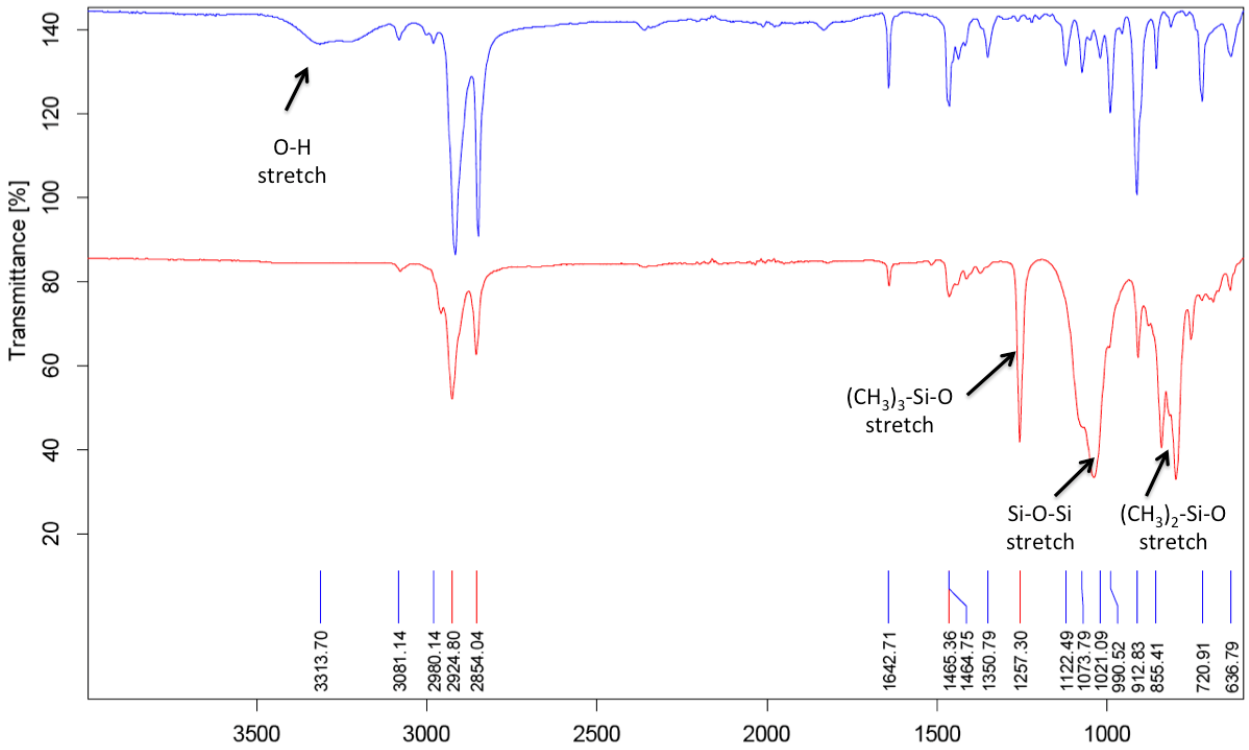


Figure 5-21. FT-IR spectra of **(5-9)** (blue) and **(5-16)** (red).

**(5-16)** (2.5g) was polymerized in 1mL of dibenzyl carbonate at 55°C, using 1mol % of 2nd generation Grubbs' to yield **UP(5-16)** shown in Figure 5-22. Thirty minutes after the addition of the catalyst, the formation of a viscous polymer was observed, and full vacuum was applied. Within 3 hours, stirring of the polymer was almost impossible, and the polymer precipitated from the solution. To insure that all the monomer had reacted, additional catalyst was added 24 hours later, and stirring was induced manually using a strong magnet on the outside of the flask, to move the stir bar. The polymerization was allowed to continue for another 24 hours after which a mixture of ethyl vinyl ether and toluene was used to quench the polymerization. The polymer **UP(5-16)** obtained was insoluble and has the same texture as the unsaturated polymers obtained in Chapter 4.

The standard spectroscopic measurments ($^{1}$H NMR, $^{13}$C NMR) and molecular weight determination by gel-permeation chromatography (GPC) could not be performed,

however, the structure of the polymer was analyzed by FT-IR and its thermal properties measured using DSC and TGA.

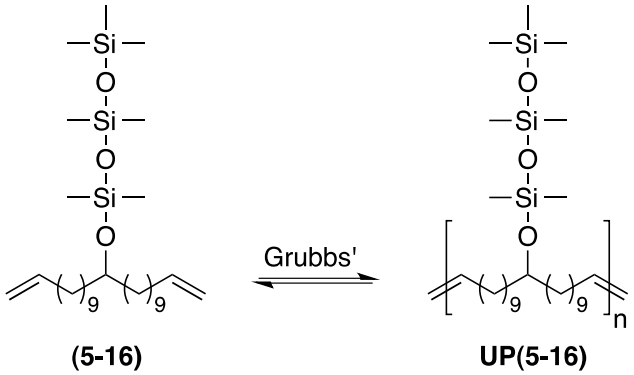


Figure 5-22. Polymerization of **(5-16)**.

The thermal degradation behavior of polymer **UP(5-16)** is shown in the TGA thermograms in Figure 5-23 and compared to the degradation behavior of **UP(4-9)**. These were measured in an inert atmosphere ($N_2$), as percentage of weight loss versus temperature in the 0°C-500°C range

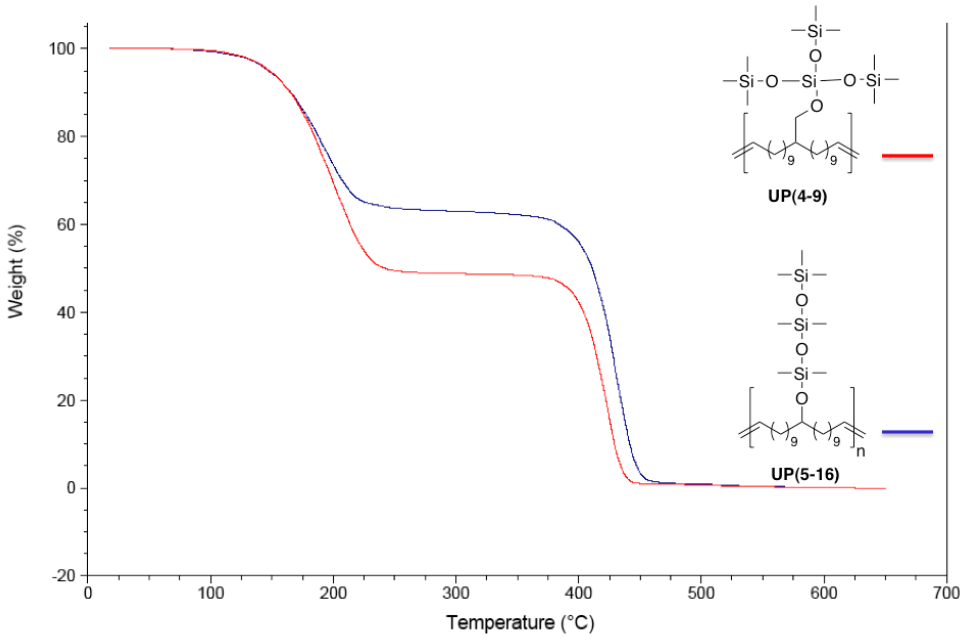


Figure 5-23. TGA thermograms of **UP(4-9)** (red) and **UP(5-16)**.

. Both polymers clearly show a comparable degradation behavior leading us to conclude that polymer **UP(5-16)** has a similar structure to **UP(4-9)**.

The DSC heating traces for polymers **UP(4-9)** and **UP(5-16)** are shown in Figure 5-24. Thermograms of both polymers are similar and show a cold crystallization peak followed by a melting peak around the same temperature. **UP(5-16)** shows two melting peaks, which can be due to the presence of both low and high molecular weight polymer.

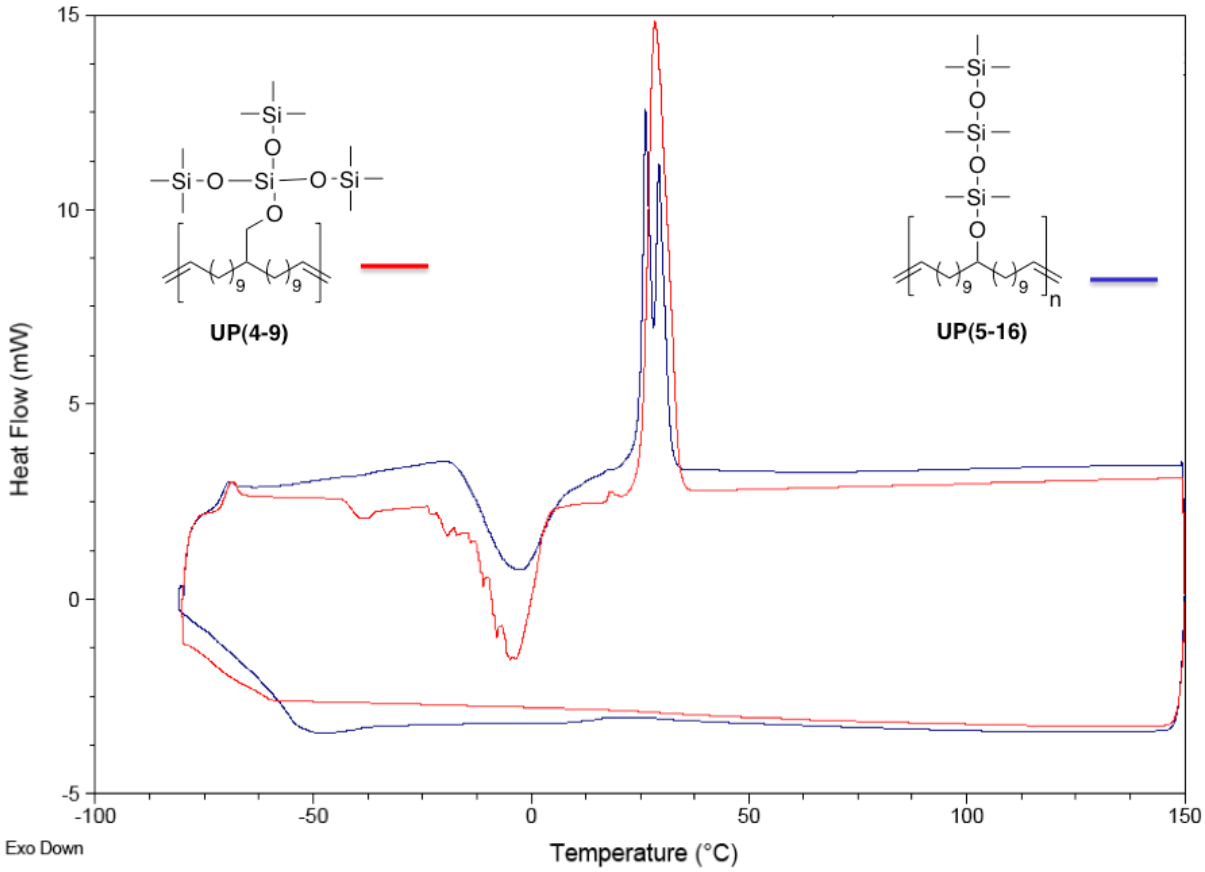


Figure 5-24. DSC thermograms of **UP(4-9)** (red) and **UP(5-16)**.

## 5.3 Conclusions

This chapter discussed the attachment of the siloxane branch on the polyethylene backbone via hydrosilylation and dehydrogenative coupling. Post-polymerization functionalization of the polyethylene backbone was not successful, and

only minimal functionalization occurred, while reduction reactions were predominant. The polymers obtained behaved like high density polyethylene, rather than polysiloxane.

The highlight of this chapter was the successful synthesis of a siloxane branched monomer using dehydrogenative coupling between the secondary alcohol monomer and a silicon-hydride. A total of two steps were required for the synthesis of the monomer, in almost quantitative yield, and only minimal purification was required. This method is very attractive as it can easily be scaled-up and adapted for industrial commercialization. In addition, there are various sizes of silicon-hydrides available commercially, which would allow synthesis of monomers with various siloxane branch sizes. The polymer **UP(5-16)** obtained through this method, showed similar degradation behavior and thermal behavior as polymer **UP(4-9)** obtained from the multi-step synthesis described in Chapter 4.

Now that an effective method has been identified for the synthesis of the siloxane branched monomer, the next step would be to synthesize families of polymers with various branch sizes and run lengths.

## 5.4 Experimental

### 5.4.1 Materials and Instrumentation

All silicones were purchased from Gelest and distilled over $CaH_2$ prior to use. All other materials were purchased from Aldrich and used without further purification unless noted. Grubbs 1$^{st}$ generation catalyst, bis(tricyclohexylphosphine)benzylidineruthenium (IV) dichloride (G1), was kindly provided by Materia, Inc. Anhydrous solvents were obtained from an anhydrous solvent system. All $^{1}H$ NMR and $^{13}C$ NMR were obtained on a Varian Mercury 300MHz spectrometer and recorded in $CDCl_3$. $^{1}H$ NMR and $^{13}C$

NMR shifts were referenced to residual signals from $CDCl_3$ ($^1H$ = 7.24 ppm and $^{13}C$ = 77,23 ppm). Mass spectrograms were aquired on a Thermo Scientific DSQ MS using the chemical ionization mode. Thin layer chromatography (TLC) was used to monitor all reactions and was performed on plastic backed neutral alumina plates. Column chromatography was performed using neutral alumina. Thermogravimetric analysis (TGA) was performed on TA Instruments TGA Q1000 Series using dynamic scans under nitrogen. Differential scanning calorimetry (DSC) analysis was performed using a TA Instruments Q1000 series equipped with a controlled cooling accessory (refrigerated cooling system) at 10°C/min. All samples were prepared in hermetically sealed pans (4-7 mg/sample) and were referenced to an empty pan. Melting temperatures were taken as the peak of the melting transition, glass transition temperatures as the mid point of a step change in heat capacity. Thermal experiments were conducted as follows: samples were heated through the melt to erase thermal history, followed by cooling at 10°C/min to -80°C, and then heated through the melt at 10°C/min. Data reported reflects this second heating scan. Gel permeation chromatography (GPC) was performed at 40 °C using a Waters Associates GPCV2000 liquid chromatography system with an internal differential refractive index detector and two Waters Styragel HR-5E columns (10 μm PD, 7.8 mm i.d., 300 mm length) using HPLC grade THF as the mobile phase at a flow rate of 1.0 mL/min. FT-IR data was gathered from a Bruker Vertex 80v using a Pike GladiATR stage and the data were processed using the OPUS 6.5 software.

### 5.4.2 Procedures

**3-(3-bromopropyl)-1,1,1,3,5,5,5-heptamethyltrisiloxane (5-2):** Allyl bromide **(5-1)** (1.50 g, 12.50 mmol) was dissolved in anhydrous toluene (15 mL) under an argon atmosphere. 1,1,3,3,5,5,5-heptamethyltrisiloxane (6.40 g, 28.75 mmol) was injected

through a septum, followed by the addition of a drop of Karstedt's catalyst (platinum-divinyltetramethyl-siloxane complex in xylene, 5 wt%). The resulting mixture was stirred at 50°C under argon for 48 hours. The reaction did not proceed and the starting material was recovered.

**Synthesis of unsaturated polyethylene (5-6):** Under constant argon flow, 2.5 g of 1,9 decadiene **(5-5)** was added to flame-dried Schlenk flask equipped with a magnetic stir bar. Grubbs 1st generation catalyst (1 mol%) was then added to the reaction mixture. The reaction was placed under high vacuum at 50°C while stirring. After 48 hours the reaction was quenched with a solution of 2mL of ethyl vinyl ether in 10mL of toluene. The solvents were reduced to a minimal amount under vacuum and the polymer was precipitated into 250mL of cold methanol and isolated via filtration. The polymer was characterized using $^{1}$H NMR and the molecular weight was measured by GPC. $^{1}$H NMR (300 MHz, $CDCl_3$): $\delta$(ppm) 5.55-5.35 (m, 2H), 2.05 ppm (q, J=7.0Hz, 4H), 1.40-1.21 (m, 8H). FT-IR: 2918, 2849, 1468, 1170, 1071, 965, 841, 720 $cm^{-1}$. GPC data (THF vs. polystyrene standards): $M_n$= 15,230 g/mol; PDI ($M_w$/ $M_n$)=2.20. DSC Results: $T_m$=70.7°C

**Palladium catalyzed synthesis of polymer Pd(5-8):** Unsaturated polyethylene (**5-6)** (0.25g, 2.27 mmol) was dissolved in a minimal amount of toluene under constant argon flow. Palladium-on-carbon (2mg) was added to the reaction mixture, which turned brown. 1,1,1,3,3-pentamethyldisiloxane (0.44 g, 2.95 mmol) was added to the reaction at 0°C and the reaction was stirred for 30 min, after which it was allowed to stir at room temperature for an hour and at 50°C overnight. The reaction was then sampled and assessed for complete conversion of the internal olefin by $^{1}$H NMR. Upon completion,

the catalyst was removed by filtration and the solvent was evaporated under vacuum to a minimal amount. The polymer was precipitated into 250mL of cold methanol for purification and was isolated via filtration. FT-IR: 2915, 2849, 1471, 1366, 1260, 1073, 963, 844, 805, 718 $cm^{-1}$. DSC Results: $T_m$=111.4°C

**Speir's catalyzed synthesis of polymer Pt(5-8):** Unsaturated polyethylene **(5-6)** (0.25g, 2.27 mmol) was dissolved in a minimal amount of toluene under constant argon flow. Speir's catalyst ($H_2PtCl_6$) (8mg) was added to the reaction mixture, which turned orange. 1,1,1,3,3-pentamethyldisiloxane (0.44 g, 2.95 mmol) was added to the reaction at 0°C and the reaction was stirred for 30 min, after which it was allowed to stir at room temperature for an hour and at 50°C overnight. The reaction was then sampled and assessed for complete conversion of the internal olefin by $^1$H NMR. Upon completion, the catalyst was removed by filtration and the solvent was evaporated under vacuum to a minimal amount. The polymer was precipitated into 250mL of cold methanol for purification and was isolated via filtration. FT-IR: 2917, 2849, 1470, 1364, 1260, 1073, 963, 803, 720 $cm^{-1}$. DSC Results: $T_m$=82.3°C

**Synthesis of tricosa-1,22-dien-12-ol (5-9):** A flame dried three-neck flask with a stir bar was charged with 40mL of THF and Mg (5.78 g, 237.7 mmol) under argon. The flask was chilled in an ice bath, and 1,2-dibromoethane (12.3 g, 65 mmol) was added to the solution and stirred at RT for 30 minutes. 11-bromo-1-undecene **(3-5)** (30.5 g, 130 mmol) was added drop-wise to the reaction mixture, which was refluxed for 24 hours. The reaction was then cooled to RT and ethyl formate (4.4 g, 59.4 mmol) was added to the reaction. The mixture was refluxed for another 24 hours under argon. The reaction was then cooled in an ice bath and neutralized with 1M HCl and extracted in ether. The

solvent was removed under vacuum, and the resulting white solid was recrystallized in acetone (Yield: 90%). $^{1}$H NMR (300 MHz, $CDCl_3$): $\delta$(ppm) 5.9-5.73 (m, 2H), 5.05-4.85 (m, 4H), 3.60 (q, J=6.4 Hz, 1H), 2.05 ppm (q, J=7.0Hz, 4H), 1.58 ppm (s,1H), 1.49-1.23 (m, 32H).$^{13}$C NMR (75 MHz, CDCl3): δ(ppm) 139.44, 114.28, 72.22, 37.7, 34.03, 29.92, 29.83, 29.77, 29.70, 29.35, 29.15, 25.87. HRMS Actual $[M]^+$=336.3308 Theory $[M]^+$=336.3314.

**Synthesis of tricosa-1,22-dien-12-one (5-10).** In a flame-dried 1L flask equipped with a stir bar, pyridinium chlorochromate (15.5 g, 71.90 mmol) and 15.5g of Celite were suspended in 100mL of dry dichloromethane. Tricosa-1,22-dien-12-ol **(5-9)** (16 g, 47.53 mmol) was dissolved in 30mL of dichloromethane and added drop-wise to the slurry. The reaction was stirred overnight and quenched with addition of 200mL of diethyl ether. The slurry was then filtered through a silica plug and the solvent was evaporated under vacuum. The crude ketone was then recrystallized in acetone to yield 13.5g of **(5-10)** (Yield: 85%). $^{1}$H NMR (300MHz, $CDCl_3$, ppm): δ= 5.9-5.7 (m, 2H); 5.05-4.85 (m, 4H); 2.41-2.32 (t, 4H); 2.10-1.95 (q, 4H); 1.61-1.49 (m, 4H); 1.91-1.70 (m, 24H)

**Synthesis of saturated ketone polymer (5-12).** Under constant argon flow, 2.5 g of tricosa-1,22-dien-12-one **(5-10)** was dissolved in 2 mL of dibenzylcarbonate and then added to a flame-dried Schlenk flask equipped with a magnetic stir bar. Grubbs 2nd generation catalyst (1 mol%) was added to the reaction mixture. The reaction was placed under high vacuum at 50°C while stirring. After 48 hours the reaction was quenched with a solution of 2mL of ethyl vinyl ether in 10mL of toluene. The solvents were reduced to a minimal amount by vacuum and the polymer **(5-11)** was precipitated into 250mL of cold methanol and was isolated via filtration. The unsaturated polymer **(5-**

**11)** was then hydrogenated to yield the saturated polymer **(5-12)**. In a 250 mL Parr bomb glass sleeve, unsaturated polymer **(5-11)** was dissolved in 40 mL of degassed toluene. Wilkinson's hydrogenation catalyst (catalyst-to-monomer ratio 1:250) was added to the solution and the bomb was charged with 800 psi of hydrogen. The reaction was allowed to proceed for 3 days at 90°C. The polymer solution was concentrated and precipitated in cold methanol. The polymer was isolated by filtration as a white solid. $^{1}$H NMR (300MHz, Toluene-d8, 108 °C, ppm): δ= 2.16 (t, 2H); 1.55 (m, 4H); 1.33 (br, 30H); 0.89 (t, 0.10, $CH_3$ end groups); FT-IR: 2962, 2916, 2849, 1705, 1462, 1380, 1259, 1014, 903, 864, 795, 685 $cm^{-1}$. $M_n$= 4,630 g/mol; PDI ($M_w$/ $M_n$)=3.90.

**Hydrosilylation of ketone polymer (5-12).** In a round-bottomed flask, under inert atmosphere, **(5-12)** (0.5g, 1.5 mmol) was dissolved in a minimal amount of dry toluene at 60°C. Pd/C (1.2 mol%, 1.9 mg, 0.018 mmol) was added to the reaction flask followed by dropwise addition of 1,1,1,3,3,5,5-heptamethyldisiloxane (0.33g, 1.5 mmol). After 20 h, the reaction mixture was concentrated under vacuum and the polymer was precipitated in cold methanol. The polymer was separated by filtration yielding a white insoluble solid. FT-IR: 3316, 2917, 2849, 1747, 1465, 1264, 1122, 1071, 963, 909, 789, 721, 696 $cm^{-1}$.

**Synthesis of unsaturated alcohol polymer (5-14).** Under constant argon flow, 2.5 g of tricosa-1,22-dien-12-ol **(5-9)** was dissolved in 2 mL of dibenzylcarbonate and then added to a flame-dried Schlenk flask equipped with a magnetic stir bar. Grubbs 1$^{st}$ generation catalyst (1 mol%) was added to the reaction mixture, and the reaction was placed under high vacuum at 50°C while stirring. After 48 hours the reaction was quenched with a solution of 2mL of ethyl vinyl ether in 10mL of toluene. The solvents

were reduced to a minimal amount and the polymer was precipitated into 250mL of cold methanol and was isolated via filtration. The polymer was characterized using FT-IR and the molecular weight was measured by GPC. $^{1}$H NMR (300MHz, $CDCl_3$, ppm): **δ=** 5.46-5.32 (s, 2H); 5.62-5.58 (s, 1H); 2.08-1.88 (s, 4H); 1.48-1.2 (s, 32H). FT-IR: 3341, 3005, 2926, 2856, 1725, 1456, 1432, 1036, 967, 868 $cm^{-1}$. $M_n$= 5,280 g/mol; PDI ($M_w$/ $M_n$)=3.20.

**Synthesis of saturated alcohol polymer (5-15).** In a 250 mL Parr bomb glass sleeve, unsaturated polymer **(5-11)** was dissolved in 40 mL of degassed toluene. Wilkinson's hydrogenation catalyst (catalyst-to-monomer ratio 1:250) was added to the solution and the bomb was charged with 800 psi of hydrogen. The reaction was allowed to proceed for 3 days at 90°C. The polymer solution was concentrated and precipitated in cold methanol. The polymer was isolated by filtration as a white solid. The saturated alcohol polymer is insoluble and was only characterized by FT-IR. FT-IR: 3341, 2926, 2856, 1725, 1456, 1036, 967, 760 $cm^{-1}$.

**Palladium-on-carbon dehydrogenative coupling of alcohol polymer (5-15).** In a round-bottomed flask under inert atmosphere **(5-15)** (0.5g, 1.48 mmol) was dissolved in a mixture of methanol/toluene (5/95) at 60°C. Pd/C (1.2 mol%, 1.9 mg, 0.018 mmol) was added to the reaction flask followed by the dropwise addition of 1,1,1,3,3,5,5-heptamethyldisiloxane (0.63g, 2.98 mmol). After 20 h, the reaction mixture was concentrated under vacuum and the polymer was precipitated in cold methanol. The polymer was separated by filtration yielding a white insoluble solid. FT-IR: 3309, 2917, 2849, 1465, 1350, 1260, 1122, 1070, 963, 858, 809, 721$cm^{-1}$.

**Dehydrogenative coupling of alcohol polymer (5-15) via $B(C_6F_5)_3$.** In a round-bottomed flask, under inert atmosphere, **(5-15)** (0.5g, 1.48 mmol) was dissolved in a mixture of methanol/toluene (5/95) at 60°C. $B(C_6F_5)_3$ (1.2 mol%, 10.8 mg, 0.018 mmol) was added to the reaction flask followed by the dropwise addition of 1,1,1,3,3,5,5-heptamethyldisiloxane (0.63g, 2.98 mmol). After 20 h, the reaction mixture was concentrated under vacuum and the polymer was precipitated in cold methanol. The polymer was separated by filtration yielding a white insoluble solid. FT-IR: 3322, 2917, 2849, 1465, 1349, 1257, 1070, 963, 841, 800, 721$cm^{-1}$.

**Synthesis of 1,1,1,3,3,5,5-heptamethyl-3-(tricosa-1,22-dien-12-yloxy)disiloxane (5-16).** To a mixture of tricosa-1,22-dien-12-ol **(5-9)** (5 g, 15 mmol) and $B(C_6F_5)_3$ (0.15 g, 0.3 mmol) in 15 mL of dry toluene was added by syringe 1,1,1,3,3,5,5-heptamethyldisiloxane (3.3 g, 15 mmol) over the course of 5 min. Vigorous evolution of $H_2$ and gentle warming was noted, but a cautious rate of addition kept the exotherm in check. The reaction was allowed to stir overnight. The catalyst was removed from the reaction by filtration and the solvent was removed under vacuum. Proton NMR of the reaction product showed no residual starting materials and **(5-17)** was obtained with no further purification (Yield: >99%). $^1$H NMR (300MHz, $CDCl_3$, ppm): δ= 5.91-5.72 (m, 2H); 5.06-4.88 (m, 4H); 3.73 (q, J= 5.7 Hz, 1H), 2.04 (q, J=7.0 Hz, 4H); 1.45-1.2 (m, 32H); 0.09 (s, 12H); 0.05 (s, 9H). $^{13}$C NMR (75 MHz, $CDCl_3$): δ(ppm) 139.21, 114.05, 72.45, 37.31, 33.81, 29.82, 29.67, 29.65, 29.61, 29.58, 29.53, 29.48, 29.13, 28.94, 25.64, 1.80, 1.04, -0.14. FT-IR: 3078, 2925, 2854, 1465, 1257, 1039, 909, 841, 798, 753 $cm^{-1}$. HRMS Actual $[M-H]^+$=557.4221 Theory $[M-H]^+$=557.4242.

# CHAPTER 6
# SUMMARY AND FUTURE WORK

## 6.1 Summary

ADMET polymerization has been used in the past by the Wagener group for the synthesis of in-chain siloxane copolymers as well as crosslinked polymers. However, this work constitutes the first attempt to synthesize polyethylene with pendant siloxane branches. The approaches and synthetic methods used in previous work to produce siloxane ADMET monomers cannot be applied for the synthesis of siloxane branched polyethylene, therefore the primary goal of this project was to identify suitable synthetic methods. Several challenges were identified and overcome along the way, such as limitations in commercially available reactive siloxanes, reaction constraint due to the combination of symmetrical diene and siloxane functionalities and finally purification challenges.

The Grignard functionalization method, which was expected to be the most successful, was actually the most problematic and did not have a positive outcome. The use of nuclephilic reactions to create Si-O-C linkages was very effective and yielded four unsaturated polymers. However, this method requires many low-yield reaction steps for the synthesis of the alcohol functionalized pre-monomer. Therefore, and alternative to this method was investigated.

Post-polymerization functionalization of the polymers via hydrosilylation of unsaturated polyethylene and saturated ketone branched polyethylene led to limited or no incorporation of the siloxane branch onto the polymer backbone. Instead, the reduction of the functional group was observed in both cases. The same results were observed when post-polymerization dehydrogenative coupling was attempted on the

saturated alcohol polymer. However, excellent results were observed when this reaction was applied to the alcohol functionalized symmetrical diene monomer. This method led to the introduction of the siloxane branch onto the polyethylene backbone in high yields using $B(C_6F_5)_3$ as a catalyst. This is a “clean” reaction, as both starting materials are entirely consumed, and the only by-product is $H_2$(g). The advantages of this method are many: i) it allows for the synthesis of siloxane branched monomers in 2 steps, with close to quantitative yields; ii) recrystallization is the only purification method required; iii) a wide family of reactive silicon-hydrides is commercially available; and finally (iv) the reaction can be scaled-up, since none of the chemicals used are considered dangerous. This work has allowed us to successfully identify a synthetic route for the production of siloxane branched diene monomers that can be further pursued to synthesize a series of polymers with different siloxane branches and various distances between the branches.

## 6.2 Future Work

### 6.2.1 Polymer characterization

The unsaturated siloxane polymers that were synthesized in Chapter 4 have been characterized to the extent of our ability. Due to their insolubility, the primary structure of the polymers could not be properly analyzed, and only FT-IR spectra were obtained. In order to better understand the structure of these polymers, solid-state NMR is required. TGA and DSC thermograms were obtained for these polymers as well. However, the information gathered from these experiments gives us very little insight concerning the morphology of the polymers. Additional experiments such as WAXS diffraction should allow us to better understand the secondary structure of these polymers, and perhaps identify the cause of their insolubility. Finally, the most important

study will be the measurements of the rheological properties of these polymers in order to determine if they are suitable additives for polyethylene extrusion.

### 6.2.2 Synthesis of a library of siloxane containing polymers

As mentioned earlier, the dehydrogenative coupling reaction provides an excellent method for the attachment of the siloxane branch onto the polyethylene backbone, and there are various silicon-hydride reactive materials available commercially. This method opens the door to the synthesis of a library of monomers in which the siloxane branch and the length between the alkyl chain can be modified. The various monomers that will be synthesized are shown in Figure 6-1.

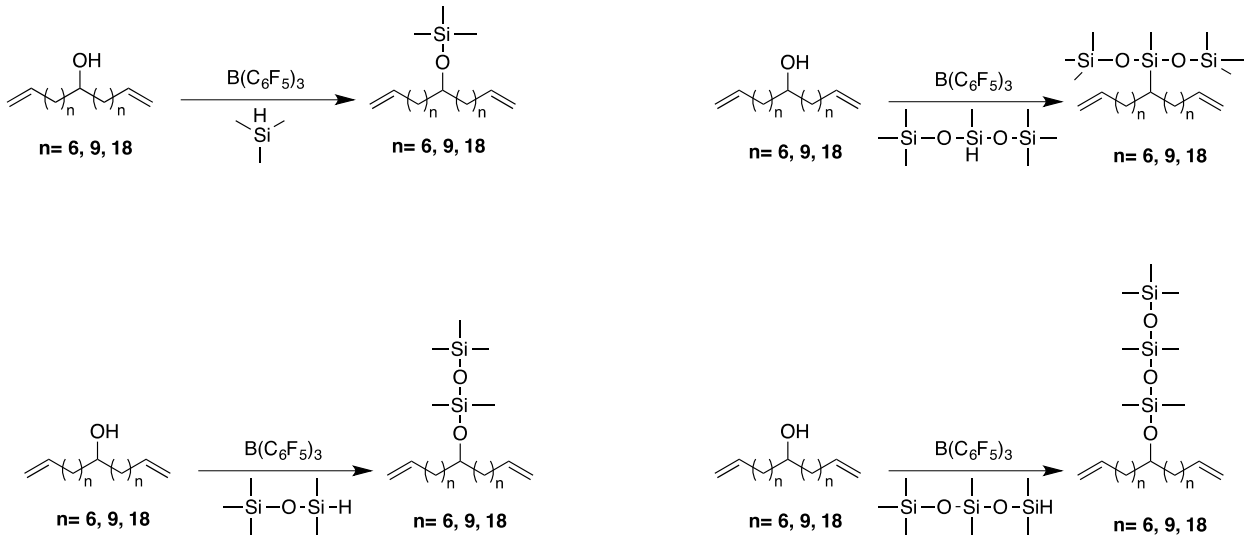


Figure 6-1. Library of siloxane branched symmetrical diene.

After these polymers have been synthesized, they can be polymerized and characterized using the same methods mentioned in section 6.2.1.

### 6.2.3 Fluorine branched polyethylene

Many drawbacks have been identified for the synthesis and use of siloxane branched polyethylene. However, the main concern is related to their insolubility. The insolubility of the polymers can be attributed to the solubility parameter of siloxane (7.3

$(cal/cm^3)^{1/2}$ for PDMS), which is similar to the solubility parameter of organic solvents ($7.2\ (cal/cm^3)^{1/2}$ for hexane), thereby leading to swelling of the polymer.[179] Fluorocarbon polymers have been shown to be efficient slippery agents, reducing the defects related to polyethylene extrusion.[31] However, similar to siloxane polymers, fluorocarbons do not mix well with polyethylene, and until now have not been succesfully used in large-scale productions. Fluorocarbons, are also very expensive, which limits their use industrially.

Studies have shown that polymers possessing both silicone and fluorocarbon moieties swell less than polymers with only silicone moieties.[180] The silicone on the other hand, acts as a chaperone, and guides the fluorine chains to the surface. Based on these studies, would a polymer with two branches side by side, a silicone branch and a fluorocarbon branch, perform in that same manner? If so, does this happen with all size branches and how does the distance between the branches affect this process? Finally, would this polymer combine the properties of both silicone and fluorocarbon therefore making for a highly efficient extruding aid? The synthesis of such a polymer can be achieved via the 4 steps synthesis shown in Figure 6-2.

This synthetic route can produce high yields, and requires little purification. The synthesis of **(3-5)**, **(5-9)** and **(5-10)** was described throughout this dissertation. Ketone **(5-10)** is highly reactive with Grignards, and can produce **(6-1)** using very mild conditions, and with no by-product if (trimethylsilylmethyl)magnesium is used in great excess. Using the Grignard in excess for this reaction is not problematic, since any unreacted Grignard will become tertamethylsilane once the reaction is quenched. Tetramethylsilane has a low boiling point, and can be evaporated with the solvent under vacuum. Another advantage to this reaction is that it takes place at 0°C; therefore, side

reactions with the solvents should no longer be an issue.12-((trimethylsilyl)methyl)tricosa-1,22-dien-12-ol **(6-1)** possesses a reactive hydroxyl group along with the silane branch.

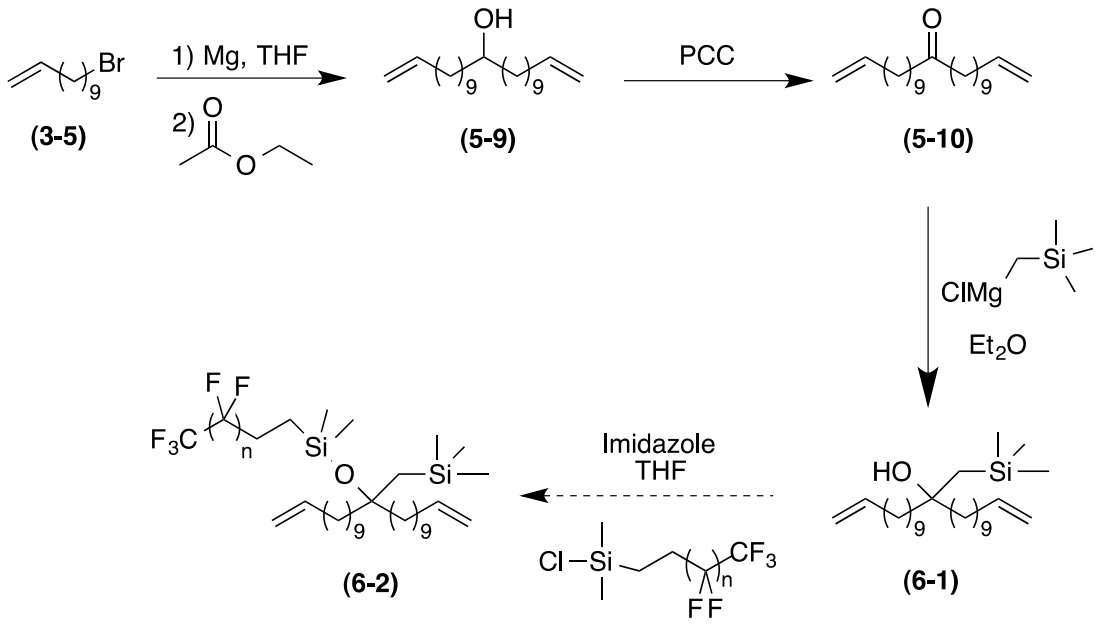


Figure 6-2. Four steps synthesis of fluorine branched polyethylene.

The alcohol can undergo an SN2 reaction with (3,3,3-Trifluoropropyl)chlorodimethylsilane and other derivatives to produce the difunctional diene **(6-2)**. This reaction was not performed with compound **(6-1)**, but it was tested with undec-10-en-1-ol as shown in Figure 6-2.

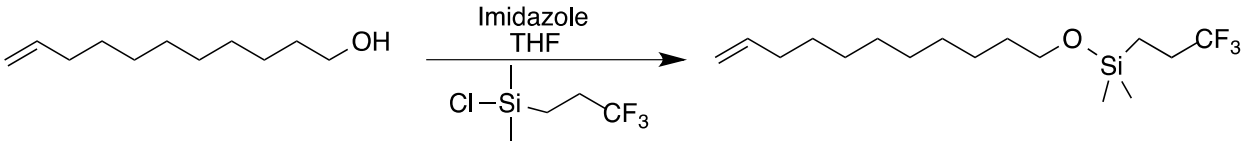


Figure 6-3. Model SN2 reaction.

This synthetic route seems like a great alternative for the silicone branched polyethylene, with limited purification required, high yields and commercially available compounds. Once these polymers are synthesized, rheological measurements would answer all the application related questions.

## 6.3 Experimental

### 6.3.1 Materials and Instrumentation

All silicones were purchased from Gelest and distilled over $CaH_2$ prior to use. All other materials were purchased from Aldrich and used without further purification unless noted. Anhydrous solvents were obtained from an anhydrous solvent system. All $^{1}H$ NMR and $^{13}C$ NMR were obtained on a Varian Mercury 300MHz spectrometer and recorded in $CDCl_3$. $^{1}H$ NMR and $^{13}C$ NMR shifts were referenced to residual signals from $CDCl_3$ ($^{1}H$ = 7.24 ppm and $^{13}C$ = 77,23 ppm). Mass spectrograms were acquired on a Thermo Scientific DSQ MS using the chemical ionization mode. Thin layer chromatography (TLC) was used to monitor all reactions and was performed on plastic-backed neutral alumina plates.

### 6.3.2 Procedures

**12-((trimethylsilyl)methyl)tricosa-1,22-dien-12-ol (6-1):** A flame dried three neck flask with a stir bar was charged with 40mL of diethyl ether and Mg (5.78 g, 237.7 mmol) under argon. The flask was chilled in an ice bath, and 1,2-dibromoethane (12.3 g, 65 mmol) was added to the solution and stirred at RT for 30 minutes. (Bromomethyl)trimethylsilane (21.58 g, 130 mmol) was added drop-wise to the reaction mixture followed by refluxing for 24 hours. The reaction was then cooled to 0°C and tricosa-1,22-dien-12-one **(5-10)** ( 4.34 g, 13 mmol) dissolved in 10 mL of ether was added dropwise to the reaction. The reaction was allowed to proceed for 24 hours on ice. The reaction neutralized with saturated $NH_4Cl$, extracted in ether, washed with brine and dried over magnesium sulfate. The solvent was removed under vacuum to yield a clear oil (Yield: 73%). $^{1}H$ NMR (300 MHz, $CDCl_3$): $\delta$(ppm) 5.93-5.71 (m, 2H), 5.07-4.86 (m, 4H), 2.04 ppm (q, J=7.0Hz, 4H), 1.57 ppm (s,1H), 1.43-1.27 (m, 32H), 0.95(s, 2H),

0.06 (s, 9H).$^{13}$C NMR (75 MHz, CDCl3): δ(ppm) 139.32, 114.57, 69.46, 40.7, 37.61, 33.02, 29.92, 29.83, 29.77, 29.70, 29.35, 29.15, 25.87, -0.8.

LIST OF REFERENCES

(1) Piringer, O. G. *Plastic Packaging; Interactions with Food and Pharmaceuticals*; Wiley-VCH Verlag GmbH&Co. KGaA: Weinheim, Germany, 2008.

(2) Peacock, A. J. *Handbook of polyethylene: Structures, properties and applications*; Marcel Dekker: New York, 2000.

(3) Bamberger, E.; Tschirner, F. *Berichte Der Deutschen Chemischen Gesellschaft* **1900**, *33*, 955.

(4) Furukawa, Y. *Isis* **1987**, *78*, 102.

(5) Carothers, W. H.; Hill, J. W.; Kirby, J. E.; Jacobson, R. A. *Journal of the American Chemical Society* **1930**, *52*, 5279.

(6) Fawcett, E. W.; Gibson, R. O.; Perrin, M. H.; Patton, J. G.; Williams, E. G.; Industries, I. C., Ed.; International Chemical Industries: Great Britain, **1937** p471.

(7) Johnson, J. K.; Mecking, S.; Brookhart, M. *Abstracts of Papers of the American Chemical Society* **1995**, *210*, 242.

(8) Killian, C. M.; Tempel, D. J.; Johnson, L. K.; Brookhart, M. *Journal of the American Chemical Society* **1996**, *118*, 11664.

(9) Johnson, L. K.; Mecking, S.; Brookhart, M. *Journal of the American Chemical Society* **1996**, *118*, 267.

(10) Tempel, D. J.; Johnson, L. K.; Huff, R. L.; White, P. S.; Brookhart, M. *Journal of the American Chemical Society* **2000**, *122*, 6686.

(11) Ittel, S. D.; Johnson, L. K.; Brookhart, M. *Chemical Reviews* **2000**, *100*, 1169.

(12) Svejda, S. A.; Johnson, L. K.; Brookhart, M. *Journal of the American Chemical Society* **1999**, *121*, 10634.

(13) Leatherman, M. D.; Svejda, S. A.; Johnson, L. K.; Brookhart, M. *Journal of the American Chemical Society* **2003**, *125*, 3068.

(14) Mecking, S.; Johnson, L. K.; Wang, L.; Brookhart, M. *Journal of the American Chemical Society* **1998**, *120*, 888.

(15) Killian, C. M.; Johnson, L. K.; Brookhart, M. *Organometallics* **1997**, *16*, 2005.

(16) Gates, D. P.; Svejda, S. K.; Onate, E.; Killian, C. M.; Johnson, L. K.; White, P. S.; Brookhart, M. *Macromolecules* **2000**, *33*, 2320.

(17) Emert, J.; Rossi, A.; Gindelberger, D.; Stanat, J.; Stokes, J.; Sim, J.; Exxon: 1997, p 9803617.

(18) Geprags, M.; Mulhaupt, R.; Heinemann, J.; Aktiengesellschaft, B. 1998, p 9947569.

(19) Ziegler, K.; Pat., B., Ed. 1955.

(20) Sinn, H.; Kaminsky, W. *Ziegler-Natta Catalysts. Advances in Organometallic Chemistry*; Academic Press Inc.: London, 1980.

(21) James, D. E. *Ethylene Polymers: Encyclopedia of Polymer Science and Chemistry*; *2nd* ed.; Wiley-Interscience: New York, 1986.

(22) Florjańczyk, Z.; Peneczek, S. *Chemia Polimerów* Warszawa, 1995.

(23) Hester, D. L.; Sadik, S. A.; Trouilhet, Y. *Tappi Journal* **1990**, *73*, 117.

(24) Halle, R. W.; Simpson, D. M. In *Paper, Film and Foil Converter Magazine* 2003.

(25) Rappaport, H. *Plastics Industry Update, ANIPAC*, 2005.

(26) Wagner, P. *Brief Evaluation of the World Market for Extrusion Coating Equipment*, 2001.

(27) Rosato, M. G.; Rosato, D. V. *Concise encyclopedia of plastics*; Springer: New York, 2000.

(28) http://www.reliance.com/prodserv/standriv/appnotes/d7741.pdf: (accessed September 2013).

(29) Kaufman, M. *Plastics and Polymers* **1969**, *37*, 243.

(30) Leonov, A. I.; Prokunin, A. N. *Rheologica Acta* **1983**, *22*, 137.

(31) Macosko, C. W. *Rheology: Principles, Measurements and Applications*; VCH Publishers: New York, 1994.

(32) Cogswell, F. N. *Polymer Melt Rheology*; Woodhead Publishing: Cambridge, England, 1996.

(33) Debbaut, B. *Plastics Rubber and Composites* **2008**, *37*, 166.

(34) Latto, B.; Elriedy, O. K.; Vlachopoulos, J. *Journal of Rheology* **1981**, *25*, 583.

(35) Denn, M. M. *Annual Review of Fluid Mechanics* **2001**, *33*, 265.

(36) A.V., R. *Proceedings of X$^{th}$ International Congress of Rheology* Sydney, 1988.

(37) Hristov, V.; Takacs, E.; Vlachopoulos, J. *Polymer Engineering and Science* **2006**, *46*, 1204.

(38) Rosenbaum, E. E.; Randa, S. K.; Hatzikiriakos, S. G.; Stewart, C. W.; Henry, D. L.; Buckmaster, M. *Polymer Engineering and Science* **2000**, *40*, 179.

(39) Wang, S. Q. *Polymers in Confined Environments* **1999**, *138*, 227.

(40) Hatzikiriakos, S. G.; Hong, P.; Ho, W.; Stewart, C. W. *Journal of Applied Polymer Science* **1995**, *55*, 595.

(41) Kurtz, S. J.; Blakeslee, T. R.; Scarola, L. S. U.S., 1981; Vol. 4,282,177.

(42) Buckmaster, M. D.; Henry, D. L.; Randa, S. K.; Inc., E. I. D. d. N. a. C., Ed. U.S., 1997.

(43) Achilleos, E. C.; Georgiou, G.; Hatzikiriakos, S. G. *Journal of Vinyl & Additive Technology* **2002**, *8*, 7.

(44) Kanu, R. C.; Shaw, M. T. *Polymer Engineering and Science* **1982**, *22*, 507.

(45) Migler, K. B.; Son, Y.; Qiao, F.; Flynn, K. *Journal of Rheology* **2002**, *46*, 383.

(46) Migler, K. B.; Lavallee, C.; Dillon, M. P.; Woods, S. S.; Gettinger, C. L. *Journal of Rheology* **2001**, *45*, 565.

(47) Kazatchkov, I. B.; Hatzikiriakos, S. G.; Stewart, C. W. *Polymer Engineering and Science* **1995**, *35*, 1864.

(48) Ivin, K. J.; Mol, J. C. *Olefin Metathesis and Metathesis Polymerization* Academic: San Diego, CA, 1997.

(49) http://www.nobelprize.org/nobel_prizes/chemistry/laureates/2005/press.html: (accessed September 2013).

(50) Casey, C. P. *Journal of Chemical Education* **2006**, *83*, 192.

(51) Calderon, N.; Chen, H. Y.; Scott, K. W. *Tetrahedron Letters* **1967**, 3327.

(52) Calderon, N.; Ofstead, E. A.; Ward, J. P.; Judy, W. A.; Scott, K. W. *Journal of the American Chemical Society* **1968**, *90*, 4133.

(53) Truett, W. L.; Johnson, D. R.; Robinson, I. M.; Montague, B. A. *Journal of the American Chemical Society* **1960**, *82*, 2337.

(54) Mutlu, H.; de Espinosa, L. M.; Meier, M. A. R. *Chemical Society Reviews* **2011**, *40*, 1404.

(55) Herisson, J. L.; Chauvin, Y. *Makromolekulare Chemie* **1971**, *141*, 161.

(56) Katz, T. J.; McGinnis, J. *Journal of the American Chemical Society* **1975**, *97*, 1592.

(57) Astruc, D. *New Journal of Chemistry* **2005**, *29*, 42.

(58) Baughman, T. W.; van der Aa, E.; Lehman, S. E.; Wagener, K. B. *Macromolecules* **2005**, *38*, 2550.

(59) Buchmeiser, M. R. *Chemical Reviews* **2000**, *100*, 1565.

(60) Deiters, A.; Martin, S. F. *Chemical Reviews* **2004**, *104*, 2199.

(61) McReynolds, M. D.; Dougherty, J. M.; Hanson, P. R. *Chemical Reviews* **2004**, *104*, 2239.

(62) Blackwell, H. E.; O'Leary, D. J.; Chatterjee, A. K.; Washenfelder, R. A.; Bussmann, D. A.; Grubbs, R. H. *Journal of the American Chemical Society* **2000**, *122*, 58.

(63) Smith, A. B.; Adams, C. M.; Kozmin, S. A.; Paone, D. V. *Journal of the American Chemical Society* **2001**, *123*, 5925.

(64) Atallah, P.; Wagener, K. B.; Schulz, M. D. *Macromolecules* **2013**, *46*, 4735.

(65) Schrock, R. R. *Accounts of Chemical Research* **1990**, *23*, 158.

(66) Scrock, R. R. *Ring Opening Polymerization*; Brunelle, D.J., Ed.; Hanser:Munich, 1993.

(67) Nicolaou, K. C.; Bulger, P. G.; Sarlah, D. *Angewandte Chemie-International Edition* **2005**, *44*, 4490.

(68) Nelson, D. J.; Ashworth, I. W.; Hillier, I. H.; Kyne, S. H.; Pandian, S.; Parkinson, J. A.; Percy, J. M.; Rinaudo, G.; Vincent, M. A. *Chemistry-a European Journal* **2011**, *17*, 13087.

(69) Grubbs, R. H.; Miller, S. J.; Fu, G. C. *Accounts of Chemical Research* **1995**, *28*, 446.

(70) Furstner, A. *Topics in Catalysis* **1997**, *4*, 285.

(71) Furstner, A. *Angewandte Chemie-International Edition* **2000**, *39*, 3012.

(72) Schuster, M.; Blechert, S. *Angewandte Chemie-International Edition in English* **1997**, *36*, 2037.

(73) Grubbs, R. H.; Chang, S. *Tetrahedron* **1998**, *54*, 4413.

(74) Wright, D. L. *Current Organic Chemistry* **1999**, *3*, 211.

(75) Ivin, K. J. *Journal of Molecular Catalysis a-Chemical* **1998**, *133*, 1.

(76) O'Leary, D. J.; Blackwell, H. E.; Washenfelder, R. A.; Grubbs, R. H. *Tetrahedron Letters* **1998**, *39*, 7427.

(77) Opper, K. L.; Wagener, K. B. *Journal of Polymer Science Part a-Polymer Chemistry* **2011**, *49*, 821.

(78) Doyle, G. *Journal of Catalysis* **1973**, *30*, 118.

(79) Korshak, Y. V.; Tlenkopatchev, M. A.; Dolgoplosk, B. A.; Avdeikina, E. G.; Kutepov, D. F. *Journal of Molecular Catalysis* **1982**, *15*, 207.

(80) Dallasta, G.; Stiglian.G; Greco, A.; Motta, L. *Chimica & L Industria* **1973**, *55*, 142.

(81) Lindmarkhamberg, M.; Wagener, K. B. *Abstracts of Papers of the American Chemical Society* **1987**, *193*, 140.

(82) Wagener, K. B.; Boncella, J. M.; Nel, J. G.; Duttweiler, R. P.; Hillmyer, M. A. *Makromolekulare Chemie-Macromolecular Chemistry and Physics* **1990**, *191*, 365.

(83) Courchay, F. C.; Sworen, J. C.; Wagener, K. B. *Macromolecules* **2003**, *36*, 8231.

(84) Wagener, K. B.; Puts, R. D.; Smith, D. W. *Makromolekulare Chemie-Rapid Communications* **1991**, *12*, 419.

(85) Weychardt, H.; Plenio, H. *Organometallics* **2008**, *27*, 1479.

(86) Berda, E. B.; Wagener, K. B. *Synthesis of Polymers; New Structures and Methods* Schluter, D.; Hawker, C.; Sakamosto, J., Eds.; Wiley-VCH: Weinhein, Germany, 2012, p 587.

(87) Berda, E. B.; Wagener, K. B. *Polymer Science: A Comprehensive Reference* Matyjaszewski, K., Müllen, M., Eds.; Elsevier BV: Amsterdam 2012; Vol. 5, pp 195-216.

(88) Wagener, K. B.; Berda, E. B. *Complex Macromolecular Architecture: Synthesis, Characterization, and Self-Assembly* Hadjichristidis, N., Hirao, A., Tezuka, Y., Du Prez, F. , Eds.; John Wiley & Sons: Singapore, 2011; pp 317−347

(89) Baughman, T. W.; Wagener, K. B. *Metathesis Polymerization* **2005**, *176*, 1.

(90) Trnka, T. M.; Grubbs, R. H. *Accounts of Chemical Research* **2001**, *34*, 18.

(91) Vougioukalakis, G. C.; Grubbs, R. H. *Chemical Reviews* **2010**, *110*, 1746.

(92) Schaverien, C. J.; Dewan, J. C.; Schrock, R. R. *Journal of the American Chemical Society* **1986**, *108*, 2771.

(93) Schrock, R. R.; Depue, R. T.; Feldman, J.; Schaverien, C. J.; Dewan, J. C.; Liu, A. H. *Journal of the American Chemical Society* **1988**, *110*, 1423.

(94) Schrock, R. R.; Depue, R. T.; Feldman, J.; Yap, K. B.; Yang, D. C.; Davis, W. M.; Park, L.; Dimare, M.; Schofield, M.; Anhaus, J.; Walborsky, E.; Evitt, E.; Kruger, C.; Betz, P. *Organometallics* **1990**, *9*, 2262.

(95) Murdzek, J. S.; Schrock, R. R. *Organometallics* **1987**, *6*, 1373.

(96) Schrock, R. R.; Murdzek, J. S.; Bazan, G. C.; Robbins, J.; Dimare, M.; Oregan, M. *Journal of the American Chemical Society* **1990**, *112*, 3875.

(97) Oskam, J. H.; Fox, H. H.; Yap, K. B.; McConville, D. H.; Odell, R.; Lichtenstein, B. J.; Schrock, R. R. *Journal of Organometallic Chemistry* **1993**, *459*, 185.

(98) Kingsbury, J. S.; Harrity, J. P. A.; Bonitatebus, P. J.; Hoveyda, A. H. *Journal of the American Chemical Society* **1999**, *121*, 791.

(99) Garber, S. B.; Kingsbury, J. S.; Gray, B. L.; Hoveyda, A. H. *Journal of the American Chemical Society* **2000**, *122*, 8168.

(100) Gessler, S.; Randl, S.; Blechert, S. *Tetrahedron Letters* **2000**, *41*, 9973.

(101) Nguyen, S. T.; Grubbs, R. H.; Ziller, J. W. *Journal of the American Chemical Society* **1993**, *115*, 9858.

(102) Wu, Z.; Nguyen, S. T.; Grubbs, R. H.; Ziller, J. W. *Journal of the American Chemical Society* **1995**, *117*, 5503.

(103) Courchay, F. C.; Sworen, J. C.; Ghiviriga, I.; Abboud, K. A.; Wagener, K. B. *Organometallics* **2006**, *25*, 6074.

(104) Schmidt, B. *Journal of Organic Chemistry* **2004**, *69*, 7672.

(105) Hopkins, T. E.; Pawlow, J. H.; Koren, D. L.; Deters, K. S.; Solivan, S. M.; Davis, J. A.; Gomez, F. J.; Wagener, K. B. *Macromolecules* **2001**, *34*, 7920.

(106) Hopkins, T. E.; Wagener, K. B. *Macromolecules* **2003**, *36*, 2206.

(107) Leonard, J. K.; Turek, D.; Sloan, K. B.; Wagener, K. B. *Macromolecular Chemistry and Physics* **2010**, *211*, 154.

(108) Duncan, R. *Nature Reviews Drug Discovery* **2003**, *2*, 347.

(109) Duncan, R. *Nature Reviews Cancer* **2006**, *6*, 688.

(110) Staudinger, H.; Ashdown, A. A.; Brunner, M.; Bruson, H. A.; Wehrli, U. S. *Helvetica Chimica Acta* **1929**, *12*, 934.

(111) Odian, G. *Principles of Polymerization, 4th ed.*; John Wiley & Sons, Inc. : Hoboken, NJ, 2004; p 633.

(112) Hopkins, T. E.; Wagener, K. B. *Advanced Materials* **2002**, *14*, 1703.

(113) Inci, B.; Wagener, K. B. *Journal of the American Chemical Society* **2011**, *133*, 11872.

(114) Vouyiouka, S. N.; Karakatsani, E. K.; Papaspyrides, C. D. *Progress in Polymer Science* **2005**, *30*, 10.

(115) Oakley, G. W.; Lehman, S. E.; Smith, J. A.; van Gerven, P.; Wagener, K. B. *Macromolecules* **2003**, *36*, 539.

(116) Oakley, G. W.; Wagener, K. B. *Macromolecular Chemistry and Physics* **2005**, *206*, 15.

(117) Delgado, P. A.; Liu, D. Y.; Kean, Z.; Wagener, K. B. *Macromolecules* **2011**, *44*, 9529.

(118) Schenning, A.; Kilbinger, A. F. M.; Biscarini, F.; Cavallini, M.; Cooper, H. J.; Derrick, P. J.; Feast, W. J.; Lazzaroni, R.; Leclere, P.; McDonell, L. A.; Meijer, E. W.; Meskers, S. C. J. *Journal of the American Chemical Society* **2002**, *124*, 1269.

(119) Tsuie, B.; Wagener, K. B.; Reynolds, J. R. *Abstracts of Papers of the American Chemical Society* **1999**, *218*, U450.

(120) Kaneto, K.; Yoshino, K.; Inuishi, Y. *Japanese Journal of Applied Physics Part 2-Letters* **1983**, *22*, L412.

(121) Kaneto, K.; Yoshino, K.; Inuishi, Y. *Japanese Journal of Applied Physics Part 2-Letters* **1983**, *22*, L567.

(122) Kreja, L.; Kurzawa, M.; Kurzawa, J. *Macromolecular Chemistry and Physics* **1997**, *198*, 643.

(123) Arkles, B. *Chemtech* **1983**, *13*, 542.

(124) McDermott, P. J.; Krafft, T. E.; Rich, J. D. *Journal of Polymer Science Part a-Polymer Chemistry* **1991**, *29*, 1681.

(125) Mark, J. E.; Allcock, H. R.; West, R. *Inorganic Polymers*; Oxford University Press New York 2005

(126) Matloka, P. P.; Wagener, K. B. *Journal of Molecular Catalysis a-Chemical* **2006**, *257*, 89.

(127) Matloka, P. P.; Kean, Z.; Wagener, K. B. *Journal of Polymer Science Part a-Polymer Chemistry* **2010**, *48*, 1866.

(128) Matloka, P. P.; Sworen, J. C.; Zuluaga, F.; Wagener, K. B. *Macromolecular Chemistry and Physics* **2005**, *206*, 218.

(129) Brzezinska, K. R.; Wagener, K. B.; Burns, G. T. *Journal of Polymer Science Part a-Polymer Chemistry* **1999**, *37*, 849.

(130) Paul, D. R. *In Polymer Blends*; Paul, D. R., Newman, S., Eds.; Academic Press New York 1978; Vol. 2, Chapter 12

(131) Roland, C. M. *In Handbook of Elastomers - New Developments and Technology* New York, 1980; p 683.

(132) Kole, S.; Bhattacharya, A.; Tripathy, D. K.; Bhowmick, A. K. *Journal of Applied Polymer Science* **1993**, *48*, 529.

(133) Munoz, P. P.; Vargas, M. D.; Werlang, M. M.; Yoshida, I. V. P.; Mauler, R. S. *Journal of Applied Polymer Science* **2001**, *82*, 3460.

(134) Al-Robaidi, A. *Macromolecular Symposia* **2009**, *282*, 192−198.

(135) Wang, H.; Winnik, M. A.; Manners, I. *Macromolecules* **2007**, *40*, 3784.

(136) Kipping, F. S. *Proceedings of the Royal Society of London Series a-Mathematical and Physical Sciences* **1937**, *159*, 0139.

(137) Clarson, S. J. *Synthesis and Properties of Silicones and Silicone-Modified Materials* **2003**, *838*, 1.

(138) Yuan, Q. W.; Mark, J. E. *Macromolecular Chemistry and Physics* **1999**, *200*, 206.

(139) McCarthy, D. W.; Mark, J. E.; Schaefer, D. W. *Journal of Polymer Science Part B-Polymer Physics* **1998**, *36*, 1167.

(140) McCarthy, D. W.; Mark, J. E.; Clarson, S. J.; Schaefer, D. W. *Journal of Polymer Science Part B-Polymer Physics* **1998**, *36*, 1191.

(141) Kumudinie, C.; Mark, J. E. *Materials Science & Engineering C-Biomimetic and Supramolecular Systems* **2000**, *11*, 61.

(142) Kawakami, Y.; Li, Y. N. *Designed Monomers and Polymers* **2000**, *3*, 399.

(143) Shimojima, A.; Kuroda, K. *Chemical Record* **2006**, *6*, 53.

(144) Klempner, D.; Frisch, K. C.; Xiao, X. H.; Frisch, H. L. *Polymer Engineering and Science* **1985**, *25*, 488.

(145) Woo, E. M.; Barlow, J. W.; Paul, D. R. *Journal of Applied Polymer Science* **1986**, *32*, 3889.

(146) Baidak, A. A.; Liegeois, J. M.; Sperling, L. H. *Journal of Polymer Science Part B-Polymer Physics* **1997**, *35*, 1973.

(147) Sperling, L. H.; Mishra, V. *Macromolecular Symposia* **1997**, *118*, 363.

(148) Yilgor, I.; McGrath, J. E. *Advances in Polymer Science* **1988**, *86*, 1.

(149) Cancouet, P.; Daudet, E.; Helary, G.; Moreau, M.; Sauvet, G. *Journal of Polymer Science Part a-Polymer Chemistry* **2000**, *38*, 826.

(150) Macosko, C. W.; Guegan, P.; Khandpur, A. K.; Nakayama, A.; Marechal, P.; Inoue, T. *Macromolecules* **1996**, *29*, 5590.

(151) Eaborn, C. *Organosilicon Compounds*; Butterworths Scientific Publications: London, 1960.

(152) Noll, W. *Chemistry and Technology of Silicones*; Academic Press New York, 1968.

(153) Abedali, S. S.; Brisdon, B. J.; England, R. *Macromolecules* **1989**, *22*, 3969.

(154) Brisdon, B. J.; Watts, A. M. *Journal of the Chemical Society-Dalton Transactions* **1985**, 2191.

(155) Rappoport, Z.; Apeloig, Y. *The Chemistry of Organic Silicon Compounds*; John Wiley: Chichester, 1998.

(156) Antic, V. V.; Vuckovic, M. V.; Djonlagic, J. *Journal of the Serbian Chemical Society* **2007**, *72*, 139.

(157) Baughman, T. W.; van der Aa, E.; Wagener, K. B. *Macromolecules* **2006**, *39*, 7015.

(158) Colvin, E. W. *Silicon in Organic Synthesis;* Butterworth: London, 1980.

(159) Walsh, R. *Accounts of Chemical Research* **1981**, *14*, 246.

(160) Arkles, B. *Handbook of Grignard Reagents*; Silverman, G.S.; Rakita, P.E., Eds; Marcel Dekker: New York, 1996; pp667-675.

(161) Rosenberg, S. D.; Walburn, J. J.; Ramsden, H. E. *Journal of Organic Chemistry* **1957**, *22*, 1606.

(162) Pearson, D. E.; Cowan, D.; Beckler, J. D. *Journal of Organic Chemistry* **1959**, *24*, 504.

(163) Respess, W. L.; Ward, J. P.; Tamborsk.C *Journal of Organometallic Chemistry* **1969**, *19*, 191.

(164) Uchida, H.; Kabe, Y.; Yoshino, K.; Kawamata, A.; Tsumuraya, T.; Masamune, S. *Journal of the American Chemical Society* **1990**, *112*, 7077.

(165) Beckmann, J.; Duthie, A.; Reeske, G.; Schurmann, M. *Organometallics* **2005**, *24*, 3629.

(166) Lee, Y.; Seomoon, D.; Kim, S.; Han, H.; Chang, S.; Lee, P. H. *Journal of Organic Chemistry* **2004**, *69*, 1741.

(167) Imai, K.; Sasaki, T.; Abe, J.; Nemoto, N. *Polymer Bulletin* **2012**, *68*, 1589.

(168) Mandal, P. K.; McMurray, J. S. *Journal of Organic Chemistry* **2007**, *72*, 6599.

(169) Smetankina, N. P.; Karbovskaya, L. E. *Synthesis and Physical Chemistry of Urethanes*; Schiller, A.M., Ed.; Technomic Publications: Westport, Conneticut, 1975.

(170) Matloka, P., University of Florida, 2006.

(171) Kawakami, Y.; Kakihana, Y.; Miyazato, A.; Tateyama, S.; Hoque, M. A. *Silicon Polymers* **2011**, *235*, 185.

(172) Pagliaro, M.; Ciriminna, R.; Pandarus, V.; Beland, F. *European Journal of Organic Chemistry* **2013**, *2013*, 6227.

(173) Gordillo, A.; Forigua, J.; Lopez-Mardomingo, C.; de Jesus, E. *Organometallics* **2011**, *30*, 352.

(174) Mabry, J. M.; Paulasaari, J. K.; Weber, W. P. *Polymer* **2000**, *41*, 4423.

(175) Paulasaari, J. K.; Weber, W. P. *Macromolecules* **1998**, *31*, 7105.

(176) Blackwell, J. M.; Foster, K. L.; Beck, V. H.; Piers, W. E. *Journal of Organic Chemistry* **1999**, *64*, 4887.

(177) Mei, J.; Kim, D. H.; Ayzner, A. L.; Toney, M. F.; Bao, Z. *Journal of the American Chemical Society* **2011**, *133*, 20130.

(178) Ogara, J. E.; Wagener, K. B.; Hahn, S. F. *Abstracts of Papers of the American Chemical Society* **1993**, *206*, 60.

(179) Lee, J. N.; Park, C.; Whitesides, G. M. *Analytical Chemistry* **2003**, *75*, 6544.

(180) Zhang, W.; Zheng, Y.; Orsini, L.; Morelli, A.; Galli, G.; Chiellini, E.; Carpenter, E. E.; Wynne, K. J. *Langmuir* **2010**, *26*, 5848.

# BIBLIOGRAPHICAL SKETCH

Pascale was born and raised in Lebanon. She is the daughter of Siham Haikal and Atallah Atallah. Pascale completed her BS degree in Chemistry at Saint Joseph University in Lebanon. She then moved to Bordeaux, France, to pursue higher education and received a Master in physics and chemical engineering from the Ecole Nationale Superieure de Chimie Physique de Bordeaux. After graduating, she worked for a year at the Research and Technology Center at Rhodia, Paris, where she realized she wanted to get a PhD. During her time at Rhodia, she had the opportunity to work on polymer synthesis using a high throughput innovative robot called CHEMSPEED. Pascale chose the University of Florida for her graduate studies because of the great polymer program available as well as her passion for basketball, and UF had won two National titles in a row. Her choice to join the Wagener group was made once she realized there was an opportunity to do research in an application related field.